NASA CONTRACTOR REPORT

NUMERICAL INVESTIGATION OF UNSTEADY LAMINAR INCOMPRESSIBLE CO-AXIAL BOUNDARY LAYER FLOWS

by Urmila Agarwal and T. Paul Torda

Prepared by
ILLINOIS INSTITUTE OF TECHNOLOGY
Chicago, Ill.
for Lewis Research Center

NATIONAL AERONAUTICS AND SPACE ADMINISTRATION • WASHINGTON, D. C. • OCTOBER 1967

NASA CR-908

NUMERICAL INVESTIGATION OF UNSTEADY LAMINAR INCOMPRESSIBLE CO-AXIAL BOUNDARY LAYER FLOWS

By Urmila Agarwal and T. Paul Torda

Prepared under Grant No. NsG-694 by
ILLINOIS INSTITUTE OF TECHNOLOGY
Chicago, Ill.

for Lewis Research Center

NATIONAL AERONAUTICS AND SPACE ADMINISTRATION

For sale by the Clearinghouse for Federal Scientific and Technical Information
Springfield, Virginia 22151 – Price $3.00

FOREWORD

Research related to advanced nuclear rocket propulsion is described herein. This work was performed under NASA Grant NsG-694 with Mr. Maynard F. Taylor, Nuclear Systems Division, NASA Lewis Research Center as Technical Manager.

ABSTRACT

The laminar, incompressible, time-dependent boundary layer equations are solved by the method of finite differences. The flow is assumed to possess cylindrical symmetry, finite transverse boundaries, and no swirl. Axial pressure gradient is accounted for. The non-linear governing differential equations are approximated by linear explicit finite difference equations, without linearizing the differential equations. Karplus' criterion is used to determine the finite step sizes conforming with numerical stability of the computation scheme.

The method developed is used to study the transient response of laminar confined jet mixing to axial velocity fluctuations superimposed at the jet exit, i.e., at the entrance section of the mixing region. The computer time required, though large, is comparable with that for the solution of the time-dependent Navier Stokes equations using implicit, unconditionally stable computation schemes.

For the flow configuration investigated, the initial velocites at the entrance of the mixing region correspond to a Reynolds' number of 1650 for the jet, and 1400 for the surrounding annulus, resulting in an overall flow with a Reynolds' number of 2900 in the confining pipe. A sinusoidal oscillation with an amplitude of five per cent of the local velocity is superimposed on the axial velocity at the entrance section, and the resulting transient flow is computed. The study is limited by the available computer facilities. It is found that the distortion of the introduced wave increases with increasing frequency, as does the transient time for the flow. In the cases considered, the frequency of the wave in the resulting motion is the same as that of the superimposed wave. Also, when the flow attains steady state, the amplitude in the

downstream direction is larger than that in the upstream direction.

When the Reynolds' numbers are decreased to 250 (jet), 228 (annulus) and 496 (overall flow), no distortion is observed even for the superimposed oscillations that undergo considerable distortion for the previous configuration with higher Reynolds' numbers.

As a reliability test of the method developed, first the problem of steady entrance flow in a porous pipe is solved. Close agreement (within 0.8 per cent) of the solution is obtained with the published results of an unconditionally stable computation scheme [1*]. Results are also obtained for Poiseuille flow with a superimposed oscillating pressure gradient and compare favorably with an available analytical solution [2].

In addition, the method is used to obtain velocity profiles for certain steady, confined flows for which published numerical solutions are already available [3,4,5]. However, these latter have been obtained by solving the steady Navier Stokes equations using unconditionally stable implicit schemes of computation. Comparison of the solutions shows a maximum deviation of about twelve per cent which is limited to the region close to the entrance section. The deviation is smaller in regions further downstream. The computer time needed is, however, much less using the explicit scheme developed.

---

* For all numbered references, see bibliography.

TABLE OF CONTENTS

LIST OF FIGURES

NOMENCLATURE

Symbol	Definition
Latin Letter	
A	Amplitude factor
f	frequency
k	time co-ordinate for discretized problem, $k = 1 + t/\Delta t$
m	radial co-ordinate for discretized problem, $m = 1 + r/\Delta r$
M	maximum value of radial co-ordinate for discretized problem, $M = 1 + R/\Delta r$
n	axial co-ordinate for discretized problem, $n = 1 + z/\Delta z$
p	pressure
r	radial co-ordinate
R	radius of confining pipe
R_1	radius of inner jet tube
Re	overall Reynolds' number, $= \frac{2RU}{\nu}$
Re_1	inner jet tube Reynolds' number, $= \frac{2R_1U_1}{\nu}$
Re_2	Annulus Reynolds' number, $= \frac{2(R-R_1)U_2}{\nu}$
t	time co-ordinate
U	average axial velocity of overall flow
U_1	average axial velocity of flow in inner jet tube
U_2	average axial velocity of flow in annulus
U_s	radial velocity of suction through porous boundary
v_r	radial component of velocity
v_z	axial component of velocity
v_{r_s}	radial component of steady state velocity

v_{z_s}	axial component of steady state velocity
x	general independent co-ordinate
z	axial co-ordinate

Greek Letter

α	dimensionless annulus flow group, defined in Equation (18b)
β	dimensionless annulus flow group, defined in Equation (18b)
δv_r	deviation in radial velocity from steady state
δv_z	deviation in axial velocity from steady state
Δr	radial step size
Δt	temporal step size
Δz	axial step size
ϕ	general dependent variable
ν	Kinematic viscosity
π	constant, = 3.1415927
ρ	mass density

Subscript

r	denotes radial direction
z	denotes axial direction
1	refers to inner jet tube
2	refers to outer annulus
max	maximum value
min	minimum value

Abbreviation

FDE	finite difference equation
PDE	partial differential equation

CHAPTER I
INTRODUCTION

Analytical problems of viscous fluid mechanics occur throughout many fields of science and technology - aerodynamics, heat transfer, oceanography and meteorology, to mention only a few. Such problems may be analyzed by solving the equations governing viscous fluid flow. These equations, the Navier Stokes equations, coupled with the equation of continuity, constitute a high-order differential system, and are non-linear, so that exact solutions have been found in only a few special cases. These solutions are mostly limited to steady flows. Analyses using simplified forms of the Navier Stokes equations have yielded solutions in good agreement with experimental results. The most important among these was developed by Prandtl who assumed that the viscosity effects are important in a thin fluid layer near the flow boundaries. The Navier Stokes equations then reduce to the boundary layer equations.

Due to the mathematical nature of the Navier Stokes equations (elliptic partial differential equations), their complete solution requires specification of the conditions on the closed boundary of a region. Hence, investigation of flows by solution of the Navier Stokes equations necessitates that a boundary condition be also prescribed on the downstream end of the flow field. This may offer no difficulty in some cases, as, for example, in the investigation of developing flows for which the fully developed flow pattern is already known. However, interest may often lie in studying exclusively the effects of an upstream condition on the flow field when no prior information is available regarding the condition on the downstream end. A proper

downstream boundary condition for such flows is one that does not appreciably affect the flow upstream. The selection of such a condition is not always impossible, but has to be made by trial and hence requires considerable numerical experimentation [6]; certain assumptions and approximations may also be sometimes necessary [7]. In addition, the elliptic Navier Stokes equations require an iterative method of solution.

However, a flow satisfying the basic assumptions of the boundary layer theory may be studied with the help of the boundary layer equations. The flow is then considered to have an "open" downstream boundary. Prior knowledge of the downstream boundary condition is no longer required. Also, the solution may be obtained by "marching" forward in the downstream direction, conditions downstream being uniquely and explicitly determined by the conditions upstream. Hence, flows with obstacles in their path may not be studied by using the boundary layer equations.

Until about two decades ago, not much attention was paid to the subject of unsteady laminar boundary layer flows. It was felt that boundary layer growth took place in such a short time that the flow may be considered steady. Early attempts to discuss unsteady laminar boundary layer flows were mainly restricted to initial phases of a motion starting from rest and to oscillatory motions without a mean flow. However, time-dependent boundary layer flow problems arise in connection with many interesting and important fluid mechanics problems and then a detailed investigation of unsteady flows is required. An example of such time-dependent flows is the motion of a vehicle with variable speed over its entire trajectory. The impulsively started

flow is a special case of these types of problems.

The unsteady, laminar, boundary layer flow problem may be solved in its differential form using analytical methods or in its corresponding finite difference form using numerical techniques.

Analytical Methods For Exact Solutions

The analytical methods of obtaining exact solutions of the unsteady boundary layer equations may be classified as follows:

Method of Successive Approximations

C. C. Lin's Method

Method of Series Expansions

Method of Similar and Semi-Similar Solutions

Detailed discussion of these methods may be found in found in Reference 8. Only their applications and limitations are mentioned herein.

Method of Successive Approximations. The integration of the unsteady boundary layer equations can be carried out in most cases by a process of successive approximations which, in essence, is an iteration procedure. The method can be applied to study periodic boundary layers as well as boundary layer flows impulsively started from rest. The limitation of the method is that the complexity of the iteration process increases with the number of higher order terms included in the approximation. Also, the convergence of the final approximation to the exact solution depends on the choice of the starting approximation.

C. C. Lin's Method. C. C. Lin's method [9], based on the theory of harmonic oscillations, is applicable to problems involving periodic motions of the free stream. The quantities under consideration are

suitably averaged and the equations describing the oscillatory components are linearized. The method may be used for flow problems with high-frequency oscillations only.

Method of Series Expansions. Problems involving oscillations may be solved also by series expansion of the solution in ascending powers of a parameter related to a co-ordinate of the problem.

In 1908, Blasius [10] used this approach to obtain solutions for the impulsive motion of a cylinder and for the uniform acceleration of a cylinder in an incompressible fluid. His results were improved upon by Goldstein and Rosenhead [11] in 1936, and further generalized by Watson [12] in 1955. In 1951 Moore [13] employed the series solution method to analyze the problem of the laminar compressible boundary layer over a flat plate moving with a time-dependent velocity. In 1955, Ostrarch [14] extended Moore's results to the case of an isothermal flat plate. In 1957, Cheng and Elliot [15] studied the development of the boundary layer over a semi-infinite flat plate starting from rest in an incompressible fluid. In 1961, the method was used by Kestin, Maeder and Wang [16] to study the effect of a longitudinal sine wave on the boundary layer along a flat plate and in 1962 by Hori [17] to investigate the boundary layer along a cylinder of arbitrary cross-section in a fluctuating main stream.

This method may also be considered as a small perturbation method and is suitable when the frequency of the oscillation is small. Also, owing to mathematical difficulties, the number of terms of the expansion is limited and the solution is accurate only for small values of the perturbation parameter.

Method of Similar and Semi-Similar Solutions. The method of similar or semi-similar solutions reduces the number of independent variables of a problem through the use of a suitable transformation. This simplifies the mathematics of the problem, but is usually applicable only to a limited number of special cases.

In 1955, this class of solutions was examined by Schuh [18], and in 1960 and 1962, by Hayasi [19, 20]. In 1957, Cheng [21] and in 1960, Hassan [22] used this method to study the flat plate problem and in 1958, Yang [23] studied the stagnation point flow using a similar approach.

A general review of solutions of non-steady laminar boundary layer equations is contained in Reference 24.

Analytical Methods For Approximate Solutions

The mathematical difficulties associated with obtaining exact solutions of the unsteady laminar boundary layer equations are very considerable, in spite of the fact that the actual problems considered represent only simple special cases. The general problem of the flow of a fluid around a body of arbitrary shape, which may be important in practical applications, cannot be completely solved exactly. Approximate methods have been developed which, in such general cases, lead quickly to a sufficiently accurate answer.

In 1921, von Karman [25] and Pohlhausen [26] applied the integral method to obtain solutions allowing determination of the boundary layer thickness along flat or curved surfaces. In 1954, Lighthill [27] used the von Karman-Pohlhausen method to investigate the response of a laminar boundary layer to fluctuations of the free stream velocity about a steady mean. Some other works related to the integral method are found in References 28, 29, 30 and 31. In 1940, the integral

method was improved upon by Schlichting and Ulrich [32]. The main advantage of this improved method lies in the fact that transverse gradients of velocity are obtainable more accurately. This might prove important in investigations of stability of velocity profiles in the boundary layer.

Various approximate methods have been developed by several investigators for the solution of the laminar unsteady boundary layer equations. A reasonably extensive list of references may be found in Reference 8.

In general, the approximate methods lead in most cases to a quick solution, but their accuracy is limited in spite of the complex algebraic manipulations involved.

Finite Difference Methods

Most analytical methods of solution of the boundary layer equations are either cumbersome, demanding impractical amount of work (for exact solutions), or have limited accuracy (for approximate solutions). Further, they lack generality of application. The alternative method of step-by-step integration, performed analytically or numerically, overcomes these drawbacks. The numerical integration requires an impracticable amount of work, not acceptable if a fast digital computer is not available. However, with the recent rapid development of large memory high-speed digital computing machines, numerical methods have acquired great importance in the investigation of complex fluid flow problems. No linearization or crucial simplifying assumptions are necessary. A wide variety of boundary and initial conditions may be handled with only minor changes in the basic method of solution. The potentiality of the numerical methods has drawn much attention and several schemes have been developed for the solution of steady as well as unsteady boundary layer

equations. To ensure convergence of the numerical solution to the exact solution of the differential equations, various stability criteria have also been formulated.

Among the earliest and the basic developments of numerical methods for the solution of steady boundary layer equations are the works due to Friedrich [33] and Rouleau and Osterle [34]. In 1952, Friedrich [33] developed an explicit finite difference method to obtain velocity distributions in the mixing region of unconfined co-axial jets. The computational ease of the explicit scheme was, however, accompanied by stability restrictions which severely limited the permissible grid size ratios and, hence, limited the applicability of the method.

In 1954, these limitations were eliminated by the method developed by Rouleau and Osterle [34] for constant pressure flows with rectangular geometry. The computation scheme was explicit in the direction of the flow, but implicit in the transverse direction. Non-negative axial velocity was the only requirement for numerical stability.

In 1959, the work of Rouleau and Osterle was extended by Bodoia [35] by including pressure variation. Therefore, this method became applicable to confined flows. The additional equation necessary to determine the pressure was obtained by application of the boundary conditions on the transverse component of the velocity. Essentially, this was equivalent to considering conservation of total mass flow rate across transverse sections of the flow field.

In 1961, Hornbeck [1] adapted the method of Bodoia to study flows with cylindrical geometry. Hornbeck investigated the development region of a flow in a porous pipe with either constant or local-pressure-dependent velocity through the wall for both uniform and parabolic inlet

velocity profiles. A variable-mesh technique allowed the use of small mesh sizes in regions of high velocity gradients, while still permitting larger mesh sizes in regions of slowly varying velocities. This minimized computational time and round-off errors. The flow problem was also studied by solving both the axial and the radial momentum equations together with the continuity equation. The results in both cases were essentially the same, except in regions very close to the pipe inlet (less than 1/20 pipe diameter downstream from the entrance).*

In 1960 a totally explicit computational method was developed by Wu [36] for the numerical solution of steady laminar boundary layer equations. The method was claimed to be applicable for flows over flat plates or curved walls with pressure and wall temperature variations in the direction of flow. Prescribed variations of fluid properties as functions of fluid temperature and pressure could be handled also. Excluding cases of extremely high temperatures and very low densities, the stability requirements were not as severe as believed by other investigators who devised unconditionally stable implicit schemes. For normal temperature ranges as encountered in incompressible and most compressible flows, a small amount of computer time was required to obtain a solution. For hypersonic flows involving extreme temperatures, use of the Stewartson transformation led to a reasonable computation time.

In 1966, similar explicit finite difference computation scheme and stability criteria were used by Schuyler and Torda [37] to study steady state combustion of solid propellant rockets.

---

* The second method was, however, extremely sensitive to mesh sizes and to the Reynolds number of the flow.

The numerical works referred to above were all restricted to steady flows only. In 1965, Farn [38] investigated numerically the unsteady incompressible laminar boundary layer flows with rectangular or curvilinear geometry. Velocity and temperature profiles were computed for the Blasius flow with a superimposed oscillation and for the impulsively started wedge flow. The finite difference scheme used was explicit in both space dimensions as well as in time. High accuracy was achieved. An attempt was also made to investigate the hydrodynamic stability of the Blasius flow using the method developed, but this effort did not meet with success.

Numerical solution of the unsteady boundary layer equations for flows with cylindrical geometry represents a forward step in the development of finite difference techniques. The development of such a method is the aim of the present work. An all-explicit computation scheme is devised for the numerical investigation of time-dependent, laminar, incompressible boundary layer flows with cylindrical symmetry. Pressure variation is taken into consideration so that confined flows may be included among the applications.

The flow problem is formulated as an initial-boundary value problem using the boundary layer equation in the axial direction together with the continuity equation and appropriate initial and boundary conditions. The equations are approximated by their finite difference forms such that quantities at any point may be expressed explicitly in terms of known quantities only. Numerical stability is ensured by satisfying Karplus' stability criterion [39]. Convergence of the obtained numerical solution to the exact solution of the initial-boundary value problem is then established under the hypothesis due to Lax [40].

If the initial conditions correspond to some steady state flow, they may be generated by the scheme developed prior to the solution of the time-dependent problem.

The method is applied to study the time response of the mixing region of a circular jet in a confined co-axial flow to fluctuations about the steady state velocities. The investigation is limited to the case of homogeneous mixing with no heat transfer and no chemical reaction, although the method is capable of handling the case without such simplifying restrictions.

Steady state mixing of jets in unconfined flows has been investigated experimentally as well as numerically for the past several years. Both laminar and turbulent, as well as compressible and incompressible, cases have been considered. However, confined mixing has been only recently investigated experimentally by Wood [41] and numerically by Seider [4] for the laminar, incompressible case with chemical reaction. The Navier Stokes equations were transformed to the vorticity and stream function equations which were then solved to obtain velocity profiles. Negligible axial diffusion was assumed in the determination of concentration profiles. Also, the turbulent jet in a confined outer stream has been investigated analytically by Hill [42].

Unsteady mixing of jets in confined flows is studied in the present investigation. To the best of the author's knowledge, this problem has not been previously considered, either experimentally or numerically. At the present, analytical investigation is probably beyond realization. Through the method of finite differences, not only is a solution obtainable, but a wide variety of initial and boundary conditions may be accommodated with only minor modifications of the method. If an

analytical method is used, each new type of boundary or initial condition may require a different method of solution, if indeed a solution is at all obtainable. The non-linear terms in the equations make analytical solutions difficult, but present comparatively less difficulty in the finite difference methods.

The use of finite differences is, nevertheless, not without limitations. The solution of a finite difference equation approaches the exact solution of its corresponding differential equation as the mesh point density is increased. This simultaneously increases the number of computations required for obtaining the solution for upto any reasonable values of more than two independent variables. Hence large amount of computer time and storage space become necessary. This also increases the cost of solution. Thus, numerical methods suffer from practical and economic limitations due to available computer speed and storage, and its high cost of operation.

CHAPTER II
ANALYSIS OF PROBLEM

Objective

The objective of the present work is to determine the time-dependent flow pattern in the mixing and developing region of a circular jet confined within a co-axial circular pipe. A time-dependent finite amplitude oscillation is superimposed on the steady state axial velocity at the jet exit section. The temporal reaction to such oscillation of the mixing region is then investigated. The general features of the problem are shown in Figure 1.

The problem is to be analyzed by solving the unsteady laminar boundary layer equations. These equations are based on a number of simplifying assumptions.

Assumptions

1. The flow is initially laminar.
2. The boundary layer assumptions are valid.
3. Condition of no slip exists at all walls.
4. The flow pattern possesses axial symmetry with no swirl.
5. Fluid in the inner pipe is the same as in the surrounding co-axial annulus. Therefore, there is no diffusion or chemical reaction.
6. The fluid is incompressible with constant physical properties throughout the flow field.
7. Isothermal flow conditions exist in the entire flow field.
8. Flows in the inner pipe, as well as in the annulus, are fully developed right up to the axial section where the inner pipe ends, i.e., effects due to termination of inner pipe are neglected.

These assumptions may be briefly justified as follows:

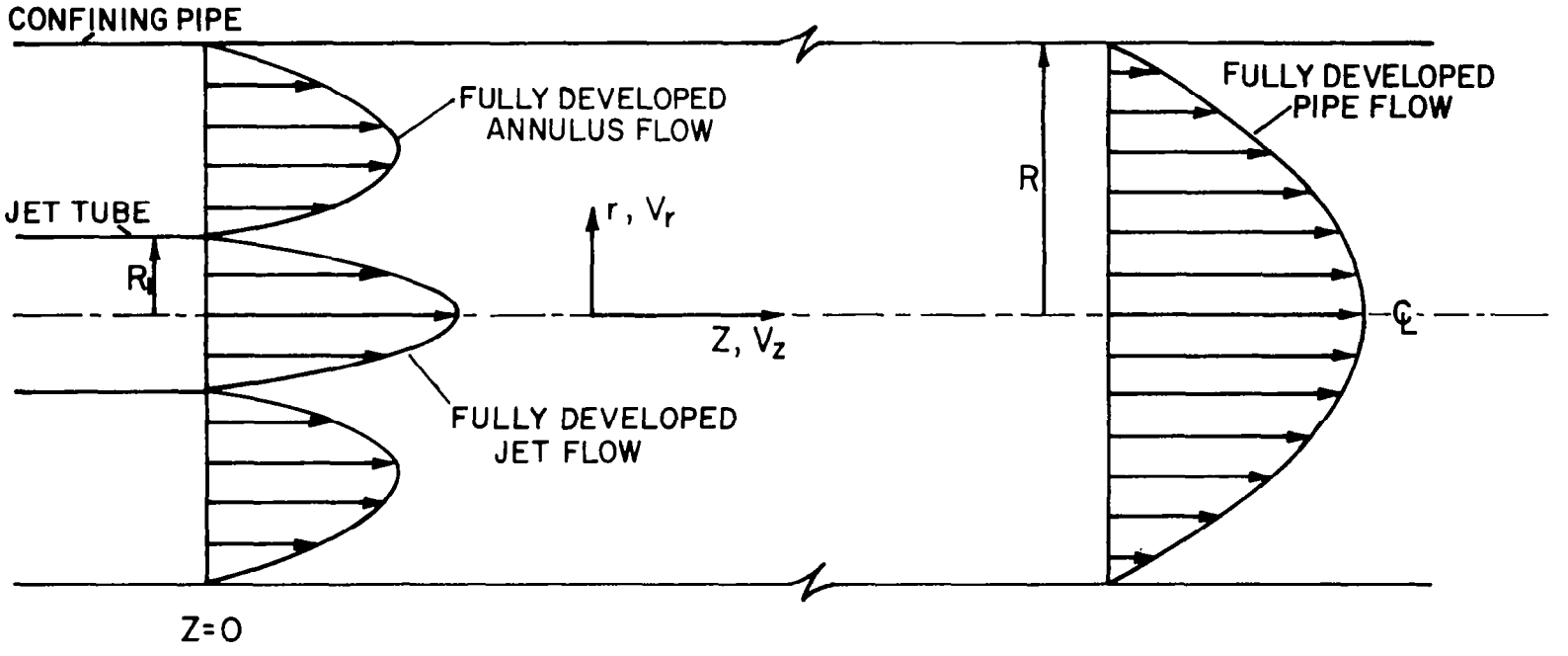

FIGURE 1. PROBLEM CONFIGURATION AND CO-ORDINATE SYSTEM

The object of the present work is to develop a method for solution of the laminar flow equations. Investigation of the order of magnitude of the terms has shown the boundary layer equations to be valid. Assumption 3 arises from the characteristics of a viscous fluid flowing along a solid, non-porous boundary. Assumptions 4, 5, 6 and 7 simplify the differential equations governing the flow and reduce the number of dependent variables to be evaluated. Since the numerical method of investigation is not basically affected by the initial and boundary conditions, the flow field may have any prescribed velocity profile at the entrance section.

Several of the above assumptions may be relaxed after this simplified problem has been solved. A more general solution may then be attempted at the expense of only increasing the number of variables to be evaluated, and hence the amount of computations. The present simplified form is of value in that it provides the basic approach to general problems of this class.

Part I
The Time-Dependent Problem

Governing Differential Equations, Initial Conditions and Boundary Conditions

Governing Differential Equations. The differential equations describing the time-dependent flow are obtained by considering conservation of mass and momentum in the flow field. These are the continuity and the Navier Stokes equations. Neglecting terms of the first order in $\frac{v_r}{v_z}$, these reduce to the boundary layer equations. Since these equations are well known, only their final form is given.

Conservation of momentum (in the axial direction) leads to the boundary

layer momentum equation.

$$\frac{\partial v_z}{\partial t} + v_r \frac{\partial v_z}{\partial r} + v_z \frac{\partial v_z}{\partial z} = - \frac{1}{\rho} \frac{\partial p}{\partial z} + \frac{\nu}{r^\gamma} \frac{\partial}{\partial r} \left[r^\gamma \frac{\partial v_z}{\partial r} \right] \qquad (1)$$

Conservation of mass leads to the continuity equation.

$$\frac{1}{r^\gamma} \frac{\partial}{\partial r} (r^\gamma v_r) + \frac{\partial v_z}{\partial z} = 0 \qquad (2)$$

where $\gamma = 0$ in the cartesian co-ordinate system

and $\gamma = 1$ in the cylindrical co-ordinate system.

The problem is formulated in cylindrical co-ordinates. Hence in cylindrical co-ordinates,

Momentum Equation

$$\frac{\partial v_z}{\partial t} + v_r \frac{\partial v_z}{\partial r} + v_z \frac{\partial v_z}{\partial z} = - \frac{1}{\rho} \frac{\partial p}{\partial z} + \nu \frac{\partial^2 v_z}{\partial z^2} + \frac{\nu}{r} \frac{\partial v_z}{\partial r} \qquad (3)$$

Continuity Equation

$$\frac{v_r}{r} + \frac{\partial v_r}{\partial r} + \frac{\partial v_z}{\partial z} = 0 \qquad (4)$$

In the above equations

$v_z = v_z (r, z, t)$ is the axial component of velocity,

$v_r = v_r (r, z, t)$ is the radial component of velocity,

$p = p (z, t)$ is the pressure.

A unique solution of Equations (3) and (4) requires specification of initial conditions and boundary conditions.

Initial Conditions.

At $t = 0$: for $0 \leq r \leq R$ and $z \geq 0$.

The velocities are given by their steady state values (i.e., for $t < 0$) together with the initial values (i.e., at $t = 0$) of the superimposed time-dependent

variations.

$$v_r(r, z, 0) = v_{r_s}(r, z) + \delta v_r(r, z, 0)$$
$$v_z(r, z, 0) = v_{z_s}(r, z) + \delta v_z(r, z, 0) \qquad (5)$$

Here, $v_{r_s}(r, z)$ and $v_{z_s}(r, z)$ are the steady state velocities determined by solving Equations (3) and (4) with $\frac{\partial v_z}{\partial t} = 0$.

δv_r and δv_z are the radial and the axial components respectively of the deviation in steady state velocities due to the superimposed time-dependent variation.

It is to be noted that the initial conditions (5) above are so defined that

$$v_z(r, z, 0) \neq v_{z_s}(r, z)$$
$$\text{and } v_r(r, z, 0) \neq v_{r_s}(r, z)$$

Boundary Conditions. The general boundary conditions of the problem for $t > 0$ are as follows:

1. At $r = 0$: for $z \geq 0$

   The condition of axial symmetry yields:

$$v_r(0, z, t) = 0$$
$$\left.\frac{\partial v_z}{\partial r}\right|_{(0, z, t)} = 0 \qquad (6)$$

2. At $r = R$: for $z \geq 0$

   The condition of no slip and no mass transfer through the stationary non-porous boundary leads to

$$v_r(R, z, t) = 0$$
$$v_z(R, z, t) = 0 \qquad (7)$$

3. At $z = 0$: for $0 \leq r \leq R$

$$v_r(r, 0, t) = v_{r_s}(r, 0) + \delta v_r(r, 0, t)$$
$$v_z(r, 0, t) = v_{z_s}(r, 0) + \delta v_z(r, 0, t) \qquad (8)$$

Equations (3) and (4) are valid in the entire flow field. However, their form becomes indeterminate at the centerline, i.e., at $r = 0$, and hence, requires some modification at this point.

Differential Equations At The Centerline. In the light of the boundary conditions (5) at $r = 0$, it is noted that the term $\frac{\nu}{r}\frac{\partial v_z}{\partial r}$ appearing in equation (3) and the term $\frac{v_r}{r}$ appearing in Equation (4) are of the indeterminate form $\frac{0}{0}$ at $r = 0$. It is necessary to replace these terms by their corresponding determinate forms thereby obtaining the modified forms of Equations (3) and (4) which are valid at the centerline. The indeterminacy is removed by using L'Hospital's rule for these terms. Thus,

$$\lim_{r\to 0}\left[\frac{1}{r}\frac{\partial v_z}{\partial r}\right] = \lim_{r\to 0}\frac{\frac{\partial v_z}{\partial r}}{r} = \lim_{r\to 0}\frac{\frac{\partial}{\partial r}\left[\frac{\partial v_z}{\partial r}\right]}{\frac{\partial}{\partial r}[r]} = \lim_{r\to 0}\frac{\frac{\partial^2 v_z}{\partial r^2}}{1}$$

Therefore,
$$\lim_{r\to 0}\left[\frac{1}{r}\frac{\partial v_z}{\partial r}\right] = \left.\frac{\partial^2 v_z}{\partial r^2}\right|_{r=0} \qquad (9)$$

Similarly,

$$\lim_{r\to 0}\left[\frac{v_r}{r}\right] = \lim_{r\to 0}\frac{\frac{\partial}{\partial r}[v_r]}{\frac{\partial}{\partial r}[r]} = \lim_{r\to 0}\left[\frac{\frac{\partial v_r}{\partial r}}{1}\right]$$

i.e.,
$$\lim_{r\to 0}\frac{v_r}{r} = \left.\frac{\partial v_r}{\partial r}\right|_{r=0} \qquad (10)$$

Hence, Equations (3) and (4) have the following form at the centerline r = 0

$$\frac{\partial v_z}{\partial t} + v_z \frac{\partial v_z}{\partial z} = -\frac{1}{\rho}\frac{\partial p}{\partial z} + 2\nu \frac{\partial^2 v_z}{\partial r^2} \tag{3a}$$

$$2\frac{\partial v_r}{\partial r} + \frac{\partial v_z}{\partial z} = 0 \tag{4a}$$

The flow problem thus reduces to an initial-boundary value problem described by the non-linear partial differential Equations (3) and (4), together with their modified form (3a) and (4a) at the centerline, subject to the initial conditions (5), and the boundary conditions (6), (7) and (8).

It is noted at this stage, that the problem involves three unknowns - $v_r(r, z, t)$, $v_z(r, z, t)$ and $p(z, t)$, but there are only two equations for their determination. Thus, apparently, an infinite number of solutions are possible. To obtain a unique solution, it is necessary to impose a valid and unique constraint on the problem.

Equation of Constraint

For a flow confined within non-porous, solid boundaries in the transverse direction, with no sources or sinks within the flow field, the mass rate of flow across a complete cross-section, is invariant with the axial location of the section.

Thus $$\int_0^R 2\pi r \, dr \, \rho \, v_z = \text{constant for all axial positions.} \tag{11}$$

Hence,

$$\frac{\partial}{\partial z}\left[\int_0^R 2\pi r \, \rho \, v_z \, dr\right] = 0 \tag{12}$$

The sequence of differentiation with respect to z and integration with

respect to r may be interchanged since the limits of integration are independent of z. Reversing the order of operations of differentiation and integration and dividing by the non-zero constant $2\pi\rho$, Equation (10) may be written as

$$\int_0^R r \frac{\partial \dot{v}_z}{\partial z} dr = 0 \qquad (13)$$

Equation (13) is the integral form of the continuity equation obtained by integrating the continuity equation (4) over an entire cross-section. (The derivation is contained in Appendix A.)

Equation (13) provides the additional necessary equation of constraint.

Thus the flow problem is governed by a system of three equations, (3), (4) and (13), (together with (3a) and (4a) for the centerline) in three unknowns v_r, v_z and p and subject to the necessary number of initial and boundary conditions (5), (6), (7), (8) so that a unique solution is now obtainable.

The steady state velocities $v_{r_s}(r, z)$ and $v_{z_s}(r, z)$ appearing in the initial conditions (5) and the boundary conditions (8) are obtained as the solution of the time-independent form of equations (3), (4), (3a) and (4a) with $\frac{\partial v_z}{\partial t} = 0$, and subject to appropriate boundary conditions.

Part II
The Time-Independent Problem

The general features and the co-ordinate system of the time-independent problem are the same as for the time-dependent problem. The governing differential equations are the steady, laminar boundary layer equations arrived at under a set of assumptions similar to those for the time-dependent case.

Governing Differential Equations and Boundary Conditions

The steady state problem is described mathematically by the following differential equations and boundary conditions:

Governing Differential Equations.

Momentum Equation in the axial direction

$$v_r \frac{\partial v_z}{\partial r} + v_z \frac{\partial v_z}{\partial z} = - \frac{1}{\rho} \frac{dp}{dz} + \nu \frac{\partial^2 v_z}{\partial r^2} + \frac{\nu}{r} \frac{\partial v_z}{\partial r} \tag{14}$$

Continuity Equation

$$\frac{v_r}{r} + \frac{\partial v_r}{\partial r} + \frac{\partial v_z}{\partial z} = 0 \tag{15}$$

where

$v_r = v_r (r, z)$ is the radial component of the steady state velocity,

$v_z = v_z (r, z)$ is the axial component of the steady state velocity,

and $p = p (z)$ is the steady state pressure.

The subscript 's' denoting steady state values of v_r, v_z and p in the time-independent problem has been omitted for brevity of notation.

Boundary Conditions

1. At r = 0: for $z \geq 0$

For an axially symmetric flow

$$v_r (0, z) = 0$$

$$\left. \frac{\partial v_z}{\partial r} \right|_{(0, z)} = 0 \tag{16}$$

2. At $r = R$: for $z \geq 0$

For no slip at a stationary solid boundary

$$v_z (R, z) = 0 \tag{17a}$$

and for no mass transfer through a non-porous boundary

$$v_r (R, z) = 0 \tag{17b}$$

3a. At $z = 0$: for $0 \leq r \leq R_1$

$$v_r (r, 0) = 0$$

$$v_z (r, 0) = 2U_1 \left\{1 - \left(\frac{r}{R_1}\right)^2\right\} \tag{18a}$$

where U_1 is the average axial velocity in the inner jet pipe.

3b. At $z = 0$: for $R_1 < r \leq R$

$$v_r (r, 0) = 0$$

$$v_z (r, 0) = 2U_2 \left\{1 - \left(\frac{r}{R}\right)^2 + \alpha \log_e \left(\frac{r}{R}\right)\right\} \frac{1}{\beta} \tag{18b}$$

where U_2 is the average axial velocity in the annular region surrounding the inner pipe,

$$\alpha = \frac{1 - \frac{R_1}{R}}{\log_e \frac{R}{R_1}}$$

and

$$\beta = 1 - \alpha + \left[\frac{R_1}{R}\right]^2$$

Equations (14) and (15) suffer the same limitation as Equations (3) and (4), i.e., they may be used throughout the flow region, except at the centerline where indeterminacy occurs in the terms involving $\frac{1}{r}$ as

seen from the boundary conditions (16) and (17b). It is therefore necessary to find versions of Equations (14) and (15) which apply for $r = 0$.

Differential Equations at the Centerline. The centerline differential equations are obtained by using L'Hospital's rule for the indeterminate terms $\frac{1}{r}\frac{\partial v_z}{\partial r}$ in Equation (14) and $\frac{v_r}{r}$ in Equation (15). In the limit as $r \to 0$, using L'Hospital's rule, these indeterminate terms may be replaced by their corresponding determinate forms derived in Equations (9) and (10). The differential equations (14) and (15) thus have the following form at $r = 0$

$$v_z \frac{\partial v_z}{\partial z} = -\frac{1}{\rho}\frac{dp}{dz} + 2\nu \frac{\partial^2 v_z}{\partial r^2} \tag{14a}$$

$$2\frac{\partial v_r}{\partial r} + \frac{\partial v_z}{\partial z} = 0 \tag{15a}$$

Thus, the steady state problem of mixing of coaxial confined jets has been represented as a boundary value problem described by the differential equations (14) and (15) (together with their modified forms (14a) and (15a) for the centerline), subject to the boundary conditions (16), (17a), (17b), (18a) and (18b).

As was the case for the time-dependent problem, it is found that the steady problem also involves determination of three unknowns v_r, v_z and p with only two equations available. The additional equation necessary for a unique solution is again obtained from a similar physical constraint.

Equation of Constraint

The total mass flow rate across any cross-section in the flow field

is independent of the axial position. The mathematical statement of this constraint is obtained by a similar procedure as for Equation (13) and is given by the integral form of the continuity equation

$$\int_0^R r \frac{\partial v_z}{\partial z} \, dr = 0 \qquad (19)$$

Equations (14), (15) and (19) (together with Equations (14a) and (15a) for the centerline), constitute a system of three equations in three unknowns which may then be uniquely determined.

The details of the procedure for obtaining the flow pattern are given in the next chapter. The time-independent problem is solved first. Its solution supplies the necessary initial and boundary conditions for the time-dependent problem which is to be solved subsequently.

CHAPTER III
SOLUTION BY FINITE DIFFERENCES

The non-linear partial differential equations describing the flow problem are solved numerically by the method of finite differences. A network of discrete points is superimposed on the r-z-t space-time system. The discrete configuration of the problem and the co-ordinate system are shown in Figure 2.

The differential equations, initial conditions and boundary conditions of the problem are replaced by their corresponding finite difference forms. Questions now arise regarding the finite difference forms and the numerical stability criterion to be used.

Derivatives in Finite Difference Form

Three basic forms are available for finite difference approximations to continuous derivatives, namely: forward, backward and central differences. Using the discrete subscript system shown in Figure 2, the difference approximations may be given as

Forward Difference

$$\left.\frac{\partial \phi}{\partial x}\right|_{m,n,k} = \frac{\phi_{m+1,n,k} - \phi_{m,n,k}}{\Delta x} \tag{20}$$

Backward Difference

$$\left.\frac{\partial \phi}{\partial x}\right|_{m,n,k} = \frac{\phi_{m,n,k} - \phi_{m-1,n,k}}{\Delta x} \tag{21}$$

Central Difference

$$\left.\frac{\partial \phi}{\partial x}\right|_{m,n,k} = \frac{\phi_{m+1,n,k} - \phi_{m-1,n,k}}{2\Delta x} \tag{22}$$

These are obtained by expressing ϕ in a Taylor's series and assuming

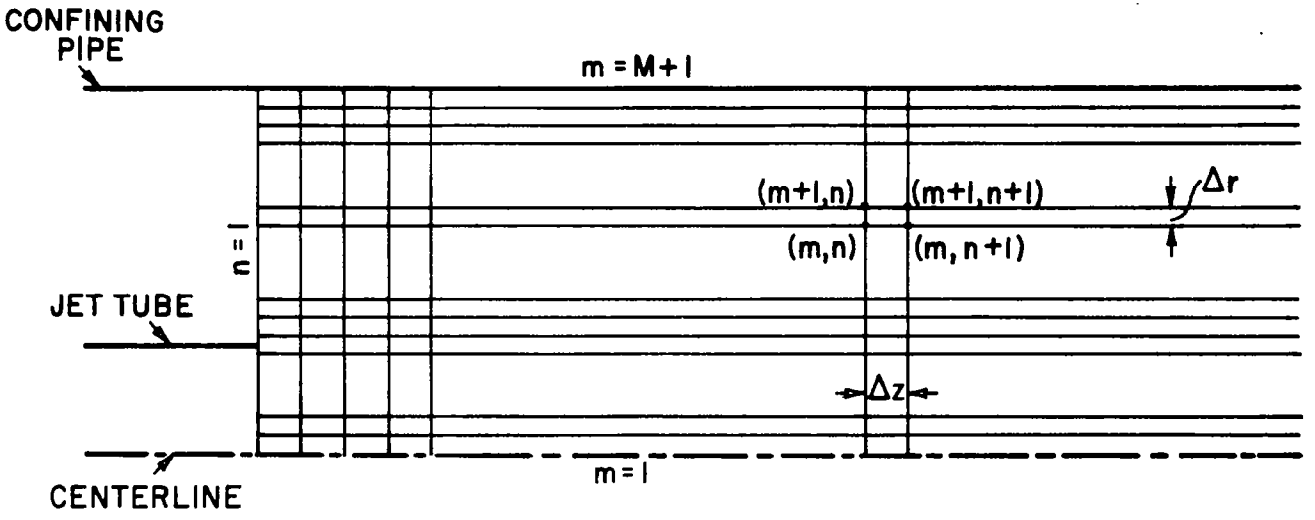

FIGURE 2. DISCRETIZED PROBLEM CONFIGURATION AND SUBSCRIPT SYSTEM

boundedness of the higher derivatives. The central difference approximation, Equation (22), involves the smallest amount of error. Hence, its use is desired so far as possible.

Criteria for Numerical Stability, Consistency and Convergence

In order that the obtained solution of the finite difference equations be meaningful, it is necessary to ensure consistency, stability and convergence of the numerical computation scheme used. Definition of these terms are included in Appendix B.

It is known from Lax's equivalence theorem [40] that, for a properly posed initial value problem, the necessary and sufficient conditions for consistency and stability are also the necessary and sufficient conditions for convergence. Hence, it is enough to ensure consistency and numerical stability of the difference equations. Convergence will then be implied.

Consistency is determined by simply examining the truncation error of the difference equations. This is carried out in Appendix C.

In the present work, stability is investigated using the criterion developed by Karplus [39] based on an electric circuit theory approach. This criterion, very simple and straightforward to apply, yields stability conditions identical to those obtained with the more familiar stability criteria of Hildebrand [43] and von Neuman [43]. The statement of Karplus' criterion and its chief merits are included in Appendix D.

A computational scheme is explicit, semi-explicit, or implicit, depending on the finite difference approximate forms used for the various terms in a partial differential equation. For explicit schemes, the permissible step sizes are usually limited by numerical stability requirements. Hence, carrying the solution up to reasonable values of

the independent variables requires large amount of computer time, particularly when more than one of the independent variables are unbounded.

Several implicit schemes have been developed which are stable regardless of the step sizes used. Since usually an iterative procedure is used, greater accuracy is achievable. However, they are generally more complex to program and call for greater computational effort than do explicit schemes. In implicit schemes, the number of points at which computations are needed is reduced, but the number of computations at each point increases. Hence, the total time required by the problem is still considerable. Further, although stability may not restrict the step sizes, other physical considerations (like accuracy and resolution desired) may often do so. Then, the computer time required by implicit schemes may make their use prohibitive [44].

In the present work, an all-explicit scheme is used. All three difference approximations and their various combinations are investigated for use in the governing differential equations. Finally, that combination is selected for use which permits an explicit scheme and satisfies the appropriate stability criteria.

Part I
The Time-Independent Problem

Finite Difference Equations and Stability Conditions

Momentum Equation. The following three schemes are investigated:

	Finite Difference Form For r-derivatives	z-derivatives
1.	Central	Central
2.	Central	Backward
3.	Central	Forward

It is assumed that the axial velocity is non-negative in the flow field considered.

Application of Karplus' stability criteria reveals that scheme 1 above is implicit and always unstable. The second scheme is semi-explicit and always unstable; the resulting finite difference equations are transcendental. Scheme 3 leads to linear explicit finite difference equations that are stable under certain realizable conditions. Therefore, scheme 3 is found appropriate for solving Equation (14).

Thus, using central differences for the r-derivatives

and forward differences for the z-derivatives,

Equation (14) is written at the point (m,n) in the following finite difference form

$$v_r(m,n)\left[\frac{v_z(m+1,n) - v_z(m-1,n)}{2\Delta r}\right] + v_z(m,n)\left[\frac{v_z(m,n+1) - v_z(m,n)}{\Delta z}\right]$$

$$= -\frac{1}{\rho}\left[\frac{dp}{dz}\right]_n + \nu\left[\frac{v_z(m+1,n) - 2\,v_z(m,n) + v_z(m-1,n)}{(\Delta r)^2}\right]$$

$$+ \frac{\nu}{r(m)}\left[\frac{v_z(m+1,n) - v_z(m-1,n)}{2\Delta r}\right] \qquad (23)$$

Solving explicitly for $v_z(m,n+1)$, Equation (23) yields

$$v_z(m,n+1) = v_z(m,n)$$

$$+ \frac{\Delta z}{v_z(m,n)}\left\{\begin{array}{l} -\frac{1}{\rho}\left[\frac{dp}{dz}\right]_n \\ + \nu\left[\frac{v_z(m+1,n) - 2\,v_z(m,n) + v_z(m-1,n)}{(\Delta r)^2}\right] \\ + \left[\frac{\nu}{r(m)} - v_r(m,n)\right]\left[\frac{v_z(m+1,n) - v_z(m-1,n)}{2\Delta r}\right] \end{array}\right\} \qquad (24)$$

The conditions for stability of Equation (24) are obtained by

employing Karplus' method. (Derivation of these stability conditions is contained in Appendix E.)

a) If $v_r(m,n) < 0$,

the scheme is stable if

$$\Delta z < \frac{v_z(m,n)}{2\nu} (\Delta r)^2 \tag{25}$$

where Δr is not limited from stability considerations, and is selected by considering the physical problem.

b) If $v_r(m,n) > 0$,

then the conditions of stability are

$$\Delta r < \frac{2\nu}{v_r(m,n)} \tag{26}$$

and

$$\Delta z < \frac{v_z(m,n)}{2\nu} (\Delta r)^2 \tag{27}$$

Momentum Equation at the Centerline. Equation (14) becomes indeterminate at the centerline, i.e., at m = 1, so does its corresponding finite difference form given by Equation (23). Therefore, it is necessary to replace Equation (14a) by a finite difference form which is valid at m = 1. Using central difference approximations for the r-derivatives and forward difference approximations for the z-derivatives, Equation (14a) may be written as

$$v_z(m,n)\left[\frac{v_z(m,n+1) - v_z(m,n)}{\Delta z}\right] = -\frac{1}{\rho}\left[\frac{dp}{dz}\right]_n + 2\nu\left[\frac{v_z(m+1,n) - 2\,v_z(m,n) + v_z(m-1,n)}{(\Delta r)^2}\right] \tag{28}$$

Here m = 1, so that the point corresponding to (m - 1) is not within the flow field considered. However, under the assumption of axial symmetry, the value of the axial velocity at (m-1,n) may be replaced by its value at (m+1,n).

Therefore, Equation (28) becomes

$$v_z(m,n)\left[\frac{v_z(m,n+1) - v_z(m,n)}{\Delta z}\right] = -\frac{1}{\rho}\left[\frac{dp}{dz}\right]_n + 4\nu\left[\frac{v_z(m+1,n) - v_z(m,n)}{(\Delta r)^2}\right] \tag{29}$$

where m = 1.

Solving explicitly for $v_z(m,n+1)$, Equation (29) yields

$$v_z(m,n+1) = v_z(m,n) + \frac{\Delta z}{v_z(m,n)}\left\{-\frac{1}{\rho}\left[\frac{dp}{dz}\right]_n + 4\nu\left[\frac{v_z(m+1,n) - v_z(m,n)}{(\Delta r)^2}\right]\right\} \tag{30}$$

where m = 1.

The stability conditions for this equation are derived in Appendix E.

Thus, Equation (30) is stable if, for m = 1,

$$\Delta z < \frac{v_z(m,n)}{4\nu}(\Delta r)^2 \tag{31}$$

where stability imposes no restriction on the size of Δr.

To ensure stability of the scheme throughout the flow field, conditions (26) and (27) together with (31) for m = 1 must be satisfied at each point of the region. Thus, if uniform step sizes are to be used, condition (26) must hold for the absolute maximum of all positive

$v_r(m,n)$ for all m,n (except m = 1), condition (27) for the absolute minimum $v_z(m,n)$ for all m,n (except m = 1) and (31) must be true for minimum $v_z(m,n)$ for m = 1 and for all n. If variable step sizes are to be used, then it is enough to satisfy these stability conditions only locally.

It is noted that for a given n, condition (31) is apparently more restrictive than condition (27). Recalling that m = 1 in (31) and that at given n, v_z is maximum at m = 1, the following inequality is claimed:

$$v_z(1,n) > 2\left[v_z(m,n)\right]_{min} \qquad (32)$$

Hence, at each n, it is enough to satisfy conditions (26) and (27), and then (31) will be automatically satisfied because of inequality (32).

Attention is here called to one other point. The pressure gradient term appearing in Equations (14) and (14a) does not enter the stability conditions. Is the stability of the momentum equation independent of this term or is it necessary to devise some means of taking this term into account? The question may be answered by recalling that the momentum equation is used to compute $v_z(m,n+1)$ by an explicit scheme. The values of all quantities, other than $v_z(m,n+1)$, appearing in this equation are available at this stage (either specified or computed prior to this stage). In particular, $\left[\frac{dp}{dz}\right]_n$ appearing in Equation (23) and (29) is a known quantity. A term that is specified or computed previously using a stable scheme cannot contribute to instability.

Continuity Equation. After the axial velocities $v_z(m,n+1)$ have been determined at a given (n+1) for all m using the momentum equation, the radial velocities $v_r(m,n+1)$ are computed with the help of the continuity equation (15). Since no axial derivative of radial velocities

appear, Equation (15) must be written at the section (n+1) in order to advance downstream the information on v_r. An explicit computation scheme can then permit only backward difference approximations for any other z-derivatives involved. The r-derivatives are approximated by central differences, thus retaining the scheme used for r-derivatives in the momentum equation. However, due to the axial symmetry of the problem, no information is obtainable at m=2 when the equation is written for m=1; the computations will yield v_r not for every m but for every other m only. Hence, some modification of the approximation scheme is necessary in order to determine v_r for all m. The other alternative would be to use some implicit computation scheme. The former approach is adopted in the following.

The continuity equation is written in its finite difference form, at the fictitious points (m-1/2, n+1), instead of at (m,n+1), using the following approximations:

1. $$\frac{v_r(m-1/2,n+1)}{r(m-1/2)} = \frac{\frac{v_r(m,n+1) + v_r(m-1,n+1)}{2}}{\frac{r(m) + r(m-1)}{2}} \qquad (33)$$

i.e.,

$$\frac{v_r(m-1/2,n+1)}{r(m-1/2)} = \frac{v_r(m,n+1) + v_r(m-1,n+1)}{r(m) + r(m-1)} \qquad (34)$$

2. $$\left.\frac{\partial v_r}{\partial r}\right|_{m-1/2,n+1} = \frac{v_r(m,n+1) - v_r(m-1,n+1)}{2\,\frac{\Delta r}{2}} \qquad (35)$$

i.e.,

$$\left.\frac{\partial v_r}{\partial r}\right|_{m-1/2,n+1} = \frac{v_r(m,n+1) - v_r(m-1,n+1)}{\Delta r} \qquad (36)$$

$$3.\quad \left.\frac{\partial v_z}{\partial z}\right|_{m-1/2,n+1} = \frac{\left.\frac{\partial v_z}{\partial z}\right|_{m,n+1} + \left.\frac{\partial v_z}{\partial z}\right|_{m-1,n+1}}{2} \tag{37}$$

Using backward difference approximations for the z-derivatives on the right-hand side, Equation (37) leads to:

$$\left.\frac{\partial v_z}{\partial z}\right|_{m-1/2,n+1}$$

$$= \frac{v_z(m,n+1) - v_z(m,n) + v_z(m-1,n+1) - v_z(m-1,n)}{2\Delta z} \tag{38}$$

Using the above approximations, the continuity equation (15) has the following finite difference form

$$\frac{v_r(m,n+1) + v_r(m-1,n+1)}{r(m) + r(m-1)} + \frac{v_r(m,n+1) - v_r(m-1,n+1)}{\Delta r}$$

$$+ \frac{v_z(m,n+1) - v_z(m,n) + v_z(m-1,n+1) - v_z(m-1,n)}{2\Delta z}$$

$$= 0 \tag{39}$$

Now,

$$r(m) = (m-1)\,\Delta r$$

$$r(m-1) = (m-2)\,\Delta r \tag{40}$$

Therefore, Equation (39) may be written as

$$\frac{v_r(m,n+1) + v_r(m-1,n+1)}{(2m-3)\,\Delta r} + \frac{v_r(m,n+1) - v_r(m-1,n+1)}{\Delta r}$$

$$+ \frac{v_z(m,n+1) - v_z(m,n) + v_z(m-1,n+1) - v_z(m-1,n)}{2\Delta z}$$

$$= 0 \tag{41}$$

On simplifying the first two terms, Equation (41) becomes

$$\left[\frac{m-1}{2m-3}\right]\frac{2}{\Delta r}v_r(m,n+1) - \left[\frac{m-2}{2m-3}\right]\frac{2}{\Delta r}v_r(m-1,n+1)$$

$$+ \frac{v_z(m,n+1 - v_z(m,n) + v_z(m-1,n+1) - v_z(m-1,n)}{2\Delta z}$$

$$= 0 \qquad (42)$$

or

$$v_r(m,n+1) = \left[\frac{m-2}{m-1}\right]v_r(m-1,n+1)$$

$$- \left[\frac{2m-3}{4(m-1)}\right]\frac{\Delta r}{\Delta z}\left\{\begin{array}{l} v_z(m,n+1) - v_z(m,n) \\ + v_z(m-1,n+1) - v_z(m-1,n)\end{array}\right\} \qquad (43)$$

It is shown in Appendix E that Equation (43) is unconditionally stable.

Continuity Equation at the Centerline. The radial velocity $v_r(m,n+1)$ at $m = 1$ is available from the boundary condition at the centerline. Hence, the continuity equation never need be written at $m = 1$, so that the singular nature of the term $\frac{v_r(m,n+1)}{r(m)}$ at $m = 1$ is never encountered.

Equation (15a), the continuity equation for $m = 1$, is, therefore, given no further consideration.

Boundary Conditions. The boundary conditions, given by Equations (16), (17a), (17b), (18a) and (18b), have the following finite difference representations.

1. At $m = 1$, for all $n > 0$:

$$v_r(1,n) = 0$$
$$v_z(2,n) = v_z(0,n) \tag{44}$$

2. At $m = M+1$, for all $n > 0$

$$v_r(M+1,n) = 0$$
$$v_z(M+1,n) = 0 \tag{45}$$

3a. At $n = 1$, for $1 \leq m < \frac{R_1}{\Delta r}$

$$v_r(m,1) = 0$$
$$v_z(m,1) = 2U_1\left[1 - \left[\frac{r(m)}{R_1}\right]^2\right] \tag{46}$$

3b. At $n = 1$, for $\frac{R_1}{\Delta r} < m \leq M+1$

$$v_r(m,1) = 0$$
$$v_z(m,1) = 2U_2\left\{\begin{array}{l} 1 - \left[\frac{r(m)}{R}\right]^2 \\ \\ + \alpha \log_e\left[\frac{r(m)}{R}\right] \end{array}\right\}^{\frac{1}{\beta}} \tag{47}$$

Here, U_1, U_2, α, and β are as defined earlier in (18a) and (18b).

Thus, for each n, Equations (24) and (43) for m=2,3,...,M, and Equation (30) for m = 1, together with the above boundary conditions, comprise a system of (2M+2) linear explicit equations in the (2M+3) unknowns $v_r(1,n)$, $v_r(2,n)$, ..., $v_r(M,n)$, $v_r(M+1,n)$;
$v_z(1,n)$, $v_z(2,n)$, ..., $v_z(M,n)$, $v_z(M+1,n)$; and $\left[\frac{dp}{dz}\right]_n$.

Numerical stability of the system is ensured by satisfying conditions (26) and (27) for m=2,3,...,M-1,M and for all n.

Equation (19) provides the additional equation necessary for a unique solution of the system.

Equation of Constraint. The equation of constraint is recalled here for ready reference.

For any fixed z

$$\int_0^R r \frac{\partial v_z}{\partial r} dr = 0 \qquad (19)$$

To represent this in finite difference form, the total interval of integration $0 \leq r \leq R$ is divided into M equal sub-intervals. The width Δr of each of these sub-intervals is small enough so that the factor $\frac{\partial v_z}{\partial z}$ in the integrand of (19) may be considered to be a constant over each sub-interval. This constant may be taken as the value of $\frac{\partial v_z}{\partial z}$ at the midpoint of the respective sub-interval.

Equation (23) may be written as:

For any fixed n

$$\left[\int_0^{\Delta r} r\, dr\right] \left.\frac{\partial v_z}{\partial z}\right|_{\frac{\Delta r}{2}} + \left[\int_{\Delta r}^{2\Delta r} r\, dr\right] \left.\frac{\partial v_z}{\partial z}\right|_{\frac{3\Delta r}{2}} + \cdots$$

$$+ \left[\int_{(M-2)\Delta r}^{(M-1)\Delta r} r\, dr\right] \left.\frac{\partial v_z}{\partial z}\right|_{(2M-3)\frac{\Delta r}{2}} + \left[\int_{(M-1)\Delta r}^{M\Delta r} r\, dr\right] \left.\frac{\partial v_z}{\partial z}\right|_{(2M-1)\frac{\Delta r}{2}}$$

$$= 0 \qquad (48)$$

The value of $\frac{\partial v_z}{\partial z}$ at the midpoint of a sub-interval may be obtained as the arithmetic mean of the values at the endpoints of that sub-interval.

Hence, after performing the indicated integrations, Equation (48) becomes

$$\frac{(\Delta r)^2}{2}\left[\frac{1}{2}\left.\frac{\partial v_z}{\partial z}\right|_{r=0} + \frac{1}{2}\left.\frac{\partial v_z}{\partial z}\right|_{\Delta r}\right]$$

$$+ \frac{3}{2}(\Delta r)^2\left[\frac{1}{2}\left.\frac{\partial v_z}{\partial z}\right|_{\Delta r} + \frac{1}{2}\left.\frac{\partial v_z}{\partial z}\right|_{2\Delta r}\right] + \cdots$$

$$+ \frac{[(M-1)^2 - (M-2)^2]}{2}(\Delta r)^2\left[\frac{1}{2}\left.\frac{\partial v_z}{\partial z}\right|_{(M-2)\Delta r} + \frac{1}{2}\left.\frac{\partial v_z}{\partial z}\right|_{(M-1)\Delta r}\right]$$

$$+ \frac{[M^2 - (M-1)^2]}{2}(\Delta r)^2\left[\frac{1}{2}\left.\frac{\partial v_z}{\partial z}\right|_{(M-1)\Delta r} + \frac{1}{2}\left.\frac{\partial v_z}{\partial z}\right|_{M\Delta r}\right]$$

$$= 0 \qquad (49)$$

Now, from the wall boundary condition (45)

$$v_z(M+1,n) = 0 \quad \text{for all } n \geq 0$$

the following condition is obtained:

$$\left.\frac{\partial v_z}{\partial z}\right|_{M\Delta r} = \left.\frac{\partial v_z}{\partial z}\right|_{(M+1,n)} = 0 \quad \text{for all } n \geq 0 \qquad (50)$$

Using (50) in Equation (49), dividing through by the non-zero constant factor $(\Delta r)^2$, Equation (49) becomes, after simplication

$$\frac{1}{4}\left.\frac{\partial v_z}{\partial z}\right|_{(1,n)} + 1\left.\frac{\partial v_z}{\partial z}\right|_{(2,n)} + 2\left.\frac{\partial v_z}{\partial z}\right|_{(3,n)} + \cdots + (M-1)\left.\frac{\partial v_z}{\partial z}\right|_{(M,n)}$$

$$= 0 \qquad (51)$$

i.e.,

$$\frac{1}{4}\left.\frac{\partial v_z}{\partial z}\right|_{(1,n)} + \sum_{m=2}^{M} (m-1)\left.\frac{\partial v_z}{\partial z}\right|_{(m,n)} = 0 \qquad (52)$$

This is the finite difference form of Equation (19).

Substituting for $\left.\frac{\partial v_z}{\partial z}\right|_{(m,n)}$ from the appropriate momentum equation yields

$$\frac{1}{4}\frac{1}{v_z(1,n)}\left\{-\frac{1}{\rho}\left[\frac{dp}{dz}\right]_n + 4\nu\left[\frac{v_z(2,n) - v_z(1,n)}{(\Delta r)^2}\right]\right\}$$

$$+\sum_{m=2}^{M}\frac{(m-1)}{v_z(m,n)}\left\{\begin{array}{l} -\frac{1}{\rho}\left[\frac{dp}{dz}\right]_n - \nu\left[\frac{v_z(m+1,n) - 2v_z(m,n) + v_z(m-1,n)}{(\Delta r)^2}\right] \\ \\ +\left[\frac{\nu}{r(m)} - v_r(m,n)\right]\left[\frac{v_z(m+1,n) - v_z(m-1,n)}{2\Delta r}\right] \end{array}\right\}$$

$$= 0 \qquad (53)$$

The term $\left[\frac{dp}{dz}\right]_n$ is the only unknown appearing in the above equation and may, therefore, be evaluated as follows:

$$\left\{\frac{1}{4}\frac{1}{v_z(1,n)} + \sum_{m=2}^{M}\frac{(m-1)}{v_z(m,n)}\right\}\left\{+\frac{1}{\rho}\left[\frac{dp}{dz}\right]_n\right\}$$

$$= \frac{1}{4}\frac{1}{v_z(1,n)}\left\{4\nu\left[\frac{v_z(2,n) - v_z(1,n)}{(\Delta r)^2}\right]\right\}$$

$$+\sum_{m=2}^{M}\frac{(m-1)}{v_z(m,n)}\left\{\begin{array}{l} \nu\left[\frac{v_z(m+1,n) - 2v_z(m,n) + v_z(m-1,n)}{(\Delta r)^2}\right] \\ \\ +\left[\frac{\nu}{r(m)} - v_r(m,n)\right]\left[\frac{v_z(m+1,n) - v_z(m-1,n)}{2\Delta r}\right] \end{array}\right\} \qquad (54)$$

from which $\left[\frac{dp}{dz}\right]_n$ can be explicitly solved for.

As we noted earlier, the equation of constraint is the integral form of the continuity equation obtainable by integrating the continuity

equation (15) over a cross-section. Since integration and summation are corresponding processes in the continuous and the discrete form, Equation (52) must be obtainable by summation of Equation (43) for all values of m appearing in the problem. Verification of this statement is given in Appendix F.

Part II
The Time-Dependent Problem

Finite Difference Equations and Stability Conditions

Momentum Equation. The time-dependent momentum equation is parabolic in the t co-ordinate, as well as in the z co-ordinate. Central difference approximations for the t derivatives, and/or for the z derivatives in Equation (3) will, therefore, result in an implicit scheme that is always unstable.

With the aim of setting up an explicit scheme of computation, the following three schemes are investigated:

	Finite Difference Form For		
	r-derivatives	z-derivatives	t-derivatives
1.	Central	Forward	Forward
2.	Central	Backward	Forward
3.	Central	Forward	Backward

Scheme 1 above does not yield an explicit solution for the flow variables for the complete domain of investigation. For, each step advanced in the t direction (or z direction) reduces the possible number of steps in the z direction (or t direction) by one, if explicit methods are used. An admissible solution, using an implicit scheme,

requires prior knowledge of the downstream boundary conditions, or of the terminal time conditions. In general, these may not be prescribed.

In scheme 2, the equation of constraint is satisfied as an identity. No information is obtainable for $\frac{\partial p}{\partial z}$. A different constraint will then be necessary for a unique solution.

However, scheme 3 presents no such difficulties. Therefore, Equation (3) is written at the point (m,n,k+1) using

central difference approximations for the r-derivatives,

forward difference approximations for the z-derivatives,

and backward difference approximations for the t-derivatives,

resulting in the finite difference equation

$$\frac{v_z(m,n,k+1) - v_z(m,n,k)}{\Delta t}$$

$$+ v_r(m,n,k+1)\left[\frac{v_z(m+1,n,k+1) - v_z(m-1,n,k+1)}{2\Delta r}\right]$$

$$+ v_z(m,n,k+1)\left[\frac{v_z(m,n+1,k+1) - v_z(m,n,k+1)}{\Delta z}\right]$$

$$= -\frac{1}{\rho}\left[\frac{dp}{dz}\right]_{(n,k+1)}$$

$$+ \nu\left[\frac{v_z(m+1,n,k+1) - 2v_z(m,n,k+1) + v_z(m-1,n,k+1)}{(\Delta r)^2}\right]$$

$$+ \frac{\nu}{r(m)}\left[\frac{v_z(m+1,n,k+1) - v_z(m-1,n,k+1)}{2\Delta r}\right] \qquad (55)$$

Then, $v_z(m,n+1,k+1)$ is given explicitly by the following expression

$$v_z(m,n+1,k+1) = v_z(m,n,k+1) +$$

$$\frac{\Delta z}{v_z(m,n,k+1)} \left\{ \begin{array}{l} - \frac{1}{\rho} \left[\frac{\partial p}{\partial z}\right]_{(n,k+1)} \\ + \nu \left[\frac{v_z(m+1,n,k+1) - 2v_z(m,n,k+1) + v_z(m-1,n,k+1)}{(\Delta r)^2}\right] \\ + \frac{\nu}{r(m)} \left[\frac{v_z(m+1,n,k+1) - v_z(m-1,n,k+1)}{2\Delta r}\right] \\ - v_r(m,n,k+1) \left[\frac{v_z(m+1,n,k+1) - v_z(m-1,n,k+1)}{2\Delta r}\right] \end{array} \right\} \qquad (56)$$

The stability conditions for Equation (56) are derived in Appendix E. It is shown that

a) For $v_r(m,n,k+1) < 0$,

Equation (56) is stable if

$$\Delta z < \frac{v_z(m,n,k+1)}{\frac{2}{(\Delta r)^2} + \frac{1}{\Delta t}} \qquad (57)$$

where Δr and Δt are ascertained from physical considerations of the problem. Stability imposes no limitation on their magnitude.

b) For $v_r(m,n,k+1) > 0$,

the conditions of stability are.

$$\Delta r < \frac{2\nu}{v_r(m,n,k+1)} \qquad (58)$$

and

$$\Delta z < \frac{v_z(m,n,k+1)}{\frac{2\nu}{(\Delta r)^2} + \frac{1}{\Delta t}} \tag{59}$$

where Δt is still free from stability restrictions.

When the above conditions are satisfied, Equation (56) represents a stable explicit expression for computation of $v_z(m,n+1,k+1)$ for $m=2,3,\ldots,M-1,M$. This equation, however, is indeterminate at $m = 1$. The finite difference form of Equation (3a) for the centerline, is, therefore, now derived.

Momentum Equation at the Centerline. The differencing scheme used is the same as for Equation (3). The following finite difference form is obtained when Equation (3a) is written at (m,n,k+1)

$$\frac{v_z(m,n,k+1) - v_z(m,n,k)}{\Delta t} + v_z(m,n,k+1)\left[\frac{v_z(m,n+1,k+1) - v_z(m,n,k+1)}{\Delta z}\right]$$

$$= -\frac{1}{\rho}\left[\frac{\partial p}{\partial z}\right]_{(n,k+1)}$$

$$+ 2\nu\left[\frac{v_z(m+1,n,k+1) - 2v_z(m,n,k+1) + v_z(m-1,n,k+1)}{(\Delta r)^2}\right] \tag{60}$$

where $m = 1$.

It is noted that the point (m-1,n,k+1) lies outside the region of computation. Under the assumption of axial symmetry, therefore, for $m = 1$

$$v_z(m+1,n,k+1) = v_z(m-1,n,k+1) \tag{61}$$

Therefore, Equation (60) becomes

$$\frac{v_z(m,n,k+1) - v_z(m,n,k)}{\Delta t} + v_z(m,n,k+1)\left[\frac{v_z(m,n+1,k+1) - v_z(m,n,k+1)}{\Delta z}\right]$$

$$= -\frac{1}{\rho}\left[\frac{\partial p}{\partial z}\right]_{(n,k+1)}$$

$$+ 4\nu\left[\frac{v_z(m+1,n,k+1) - v_z(m,n,k+1)}{(\Delta r)^2}\right] \qquad (62)$$

Solving explicitly for $v_z(m,n+1,k+1)$, this gives

$$v_z(m,n+1,k+1) = v_z(m,n,k+1)$$

$$+ \frac{\Delta z}{v_z(m,n,k+1)}\left\{\begin{array}{l} -\frac{1}{\rho}\left[\frac{\partial p}{\partial z}\right]_{(n,k+1)} \\ \\ \frac{4\nu}{\Delta r^2}\left[v_z(m+1,n,k+1) - v_z(m,n,k+1)\right] \\ \\ -\frac{v_z(m,n,k+1) - v_z(m,n,k)}{\Delta t} \end{array}\right\} \qquad (63)$$

where $m = 1$.

It is shown in Appendix E that Equation (63) is stable if

$$\Delta z < \frac{v_z(m,n,k+1)}{\frac{4\nu}{(\Delta r)^2} + \frac{1}{\Delta t}} \qquad (64)$$

where Δr and Δt are not limited by stability considerations.

Again, to ensure stability throughout the entire region of computation, it is necessary to satisfy condition (64) for $m = 1$ and condition (59) for $m=2,3,\ldots,M$, togehter with condition (58) for $m=2,3,\ldots,M$. If

variable step sizes are not desired, the values of Δr, Δz and Δt must be determined from the condition for m corresponding to the worst case. Therefore, condition (58) must be satisfied for the absolute maximum of $v_r(m,n,k+1)$, and conditions (59) and (64) for the absolute minimum of $v_z(m,n,k+1)$. As for the time-independent problem, condition (59) is claimed to be more restrictive than condition (64). Therefore, conditions (58) and (59) are the stability conditions for the time-dependent momentum equation.

Also, the stability conditions are independent of the pressure gradient $\left(\frac{\partial p}{\partial z}\right)_{(n,k+1)}$.

Continuity Equation. The continuity equation contains no terms involving a time derivative. Therefore, to advance information forward in time and in the downstream direction, Equation (4) must be written at $(m-1/2,n+1,k+1)$. Central differences are used to replace r-derivatives and backward differences to replace z-derivatives; no time differences appear. The following approximations, similar to those for the corresponding terms in time-independent equation (15) are used:

$$1. \quad \frac{v_r(m-1/2,n+1,k+1)}{r(m-1/2)} = \frac{v_r(m,n+1,k+1) + v_r(m-1,n+1,k+1)}{r(m) + r(m-1)} \tag{65}$$

Using the relation (40), this becomes

$$\frac{v_r(m-1/2,n+1,k+1)}{r(m-1/2)} = \frac{v_r(m,n+1,k+1) + v_r(m-1,n+1,k+1)}{(2m-3)\ r} \tag{66}$$

$$2. \quad \left.\frac{\partial v_r}{\partial r}\right|_{(m-1/2,n+1,k+1)} = \frac{v_r(m,n+1,k+1) - v_r(m-1,n+1,k+1)}{\Delta r} \tag{67}$$

$$3.\quad \left.\frac{\partial v_z}{\partial z}\right|_{(m-1/2,n+1,k+1)} = \frac{1}{2}\left[\frac{v_z(m,n+1,k+1) - v_z(m,n,k+1)}{\Delta z}\right] + \frac{1}{2}\left[\frac{v_z(m-1,n+1,k+1) - v_z(m-1,n,k+1)}{\Delta z}\right] \tag{68}$$

Then, Equation (4) has the following finite difference form at the point (m-1/2,n+1,k+1)

$$\frac{v_r(m,n+1,k+1) + v_r(m-1,n+1,k+1)}{(2m-3)\Delta r} + \frac{v_r(m,n+1,k+1) - v_r(m-1,n+1,k+1)}{\Delta r} + \frac{v_z(m,n+1,k+1) - v_z(m,n,k+1) + v_z(m-1,n+1,k+1) - v_z(m-1,n,k+1)}{2\Delta z} = 0 \tag{69}$$

Using expression (40) and simplifying, Equation (69) yields an explicit expression for $v_r(m,n+1,k+1)$ as follows

$$v_r(m,n+1,k+1) = \left[\frac{m-2}{m-1}\right] v_r(m-1,n+1,k+1) - \frac{(2m-3)\Delta r}{4(m-1)\Delta z}\left\{\begin{array}{l} v_z(m,n+1,k+1) - v_z(m,n,k+1) \\ + v_z(m-1,n+1,k+1) - v_z(m-1,n,k+1)\end{array}\right\} \tag{70}$$

The above equation is valid for m=2,3,...,M-1,M.

The continuity equation for the time-dependent problem is of the same form as for the time-independent problem. Stability considerations for Equation (70) are the same as for Equation (43). Therefore Equation (70) is also unconditionally stable.

Continuity Equation at the Centerline. Since $v_r(m,n+1,k+1)$ at m=1 is known from the centerline boundary condition (6), the continuity equation is not used at m=1. Hence, Equation (4a) is given no further consideration.

Initial Conditions

At k = 1, for $1 \leq m \leq M+1$ and $n \geq 1$:

$$v_r(m,n,1) = v_{r_s}(m,n) + \delta v_r(m,n,1)$$
$$\text{and } v_z(m,n,1) = v_{z_s}(m,n) + \delta v_z(m,n,1) \tag{71}$$

where v_{r_s} and v_{z_s} are obtained from the solution of the time-independent problem.

Boundary Conditions

1. At m = 1, for $n \geq 1$ and $k > 1$:

$$v_r(1,n,k) = 0$$
$$\text{and } v_z(2,n,k) = v_z(0,n,k) \tag{72}$$

2. At m = M+1, for $n \geq 1$ and $k > 1$:

$$v_r(M+1,n,k) = 0$$
$$\text{and } v_z(M+1,n,k) = 0 \tag{73}$$

3. At n = 1, for $1 \leq m \leq M+1$, and $k > 1$:

$$v_r(m,1,k) = v_{r_s}(m,1) + \delta v_r(m,1,k)$$
$$\text{and } v_z(m,1,k) = v_{z_s}(m,1) + \delta v_z(m,1,k) \tag{74}$$

Equation of Constraint. Following a procedure similar to that for Equation (19), the finite difference form of Equation (13) is obtained as the following

$$\frac{1}{4}\left[\frac{v_z(1,n+1,k+1) - v_z(1,n,k+1)}{\Delta z}\right]$$

$$+ \sum_{m=2}^{M} (m-1)\left[\frac{v_z(m,n+1,k+1) - v_z(m,n,k+1)}{\Delta z}\right] = 0 \qquad (75)$$

Substituting for the bracketed quantities from the appropriate momentum equations, i.e., Equation (62) for m=1 and Equation (55) for m=2,3,...,M-1,M, Equation (75) becomes

$$\frac{1}{4}\frac{1}{v_z(1,n,k+1)}\left\{\begin{array}{l} -\frac{1}{\rho}\left[\frac{\partial p}{\partial z}\right]_{(n,k+1)} \\ +4\nu\left[\frac{v_z(2,n,k+1) - v_z(1,n,k+1)}{(\Delta r)^2}\right] \\ -\frac{v_z(1,n,k+1) - v_z(1,n,k)}{\Delta t} \end{array}\right\}$$

$$+ \sum_{m=2}^{M} \frac{(m-1)}{v_z(m,n,k+1)}\left\{\begin{array}{l} -\frac{1}{\rho}\left[\frac{\partial p}{\partial z}\right]_{(n,k+1)} \\ +\nu\left[\frac{v_z(m+1,n,k+1) - 2v_z(m,n,k+1) + v_z(m-1,n,k+1)}{(\Delta r)^2}\right] \\ +\left[\frac{\nu}{r(m)} - v_r(m,n,k+1)\right]\left[\frac{v_z(m+1,n,k+1) - v_z(m-1,n,k+1)}{2\Delta r}\right] \\ -\frac{v_z(m,n,k+1) - v_z(m,n,k)}{\Delta t} \end{array}\right\}$$

$$= 0 \qquad (76)$$

All other quantities being known, $\left[\frac{\partial p}{\partial z}\right]_{(n,k+1)}$ may be explicitly evaluated using the above equation. Thus

$$\left[\frac{1}{4}\frac{1}{v_z(1,n,k+1)} + \sum_{m=2}^{M}\frac{(m-1)}{v_z(m,n,k+1)}\right]\frac{1}{\rho}\left[\frac{\partial p}{\partial z}\right]_{(n,k+1)}$$

$$= \frac{1}{4}\frac{1}{v_z(1,n,k+1)}\left\{\begin{array}{l} 4\nu\left[\dfrac{v_z(2,n,k+1) - v_z(1,n,k+1)}{(\Delta r)^2}\right] \\ \\ - \dfrac{v_z(1,n,k+1) - v_z(1,n,k+1)}{\Delta t}\end{array}\right\}$$

$$+ \sum_{m=2}^{M}\frac{(m-1)}{v_z(m,n,k+1)}\left\{\begin{array}{l} \nu\left[\dfrac{v_z(m+1,n,k+1) - 2v_z(m,n,k+1) + v_z(m-1,n,k+1)}{(\Delta r)^2}\right] \\ \\ + \dfrac{\nu}{r(m)}\left[\dfrac{v_z(m+1,n,k+1) - v_z(m-1,n,k+1)}{2\Delta r}\right] \\ \\ - v_r(m,n,k+1)\left[\dfrac{v_z(m+1,n,k+1) - v_z(m-1,n,k+1)}{2\Delta r}\right] \\ \\ - \dfrac{v_z(m,n,k+1) - v_z(m,n,k)}{\Delta t}\end{array}\right\} \qquad (77)$$

Thus the problem is represented in finite difference form by Equation (63) for m=1, Equations (56), (70) and (77) for m=2,3,...,M-1, M, together with the initial conditions (71) and the boundary conditions (72), (73) and (74).

Sequence of Computations

Solution of the time-dependent problem requires the results of the time-independent problem, in order to obtain the initial and boundary

conditions. The procedure for solution of both problems is outlined by the following sequence of operations.

The Time-Independent Problem.

1. For a set of parameters R_1, R, U_1 and U_2, suitable values of Δr and Δz are determined such that the stability conditions (26) and (27) are satisfied.*

2. For n = 1, $v_z(m,n)$ and $v_r(m,n)$ are determined from the boundary conditions (46) and (47) for all m=1,2,...,M,M+1.

3. $\left[\frac{dp}{dz}\right]_n$ is computed using Equation (54).

4. $v_z(m,n+1)$ is computed using Equation (30) for m=1, Equation (24) for m=2,3,...,M-1,M and the boundary condition (45) for m=M+1.

5. $v_r(m,n+1)$ is computed using the boundary condition (44) for m=1, Equation (54) for m=2,3,...,M-1,M and the boundary condition (45) for m=M+1.

6. If uniform mesh sizes are not necessary to maintain, Δr and Δz are redetermined from the stability conditions (26) and (27) using the most recent values of v_z and v_r computed in steps 4 and 5 above.

7. The value of n is incremented by unity and steps 3 through 6 are repeated until the flow field is computed for the desired value of $z = n.\Delta z$.

The Time-Dependent Problem.

1. From the parameters A and f, the value of Δt is determined based on the desired resolution of the problem.

---

* The stability limit on Δz is more restrictive for the time-dependent problem than for the time-independent problem. Hence, the value of Δz used in obtaining the initial conditions is the same as that to be used later in the time-dependent problem.

2. Suitable values of Δr and Δz are determined such that the stability conditions (58) and (59) are satisfied.

3. For k=1, $v_z(m,n,k)$ and $v_r(m,n,k)$ are determined from the boundary condition (74) for n=1 and from the initial condition (71) for all n > 1.

4. For n=1, $v_z(m,n,k+1)$ and $v_r(m,n,k+1)$ are determined from the boundary conditions (74).

5. $\left[\frac{\partial p}{\partial z}\right]_{(n,k+1)}$ is computed using Equation (77).

6. $v_z(m,n+1,k+1)$ is computed using Equation (63) for m=1, Equation (56) for m=2,3,...,M-1,M, and the boundary condition (73) for m=M+1.

7. $v_r(m,n+1,k+1)$ is computed using the boundary condition (72) for m=1, Equation (70) for m=2,3,...,M-1,M, and the boundary condition (73) for m=M+1.

8. If uniform mesh sizes are not necessary, Δr and Δz are re-determined from the stability conditions using the most recent values of v_z and v_r computed in steps 6 and 7 above.

9. The value of n is incremented by unity and steps 5 through 8 are repeated until the desired axial distance has been covered.

10. The value of k is incremented by unity and steps 4 through 9 are repeated until the flow has been computed for the desired value of $t = k.\Delta t$.

CHAPTER IV
RESULTS AND DISCUSSIONS

On The Validity of Results

The significance of a mathematical solution of any physical problem lies in the validity of the results obtained. Their acceptance requires ensuring certain facts, the most important among which are briefly discussed here.

First of all, the mathematical model considered must be as correct a representation of the physical problem as possible. The other requirements for validity having been satisfied, the accuracy of the results will then depend on how exactly this model describes the actual physical situation. Secondly, if the solution is accomplished by numerical techniques, it becomes further complicated by problems of consistency, stability and convergence. Finite difference methods determine the problem variables at discrete points instead of in a continuous space. For the solution of the "discretized" problem to converge to that of the "continuous" problem, the finite difference formulation must be consistent with the mathematical problem it approximates. Also, the computation scheme must be numerically stable. When these requirements are fulfilled, the results of the numerical solution may be considered valid, although any confidence in them would still require further experimental justification. This may be achieved by checking against other available results obtained either analytically or experimentally.

The validity of the results obtained by the method developed in the present work is now demonstrated.

The mathematical model of the flow problem considered is obtained

under certain assumptions which are justified in Chapter II. The partial differential equations describing this model are approximated by finite difference equations which are verified in Appendix C to satisfy the consistency requirements. The numerical stability of the computation scheme is confirmed by satisfying Karplus' stability conditions for the difference equations (Appendix E) in the entire region of interest. Convergence of the obtained solution to the true solution is then assured under the hypothesis of Lax's equivalence theorem for initial-boundary value problems.

In particular, the method of solution herein developed is used to investigate the time response of the laminar mixing and developing region of a confined jet to velocity fluctuations superimposed on the entrance conditions. To the author's best knowledge, this specific application has not been, as yet, dealt with by others, either analytically or experimentally, so that evaluation of the results by direct comparison is not possible. An indirect approach is therefore, adopted to assess reliance on the results.

Several analytical solutions, both exact as well as approximate, as also experimental results are available for the time-dependent boundary layer equations as applied to specific flows with rectangular or curvilinear geometry. Numerical solutions are also available for the impulsively started wedge flow and oscillations in Blasius flow [38]. However, for laminar, incompressible flows with cylindrical geometry, solutions are available only for cases where the dimension in the direction of the main flow is assumed to extend to infinity. Under this assumption, the flow is taken to be independent of this dimension so that the problem involves variations only in the transverse direction

and in time.

The non-steady Navier Stokes equations have been solved (analytically and numerically) by several investigators for various flow problems. Direct comparison of results of the present investigation with these solutions can yield any meaningful conclusions only if the obtained solutions of the boundary layer equations themselves can be shown to be reliable. The comparison would then demonstrate the variation between the results obtained for a given flow problem modeled mathematically under some differing but permissible assumptions. Comparison with experimental results would be necessary to evaluate the results obtained by the present method.

Steady, laminar, incompressible boundary layer flows have been investigated (analytically, numerically as well as experimentally) for various geometrical configurations and boundary conditions. The results of these studies may be directly compared with the results of the time-independent problem in this investigation. This provides a firm basis for evaluation of the initial conditions of the specific flow configuration being presently considered. In particular, velocity profiles are obtained for the development region of a porous pipe with constant velocity through the wall. The results are compared with those obtained by Hornbeck [1] using a numerical scheme that was implicit for the radial direction, but explicit for the axial direction. Such a scheme is unconditionally stable for all mesh ratios for non-negative axial velocities, but involves inversion of an (M x M) matrix for computing the axial velocity at the M radial grid points at each axial section. The comparison (Figure 3) shows a maximum deviation of 0.8 per cent for the centerline velocity in the initial region of about

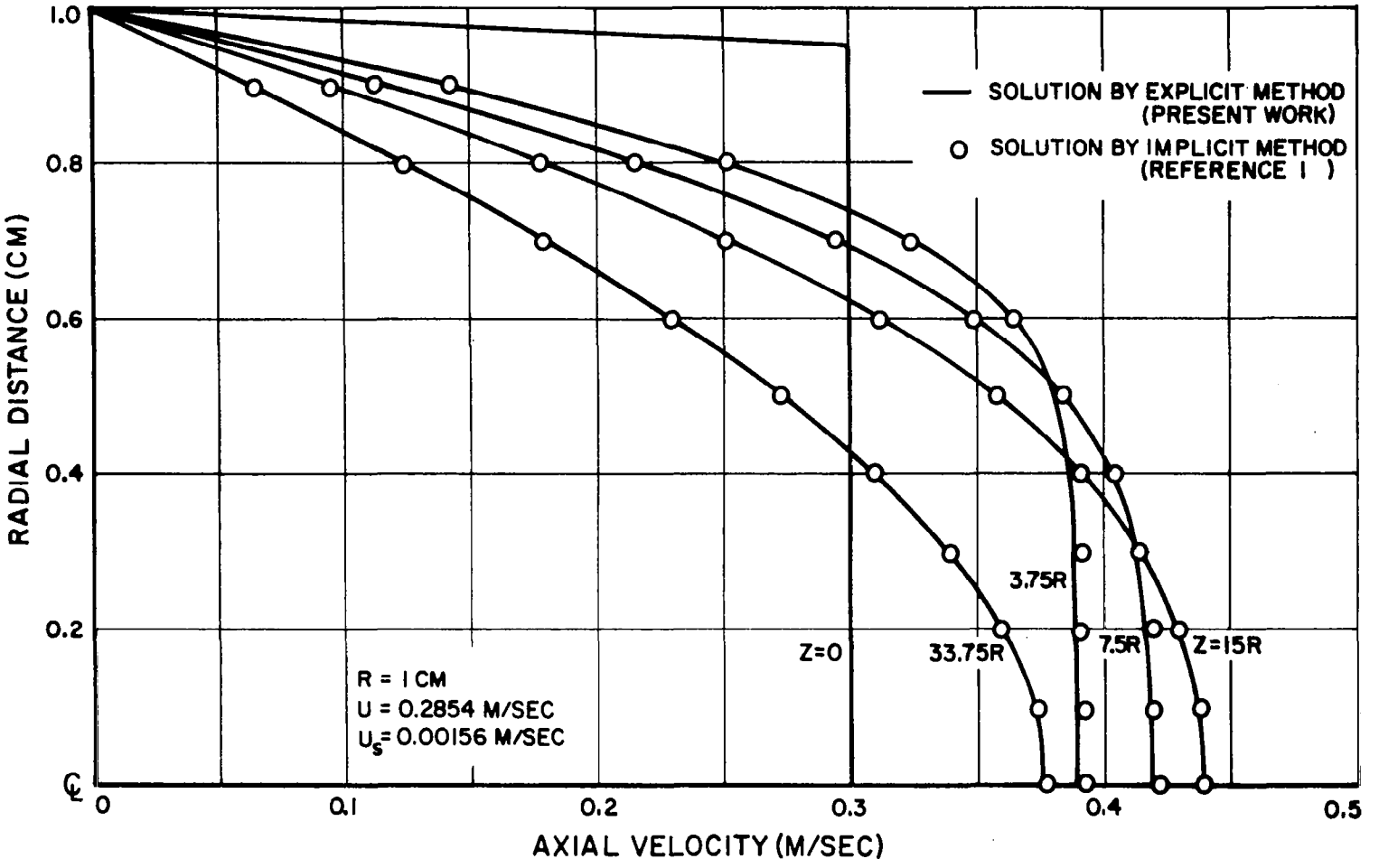

FIGURE 3. AXIAL VELOCITY PROFILES FOR ENTRANCE FLOW IN A POROUS PIPE

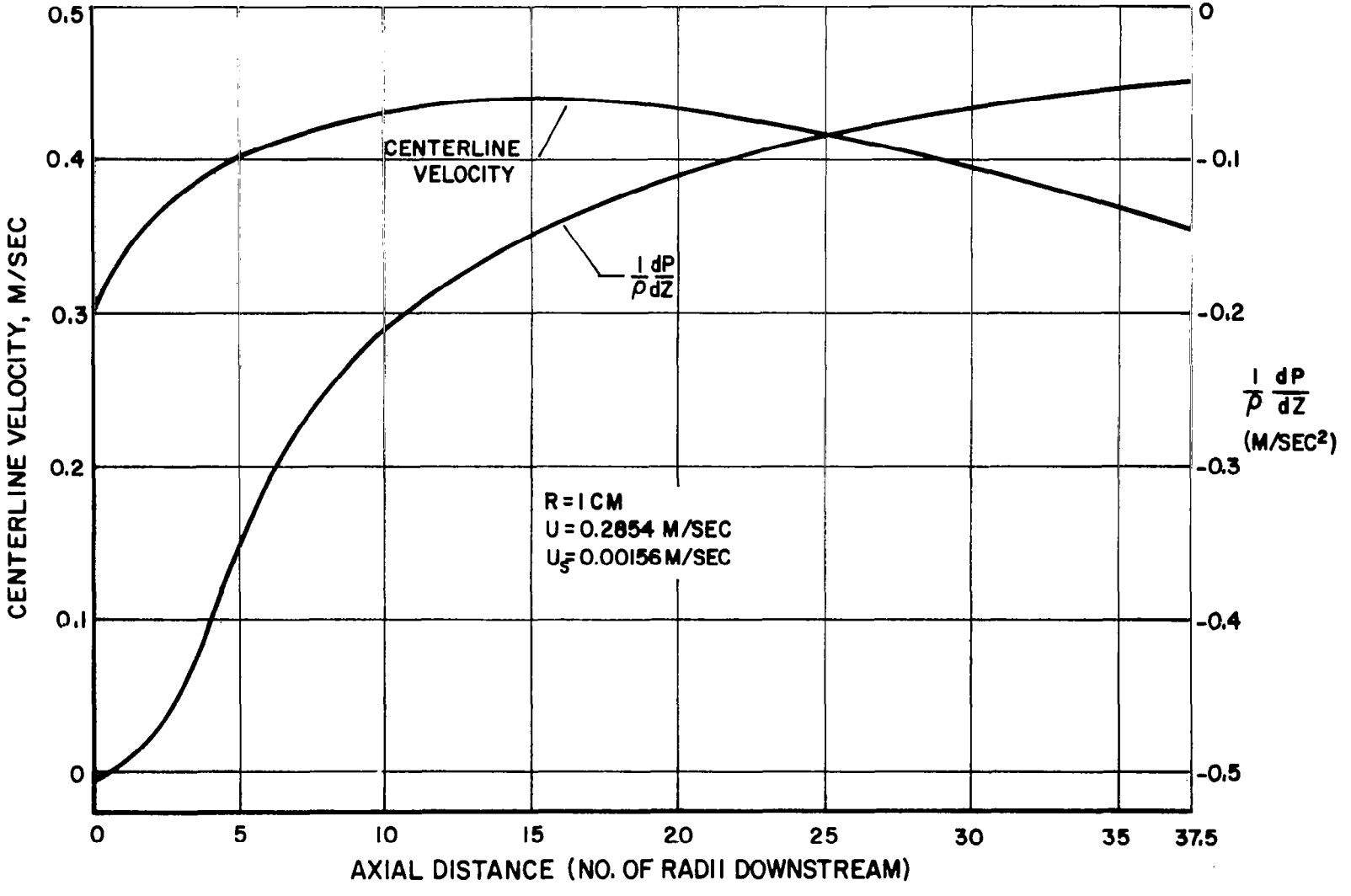

FIGURE 4. CENTERLINE VELOCITY AND $\frac{1}{\rho}\frac{dP}{dZ}$ VS AXIAL DISTANCE DOWNSTREAM FOR ENTRANCE FLOW IN A POROUS PIPE

4 pipe radii. This deviation reduces, with distance downstream to less than 0.3 per cent at about 15 radii. Also, at any axial section, the results compare more favorably in regions near the pipe wall, than near the axis. Figure 4 shows the behavior of the centerline velocity and $\frac{1}{\rho}\left[\frac{dp}{dz}\right]$ with increasing downstream distance. One further point that needs mentioning is that the all-explicit scheme developed uses less than seven minutes of computer time to solve for velocity fields for an axial distance of upto 74 pipe radii. This includes compilation as well as output time. The close agreement obtained between the two solutions confirms the quality of the results of the time-independent equations.

The validity of the time-dependent results is assured by solving the problem of a pulsating viscous flow superimposed on the steady laminar motion of incompressible fluid in a straight pipe of circular cross-section. An exact solution of this problem has been obtained by Uchida [2] in 1956. Uchida assumed that the steady flow is parallel to the pipe axis and has a zero transverse component, so that the resulting flow is independent of the axial distance. The unsteady Navier Stokes equations governing the flow thus reduce to linear parabolic partial differential equations, even though no boundary layer assumptions are made. Figure 5 shows the results for an oscillating pressure gradient of low frequency (0.024 rad/sec.) superimposed on a steady Poiseuille flow with a Reynolds number of 500. Comparison is also made for a higher frequency (0.2166 rad/sec.) of the superimposed oscillating pressure gradient (Figure 6). The close agreement of the obtained numerical solutions of Uchida, leads to reliance upon the method of solution developed in the present work.

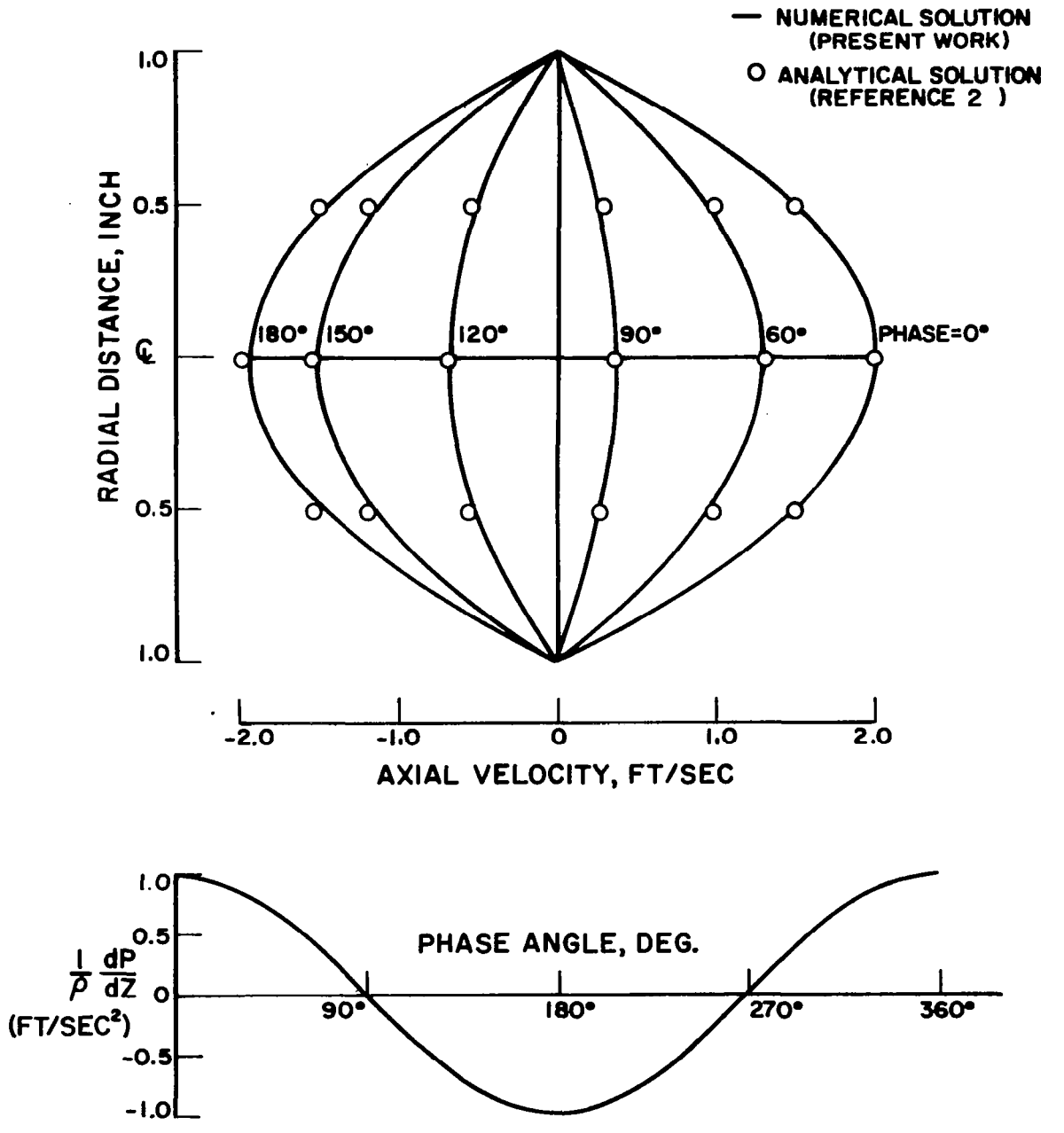

FIGURE 5. AXIAL VELOCITY PROFILES FOR POISEUILLE FLOW WITH SUPERIMPOSED OSCILLATING PRESSURE GRADIENT OF FREQUENCY = 0.024 RAD/SEC

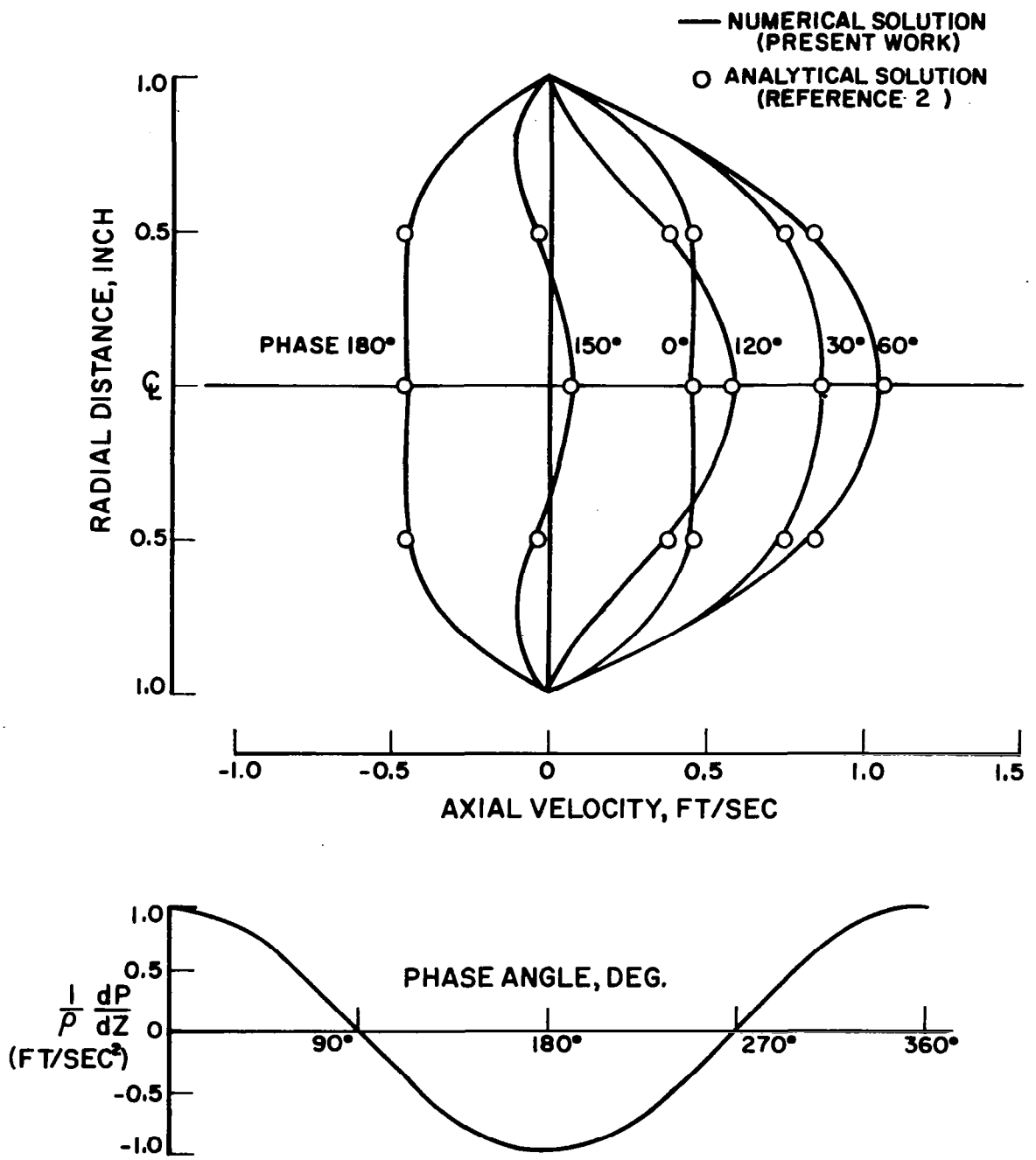

FIGURE 6. AXIAL VELOCITY PROFILES FOR POISEUILLE FLOW WITH SUPERIMPOSED OSCILLATING PRESSURE GRADIENT OF FREQUENCY = 0.2166 RAD/SEC

The scheme for the complete equations is checked out by solving for the trivial case of determining the response of a given developing flow field to zero variations superimposed on it. The validity of the scheme is assured if the flow pattern remains invariant with time, as computations progress further in time. In fact, the results showed a variation of less than 0.01 per cent at the end of twenty time levels of calculation.

Thus, the method developed is assured to yield valid results for both the steady as well as the unsteady problems.

Discussion of Present Results

The numerical computation scheme developed is employed to determine the initially steady flow pattern in the mixing and developing region of a laminar circular jet in a confined co-axial flow. The variation of this flow in response to a velocity oscillation superimposed on the entrance conditions is subsequently studied using the non-steady equations. At this stage, several practical difficulties are encountered due to the fact that the partial differential equations describing the time-dependent problem are parabolic in two independent variables. Some of these difficulties are associated, in general, with problems in three independent variables, even though they may be parabolic in only one [6,7,44]. The finite step sizes being restricted by convergence rates, a computer with a very large memory core becomes a prime necessity. Unconditionally stable schemes may be devised, but the time for solution may easily make their use prohibitive.

The IBM 7040 digital computer is used for the present numerical investigation. Its limited core may not present an insurmountable difficulty, since a larger core is easily improvised through the use

of auxiliary input-output units. The increase in computer time due to this additional input-output process is very small. However the total computer time requirement for a single run remains a serious restriction, so that only a limited study is carried out. A more complete investigation is necessary for drawing general conclusions. The present work provides a stable, convergent and efficient method for this investigation.

The flow configuration of interest involves essentially three parameters.

1. Ratio of jet radius to radius of confining pipe.

2. Reynolds' numbers at the jet exit for the flows in the jet and in the surrounding annular region.

3. The nature and distribution of the superimposed time-dependent velocity variation.

As mentioned earlier, the limited availability of computer facilities forbade a complete parametric study. Consequently, only the following set of parameters are investigated:

$R_1 = 0.5$ in.
$R = 1$ in.

$\frac{R_1}{R} = 0.5$

$U_1 = 3.30$ ft/sec.
$U_2 = 2.75$ ft/sec.
$U = 3.00$ ft/sec.

$\frac{U_1}{U_2} = 1.2$

$R_{e_1} = 1650$
$R_{e_2} = 1400$

$\frac{R_{e_1}}{R_{e_2}} = 1.18$

$R_e = 2900$

Various forms for the superimposed variations are considered. One feature common to them all is that they are confined to the axial velocity only and to the axial section where the jet pipe terminates.

The following particular profiles for the variation are investigated:

Case 1. A step increase of the local axial velocity along a circular ring near the jet exit. The magnitude of the step is five per cent of the mean flow velocity in the confining pipe.

Case 2. An impulsive increase of the local axial velocity which is then immediately restored to its original value. The location and magnitude of the impulse are the same as in (1) above.

Case 3. A pulsed increase in axial velocity introduced at a frequency of 50 cps. The amplitude and location of the pulse are the same as in (1) and (2) above.

Case 4. A sinusoidal time-variation superimposed at the jet exit section and having the form

$$\delta v_z(r, t) = A\, v_{z_s}(r, 0) \cos(2\pi f t)$$

where A = amplitude factor

f = frequency (cps)

Due to practical and economic limitations of the available facility, only a limited number of values of A and f could be investigated. The values considered are:

	A = amplitude factor	f = frequency (cps)
a)	+0.05 for $0 \leq r < R_1$	1
	-0.05 for $R_1 < r \leq R$	

b) $+0.05$ for $0 \leq r < R_1$ 50

-0.05 for $R_1 < r \leq R$

c) $+0.05$ for $0 \leq r < R_1$ 100

-0.05 for $R_1 < r \leq R$

The flow parameters listed above are shown experimentally by Seider [4] to correspond to a mixing region that undergoes transition to turbulence at an axial distance of about 3 radii of the confining pipe downstream of the jet exit. Beyond this region, the results obtained from the laminar flow equations would have no physical significance. Hence, the investigation is limited to an axial length of about 4 R. The results indicate that when the superimposed step change or impulsive change is localized to only one point along the radius, the flow merely adjusts itself to this change, but shows no abrupt behavior. The pulsed increase also shows similar results.

Figure 7 shows the steady state axial velocity profiles for the confined jet mixing configuration considered, before the oscillation of Figure 8 is superimposed on the jet exit section. Figures 9 through 11 show the results for sinusoidal oscillations of the general form listed under Case 4 above. The deviation of the axial velocity from its steady state value is plotted against the number of cycles of the superimposed oscillation, with radius r and downstream distance z as parameters.

Figure 9 shows the results for the oscillation of Case 4a superimposed on the flow entrance.

At the jet exit, i.e., at $z = 0$, the superimposed amplitude of the oscillation is 0.33 ft/sec. at the centerline. As seen from Figure 9a,

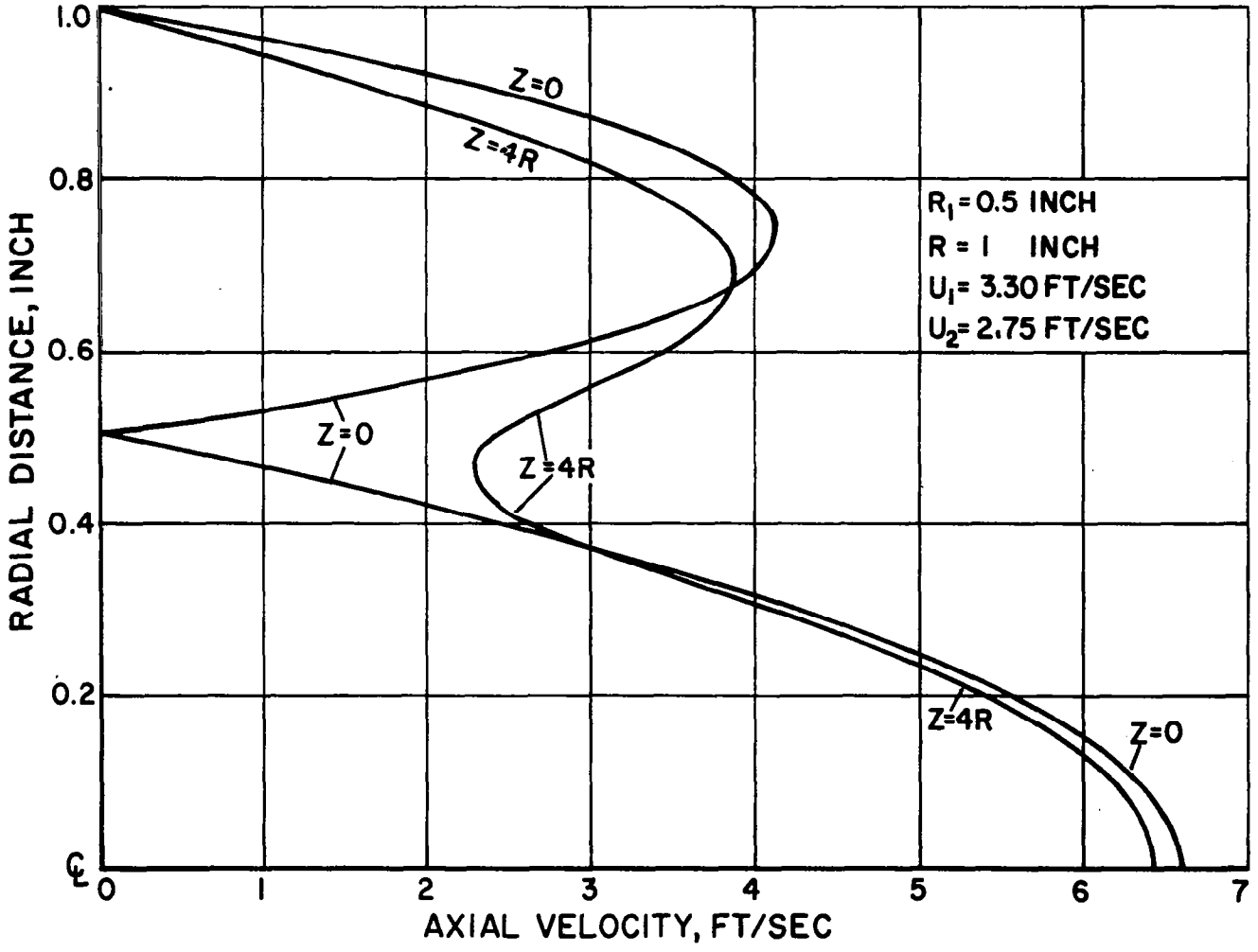

FIGURE 7. AXIAL VELOCITY PROFILES FOR CONFINED JET MIXING WITHOUT SUPERIMPOSED OSCILLATION

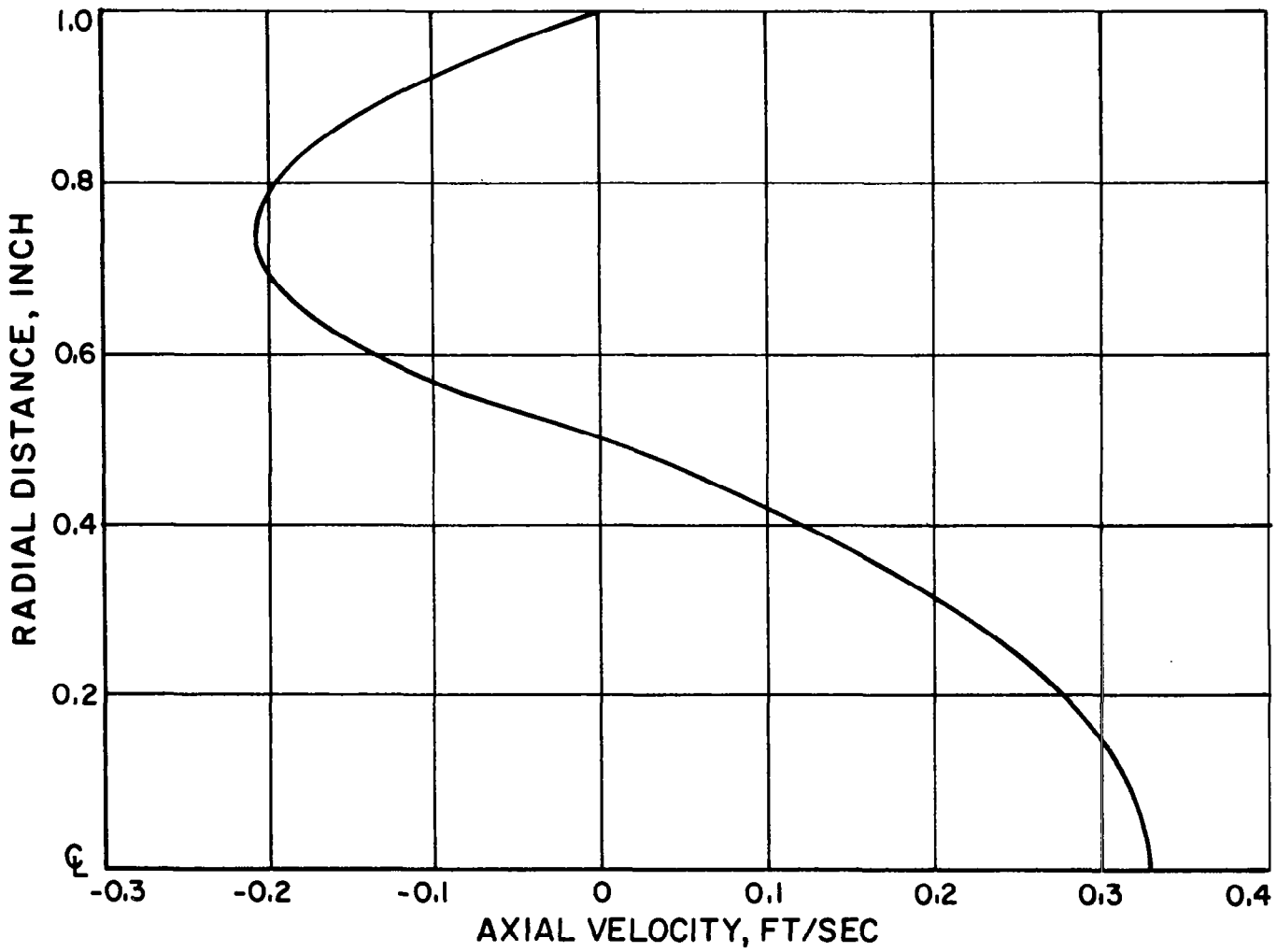

FIGURE 8. INITIAL PROFILE OF SUPERIMPOSED OSCILLATION

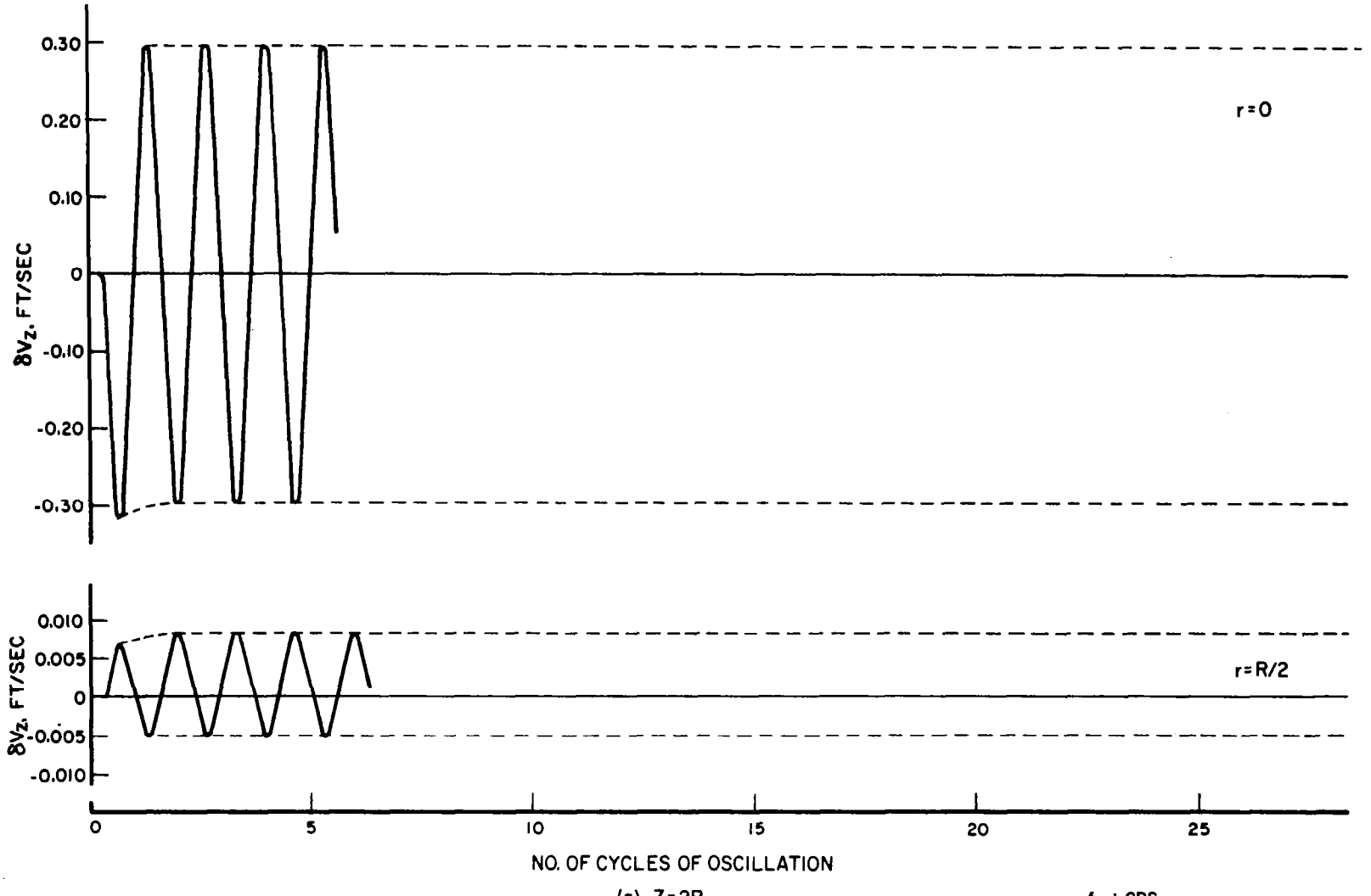

(a) Z=2R

f = 1 CPS
Re_1 = 1650
Re_2 = 1400

FIGURE 9. DEVIATION IN AXIAL VELOCITY FROM STEADY STATE VS NO. OF CYCLES OF SUPERIMPOSED OSCILLATION

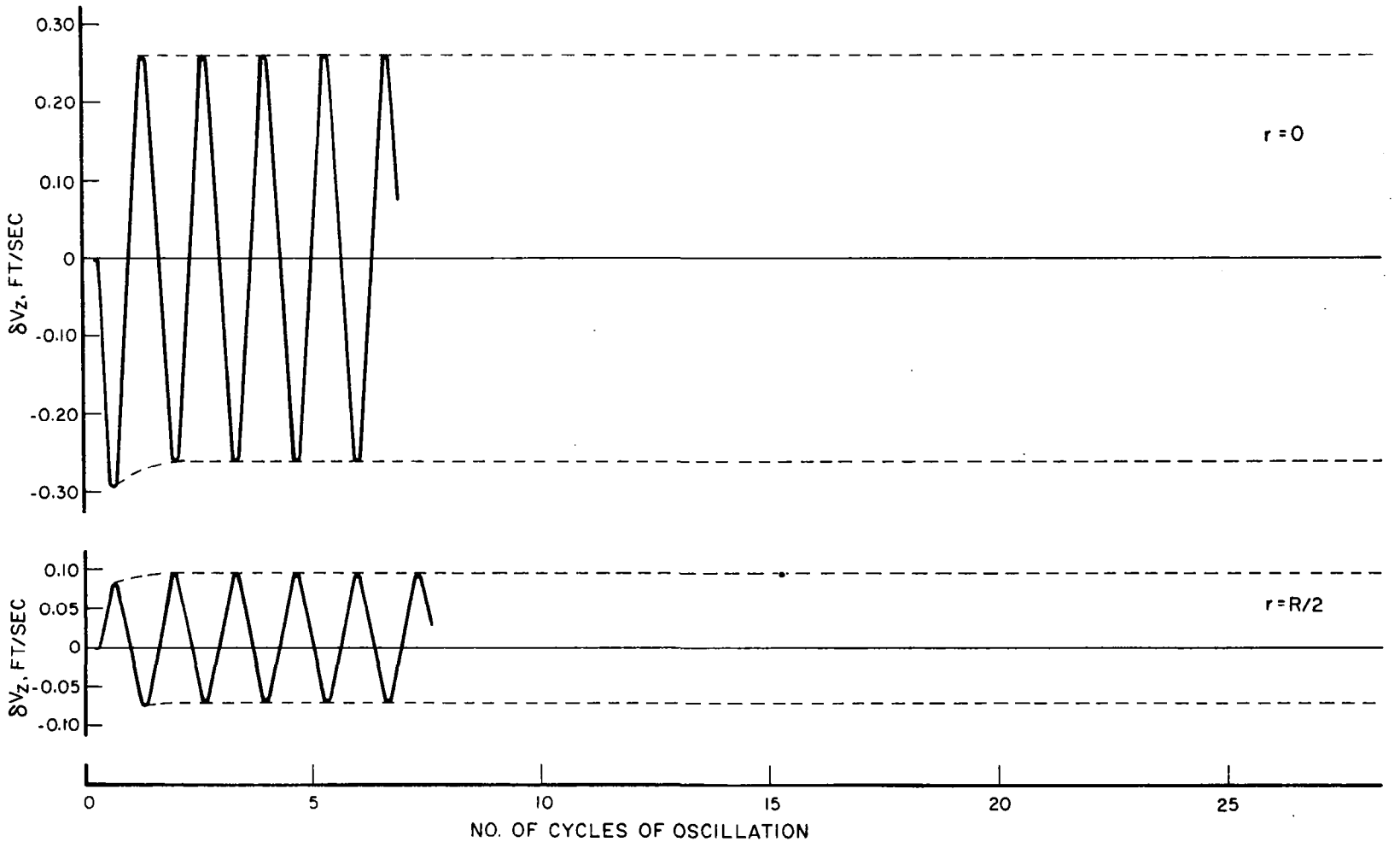

(b) Z = 4R

f = 1 CPS
Re_1 = 1650
Re_2 = 1400

FIGURE 9 concluded. DEVIATION IN AXIAL VELOCITY FROM STEADY STATE VS NO. OF CYCLES OF SUPERIMPOSED OSCILLATION

at z = 2R, this amplitude decreases to 0.315 ft/sec. at the end of the first cycle of the oscillation and further decreases to 0.295 ft/sec. at the end of the second cycle. The amplitude then remains steady at this value of 0.295 ft/sec. for the further cycles investigated.

At r = R/2, the superimposed amplitude is 0.0078 ft/sec. at z = 0. At z = 2R, this amplitude decreases to 0.0059 ft/sec. at the end of the first cycle, it increases to 0.0066 ft/sec. at the end of the second cycle, and remains constant beyond.

At r = 0, and z = 4R, the amplitude of oscillation in the resulting flow is 0.2775 ft/sec. for the first cycle. It decreases to 0.26 ft/sec. during the next cycle and remains constant at this value for the further cycles investigated.

Again at r = R/2, at z = 4R the initial amplitude of 0.0078 ft/sec. decreases to 0.00775 ft/sec. at the end of the first cycle, but increases to 0.00825 ft/sec. at the end of the second cycle remaining constant at this value for all further cycles observed.

Since information for this run was obtained for time instants corresponding to only the peaks of the oscillation for each cycle, no statement may be made regarding the distortion of the wave shape in the resulting motion.

Beyond the first two cycles, the envelope of the wave shape consists of a pair of straight lines parallel to the line $\delta v_z = 0$. At r = 0, these parallel lines are spaced symmetrically about the line $\delta v_z = 0$ for both axial locations z = 2R and z = 4R.

At r = R/2, for z = 2R the envelope of the wave is symmetric about the line $\delta v_z = 0.00175$ ft/sec., while for z = 4R, the line of symmetry shifts to $\delta v_z = 0.00125$ ft/sec.

The frequency of the introduced oscillation is increased to fifty cycles per second for the next run. Information for this run, as well as for the subsequent run, was printed out at time instants corresponding to the peaks, as well as to the zeros of the superimposed oscillations. The results are presented in Figure 10. The amplitude of the resulting wave is almost constant at 0.061 ft/sec. throughout. The wave shape is markedly distorted for the initial three or four cycles at all the four locations considered. This initial distortion is more pronounced at the centerline than at r = R/2. However, the distortion in the wave shape (after it has apparently attained steady state) is greater at z = 2R than at z = 4R, the maximum occuring at the centerline for z = 2R.

The envelope of the wave shape oscillates initially, later settling down to parallel straight lines. The oscillatory portion of the envelope is limited to a smaller initial period for the centerline than for r = R/2, the maximum spread occurring at z = 4R. At z = 4R, the envelope begins to oscillate not right from the start, but only after about the first cycle. Also, the amplitude and frequency are higher at the centerline than at r = R/2 being largest at the centerline for z = 2R. The steady state is attained faster at r = 0 than at r = R/2, and also faster at z = 2R than at z = 4R. The line of symmetry for the steady portion of the envelope is, at all locations, displaced towards positive δv_z, the shift being larger at r = R/2 than at the centerline, the maximum occurring at z = 2R and r = R/2.

The effect of a further increase in the oscillation frequency to 100 cycles/second is investigated subsequently. The results are presented in Figure 11. For the tenth and the twentieth cycles, for this

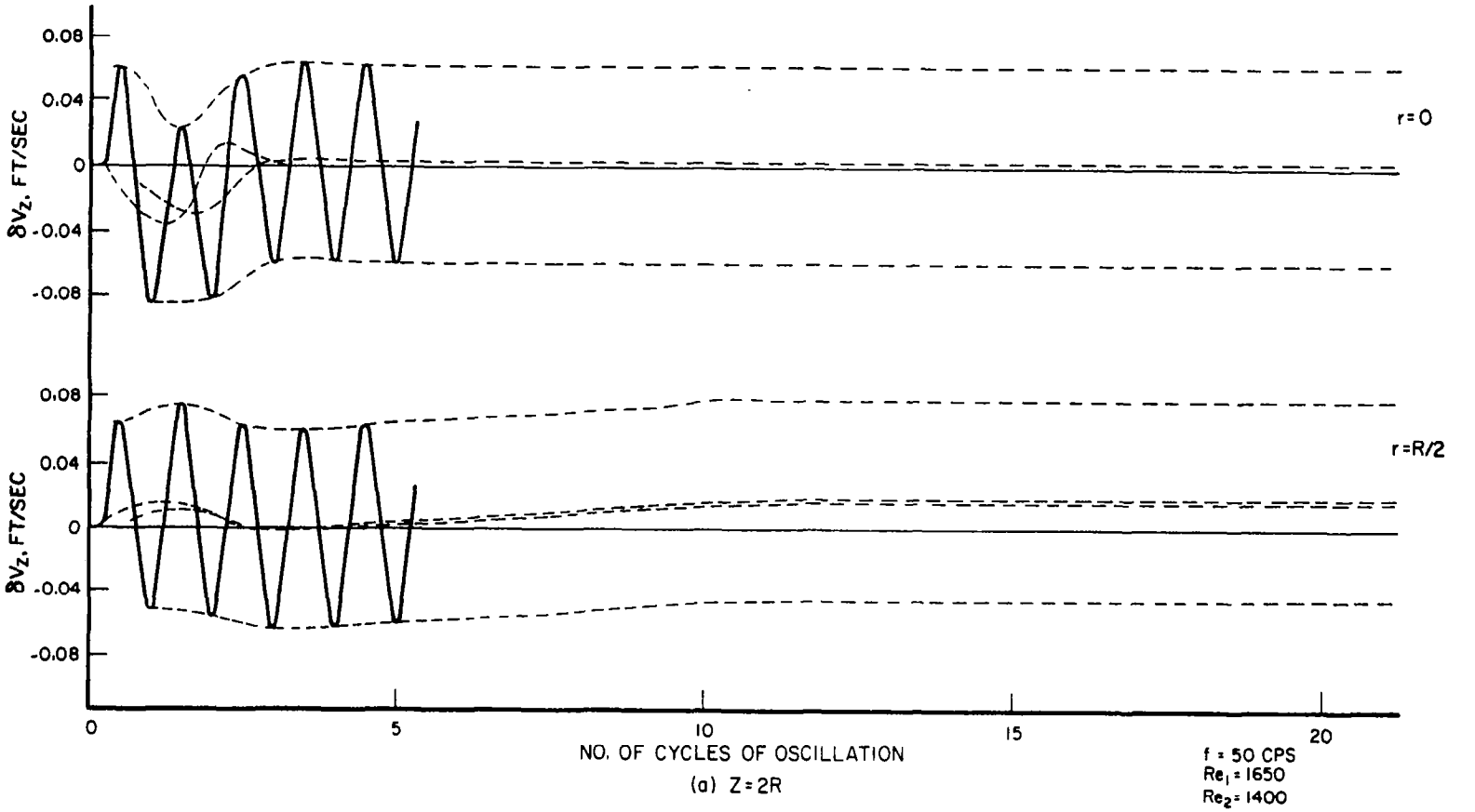

FIGURE 10. DEVIATION IN AXIAL VELOCITY FROM STEADY STATE VS NO. OF CYCLES OF SUPERIMPOSED OSCILLATION

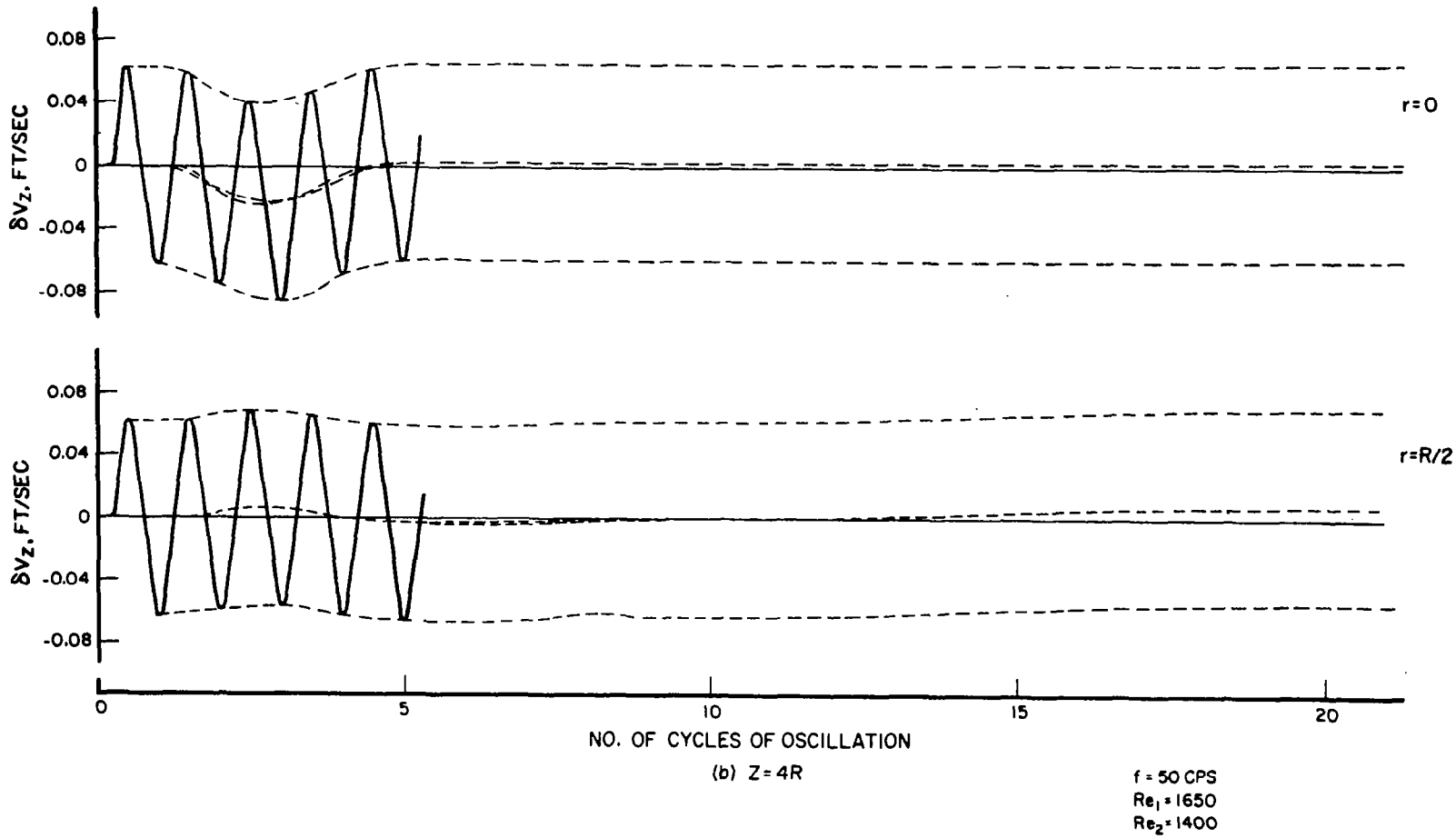

FIGURE 10 concluded. DEVIATION IN AXIAL VELOCITY FROM STEADY STATE VS NO. OF CYCLES OF SUPERIMPOSED OSCILLATION

run, printed information was obtained at twelve instants equally spaced over the period of the imposed oscillation. This information confirms that the frequency of the resulting oscillation is the same as that of the imposed oscillations.

The amplitude of the resulting wave is again almost constant at 0.061 ft/sec. throughout. The wave shape is considerably distorted at the centerline, the distortion being greater at downstream distance $z = 2R$ than at $z = 4R$. Also, at $z = 2R$, this distortion occurs over the second through the fourth cycles, and again over the eleventh through the fourteenth cycles. At $z = 4R$, these periods of distortion shift to the fourth through eighth cycles and to the thirteenth through the eighteenth cycles.

The envelope of the wave shape is oscillatory but is of much lower frequency than that of the superimposed oscillation. As in the case of superimposed oscillation frequency of 50 cps, the amplitude of the envelope oscillation is larger at the centerline than at $r = R/2$. The maximum amplitude occurs on the centerline at $z = 2R$. Also, at $z = 2R$ the envelope oscillation begins after the first cycle of the imposed oscillation and at $z = 4R$, it begins after the initial three cycles.

Without the superimposed oscillation, this flow configuration exhibits a region of positive pressure gradient close to the jet exit section. From the printed information obtained from the runs, it can only be said that this region of positive pressure gradient extends to between $z = 1.5R$ and $z = 2R$.

The effect of this high-frequency (i.e. 100 cps) oscillation of Case 4c above is also studied on the flow configuration with the

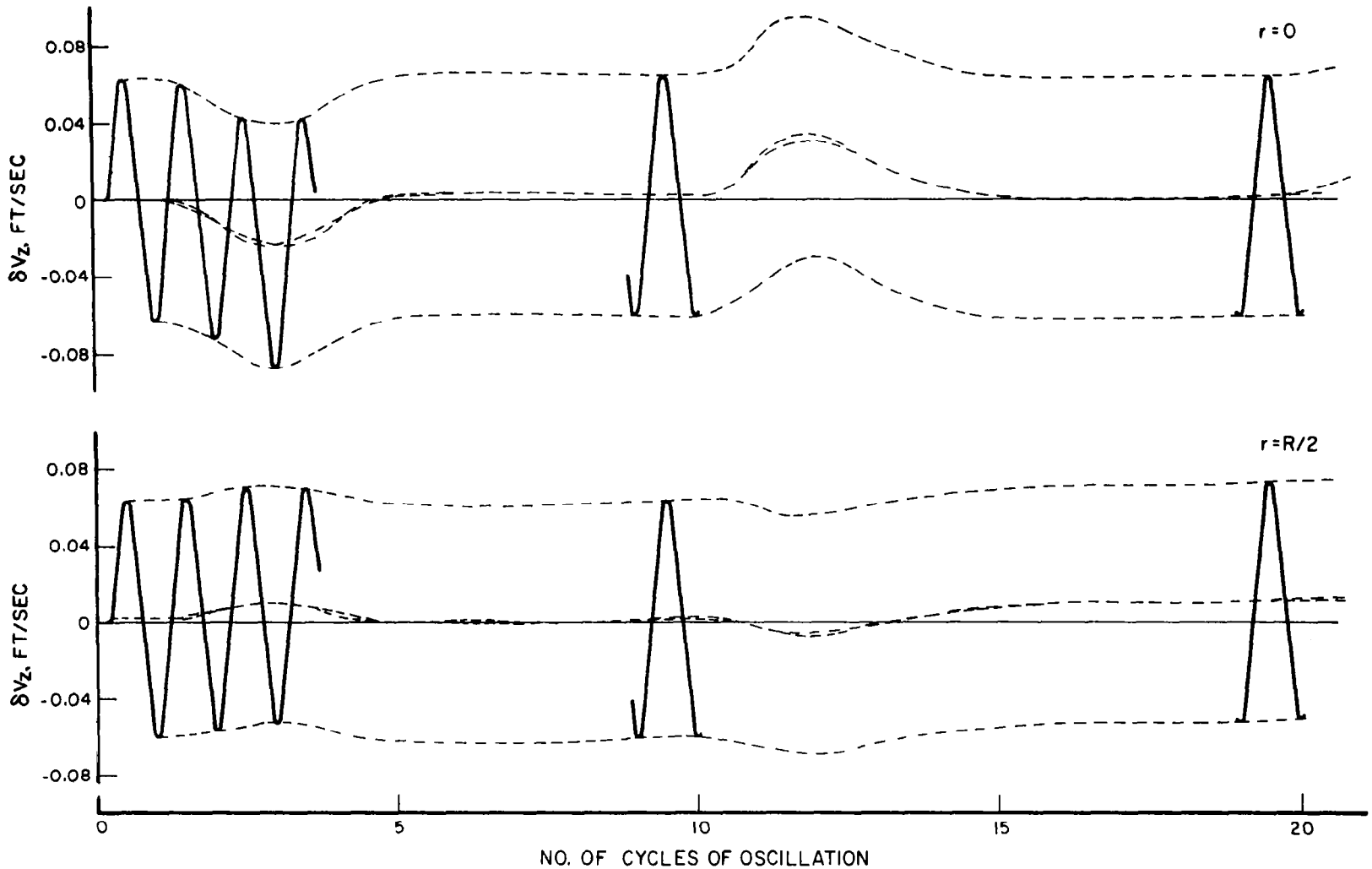

(a) Z = 2R

f = 100 CPS
Re_1 = 1650
Re_2 = 1400

FIGURE 11. DEVIATION IN AXIAL VELOCITY FROM STEADY STATE VS NO. OF CYCLES OF SUPERIMPOSED OSCILLATION

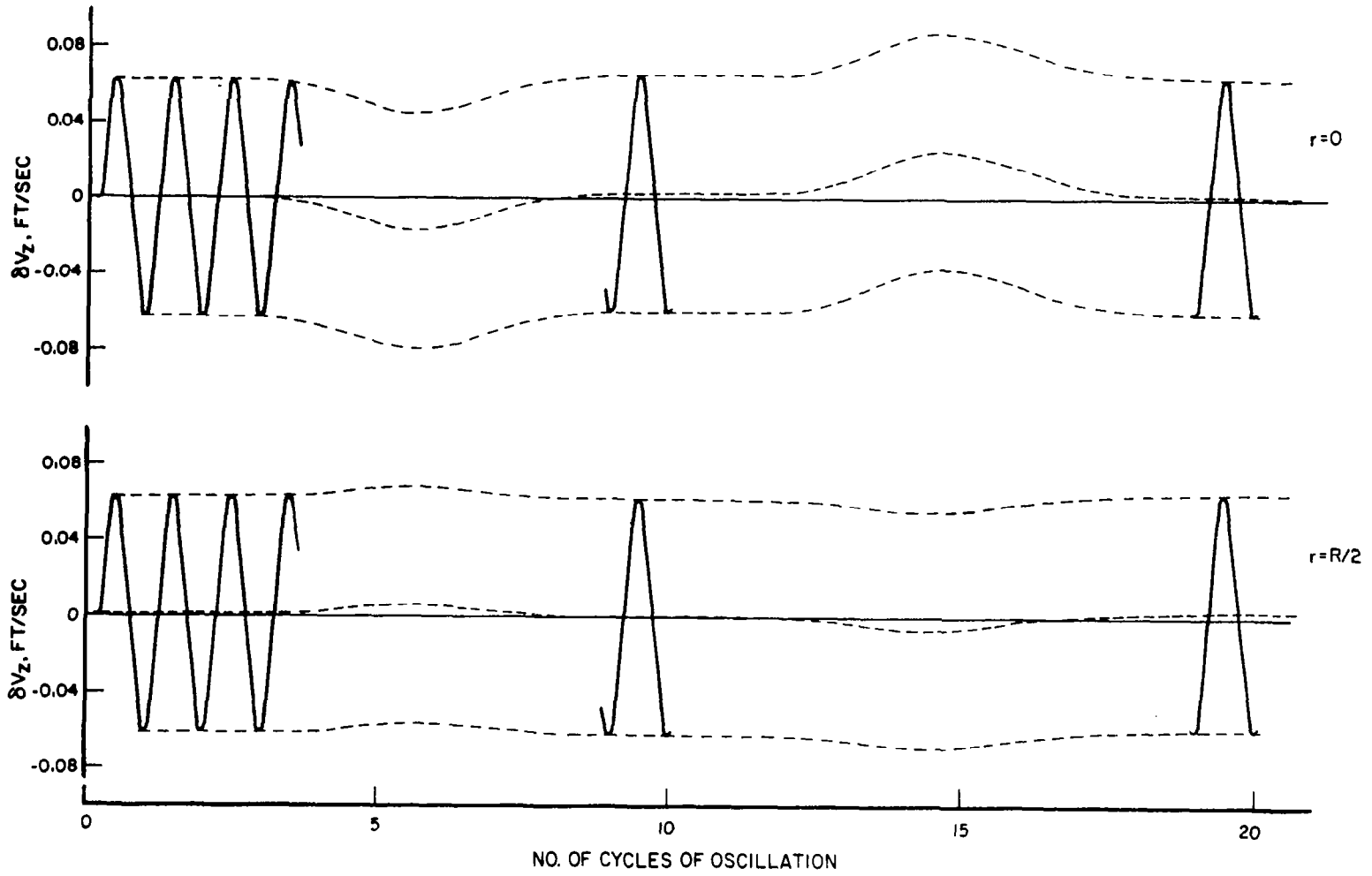

(b) Z = 4R

f = 100 CPS
Re_1 = 1650
Re_2 = 1400

FIGURE 11 concluded. DEVIATION IN AXIAL VELOCITY FROM STEADY STATE VS NO. OF CYCLES OF SUPERIMPOSED OSCILLATION

following parameters:

$R_1 = 0.563$ in.

$R = 1$ in.

$\frac{R_1}{R} = 0.563$

$U_1 = 0.442$ ft/sec.

$U_2 = 0.518$ ft/sec.

$U = 0.494$ ft/sec.

$\frac{U_1}{U_2} = 0.85$

$R_{e_1} = 250$

$R_{e_2} = 228$

$R_e = 496$

$\frac{R_{e_1}}{R_{e_2}} = 1.0965$

The experimental investigation by Seider [4] has shown that with the above parameters, the confined jet mixing region remains laminar upto 40R downstream. In the present program, the investigation is limited to a downstream distance of 8R only. The results are presented in Figure 12.

The amplitude of the oscillations introduced at z = 0 is 0.0442 ft/sec. at the centerline, and 0.0096 ft/sec. at r = R/2. The amplitude of the resulting oscillations is about 0.011 ft/sec. throughout at all locations considered. There is no distortion anywhere. The envelope of this resulting wave shape, therefore, consists of parallel straight lines symmetric about δv_z equal to zero or approximately zero.

The region of positive pressure gradient, as observed from the printed information obtained from this run, is limited to between z = 0.15R to z = 0.5R.

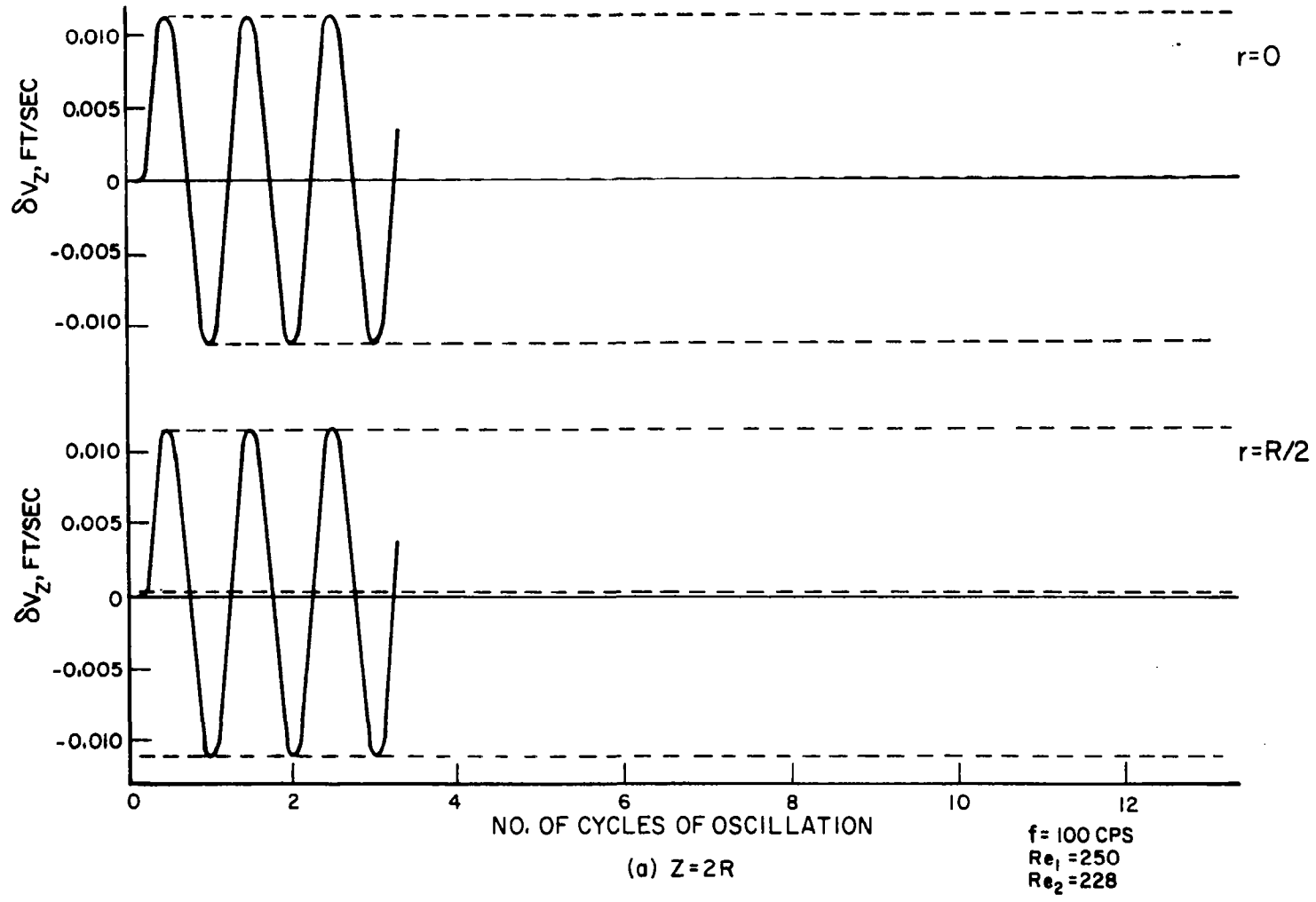

FIGURE 12. DEVIATION IN AXIAL VELOCITY FROM STEADY STATE VS NO. OF CYCLES OF SUPERIMPOSED OSCILLATION

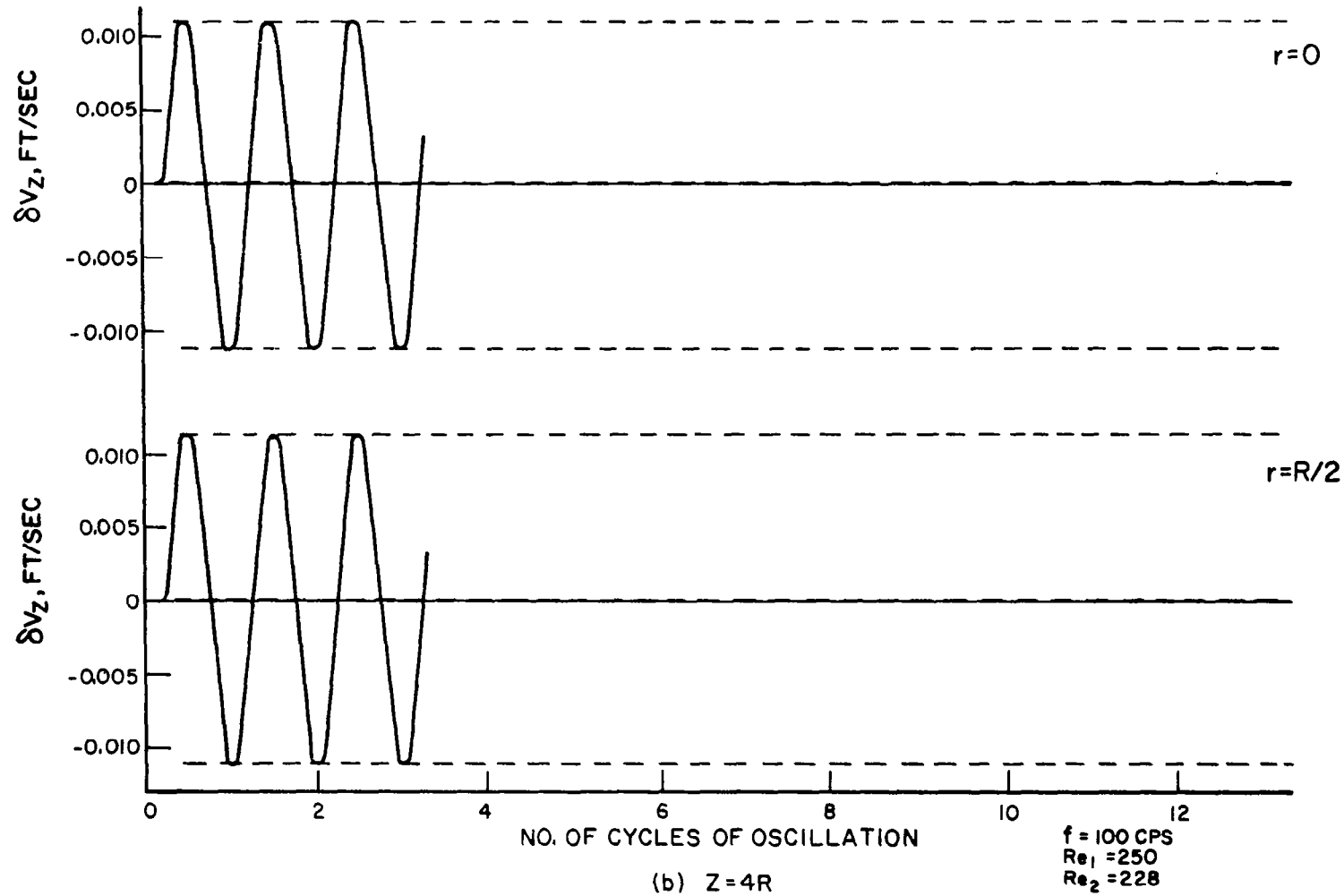

FIGURE 12 concluded. DEVIATION IN AXIAL VELOCITY FROM STEADY STATE VS NO. OF CYCLES OF SUPERIMPOSED OSCILLATION

In the light of these results for the two confined jet mixing configurations investigated and of the experimental work of Seider [4], it seems probable that hydrodynamical instability of the two flows causes them to respond differently to the same superimposed oscillations.

Comparison With Solutions of Steady Navier Stokes Equations

During the present investigation, comparison is obtained also for solutions of the boundary layer equations with solutions of the Navier Stokes equations for identical steady flow configurations. For most cases considered, the two solutions differ by a maximum of about twelve per cent near the entrance section in the vicinity of the centerline. This deviation decreases rapidly with increasing radial distance as well as with increasing axial distance downstream.

The steady boundary layer equations are solved for the classical entrance flow in a pipe using the numerical method presently developed. The results are compared in Figure 13 with those obtained by Lavan [3] who solved the Navier Stokes equations using a relaxation method.

The deviation of the centerline velocity is everywhere less than 1.5 per cent. At the half-radius, i.e., at r = R/2, the axial velocity deviates by about 3.3 per cent at a downstream distance z = 3R, but by only about 2.5 per cent at z = 9R and beyond. Near the wall at r = 0.8R the deviation is about 2.5 per cent at z = 3R, and about 1.5 per cent at z = 9R and beyond.

The steady boundary layer equations are also solved for steady jet mixing in a confined co-axial flow for three sets of parameters. The computer time for each of these runs is less than ten minutes to carry out the calculations to about 80R downstream. This also includes

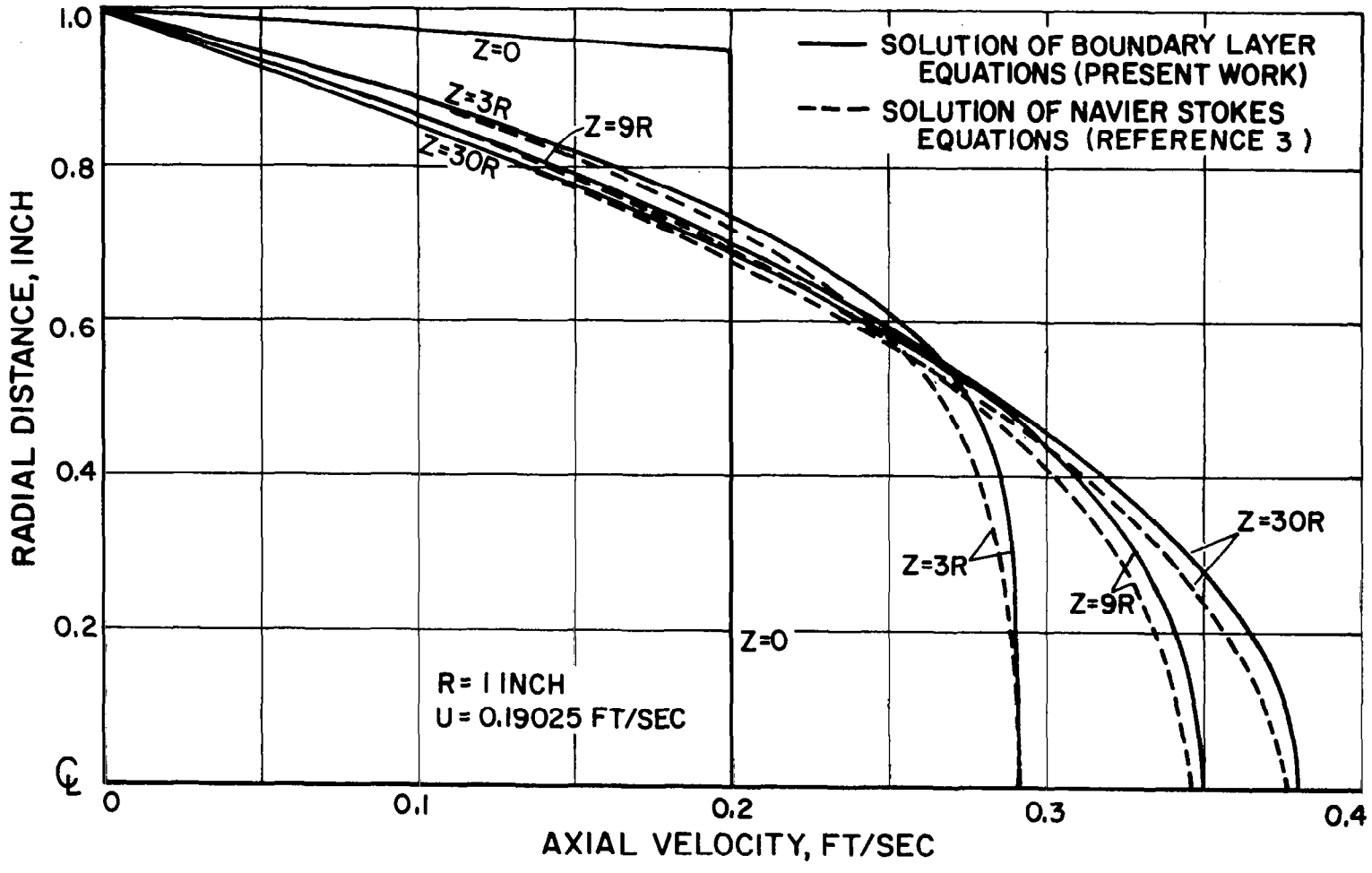

FIGURE 13. AXIAL VELOCITY PROFILES FOR CLASSICAL ENTRANCE FLOW IN A PIPE

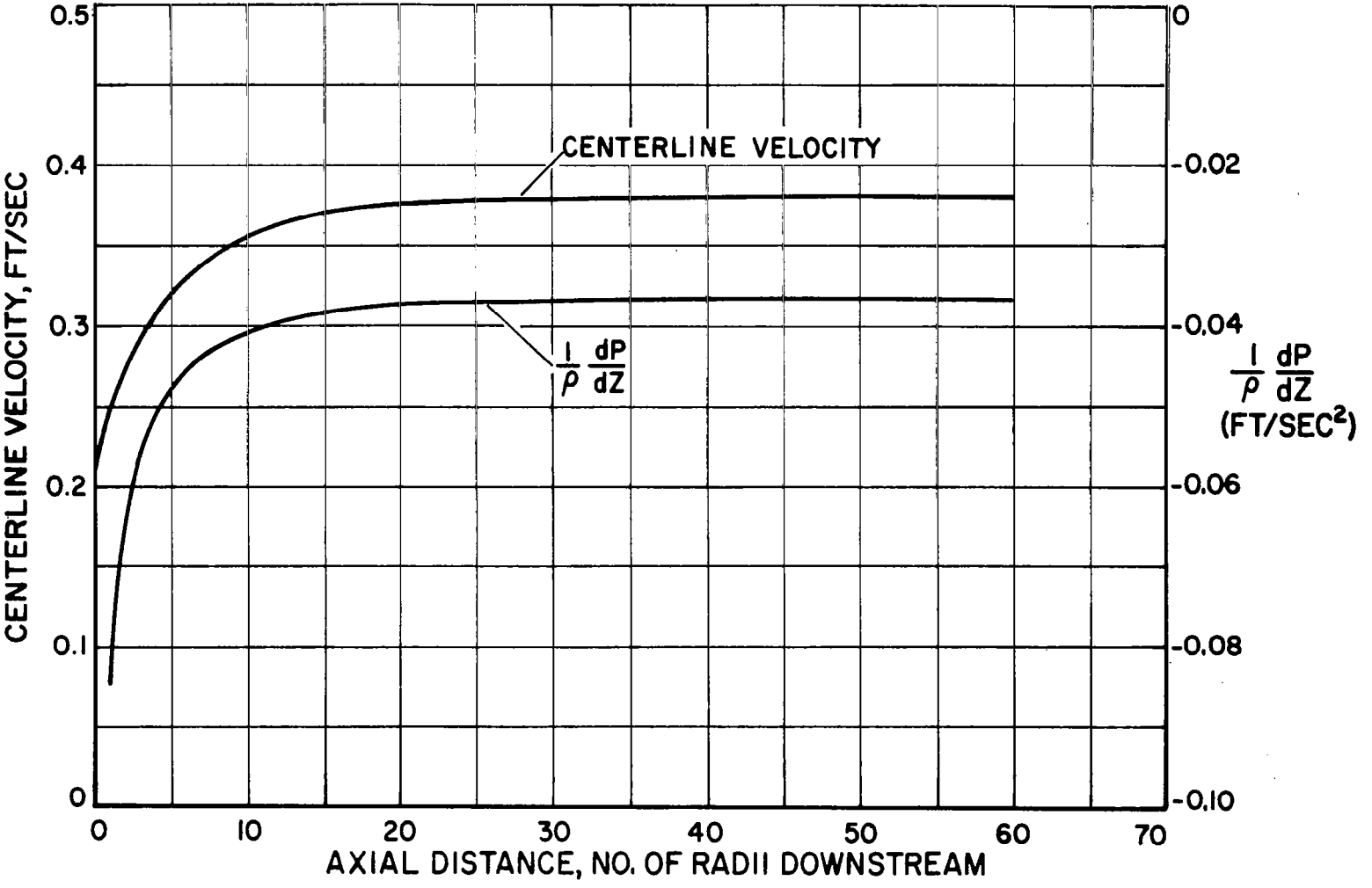

FIGURE 14. CENTERLINE VELOCITY AND $\frac{1}{\rho}\frac{dP}{dZ}$ VS AXIAL DISTANCE DOWNSTREAM FOR CLASSICAL ENTRANCE FLOW IN A PIPE

the time for output of the results.

The following are the values of the parameters for the three flow systems considered for the steady confined jet mixing problem:

	R_1 in.	R_2 in.	U_1 ft/sec	U_2 ft/sec	$\frac{U_1}{U_2}$	U ft/sec	R_{e_1}	R_{e_2}	R_e
1.	0.563	1.0	0.442	0.518	0.85	0.494	250	228	496
2.	0.470	1.0	0.621	0.224	2.77	0.312	294	119	313
3.	0.281	1.0	0.494	0.490	1.01	0.490	139	354	493

The results are compared with those of Seider [4] obtained by numerical solution of the Navier Stokes equations using the implicit alternating directions method.

Figure 15 shows the comparison of the results for the first flow configuration. The deviation of the axial velocity at the centerline is about eight to nine per cent up to a downstream distance z = 16R, but falls off to about 5.5 per cent at z = 32R. At r = 0.44R, the deviation in the axial velocity from the two solutions at z = 1R is about eleven per cent which reduces rapidly to little over two per cent at z = 16R. Also, at z = 1R downstream, the deviation of nineteen per cent at r = 0.44R, reduces to eleven per cent at r = 0.55R.

Close to the jet exit, the pressure gradient is observed to be positive. From the printed information obtained, this region of positive pressure gradient is found to be limited to between z = 0.15R to z = 0.5R.

The deviation of the two solutions is much smaller for the second and the third flow systems considered.

For the second flow configuration, as seen in Figure 16, the centerline axial velocity (obtained by the two methods), deviates by less than one per cent up to z = 5R, and by about two per cent at a downstream distance z = 10R. At r = 0.6R, the deviation, at z = 1R, is about 6.7 per cent, which decreases to about four per cent at r = 0.8R.

Figure 17 shows the comparison of the two solutions for the third flow system. The centerline velocity deviates by 1 to 1.5 per cent up to z = 3R, this deviation becoming four per cent at downstream distance z = 8R. Moving away from the centerline, i.e., at r = 0.2R, the axial velocity at z = 1R deviates by twelve per cent, but by only little over eight per cent at z = 3R.

It is to be noted that the points of largest deviation were selected for comparison in this discussion. The agreement of the two solutions is considerably better at most locations not included above.

Sufficient printed information was not obtained for the second and third configurations. Hence, no statement can be made regarding the region of positive pressure gradient that was observed for the first flow configuration.

A comparison is also obtained for the time-dependent solutions obtained from the boundary layer equations and from the Navier Stokes equation. The impulsively started entrance flow in a pipe is investigated. The results are compared with those of Lavan [5] obtained by solving the unsteady Navier Stokes equations using a relaxation method. For this flow problem, the entire flow region is initially at rest. At time t = 0+, a uniform axial velocity is imparted to the entire field, except at the pipe wall, where the no-slip condition is

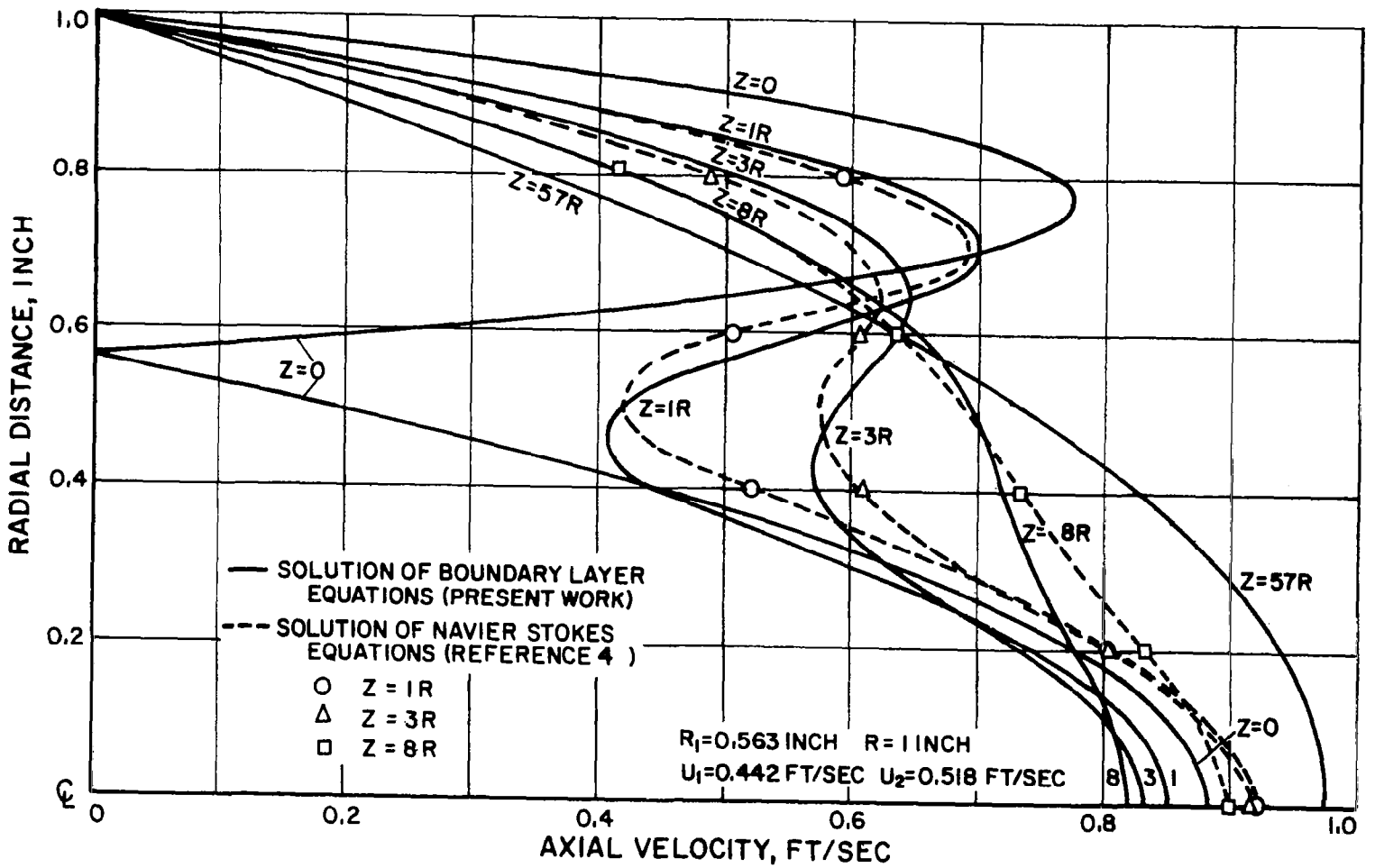

FIGURE 15. AXIAL VELOCITY PROFILES FOR STEADY CONFINED JET MIXING CONFIGURATION 1

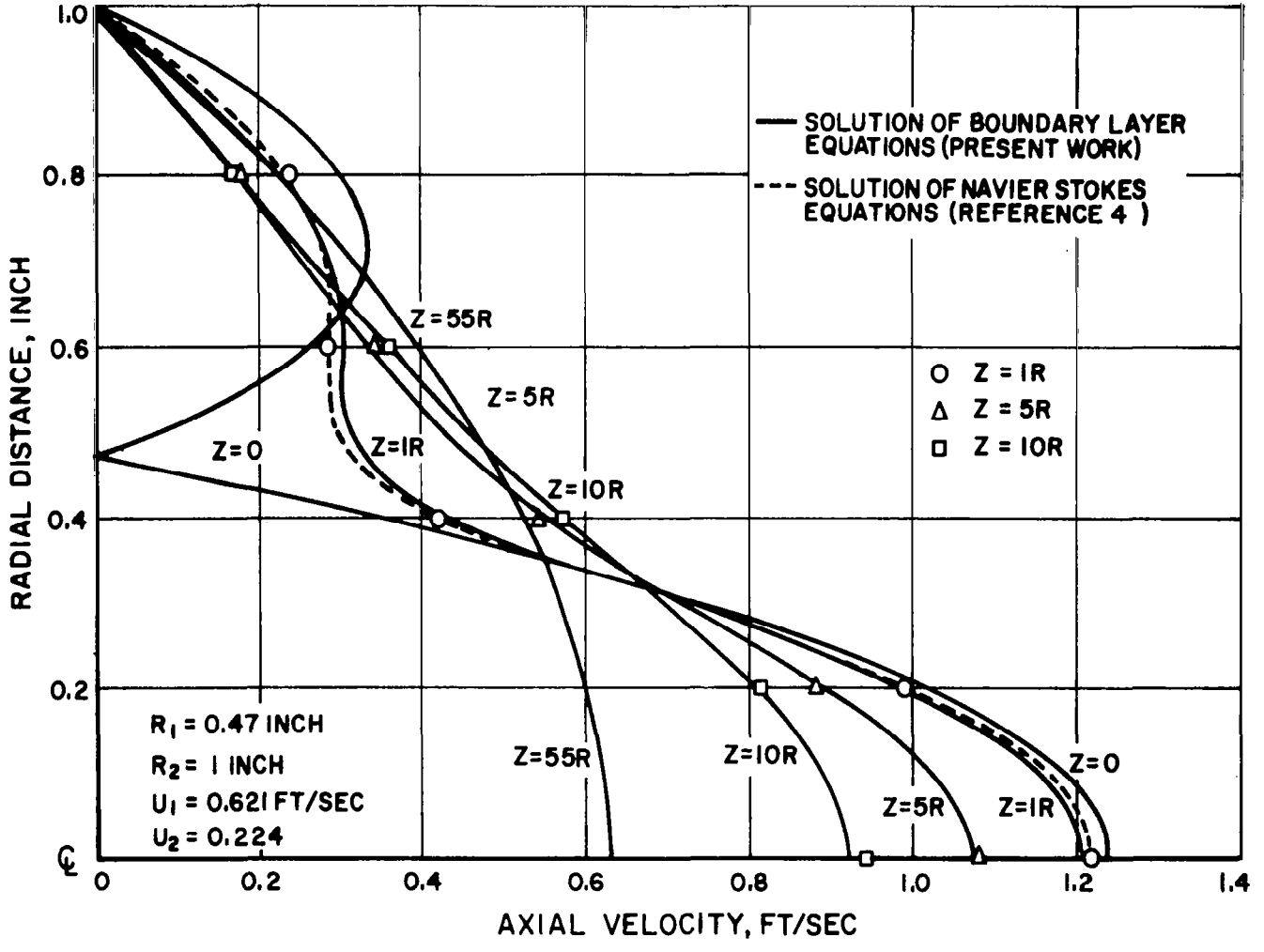

FIGURE 16. AXIAL VELOCITY PROFILES FOR STEADY CONFINED JET MIXING CONFIGURATION 2

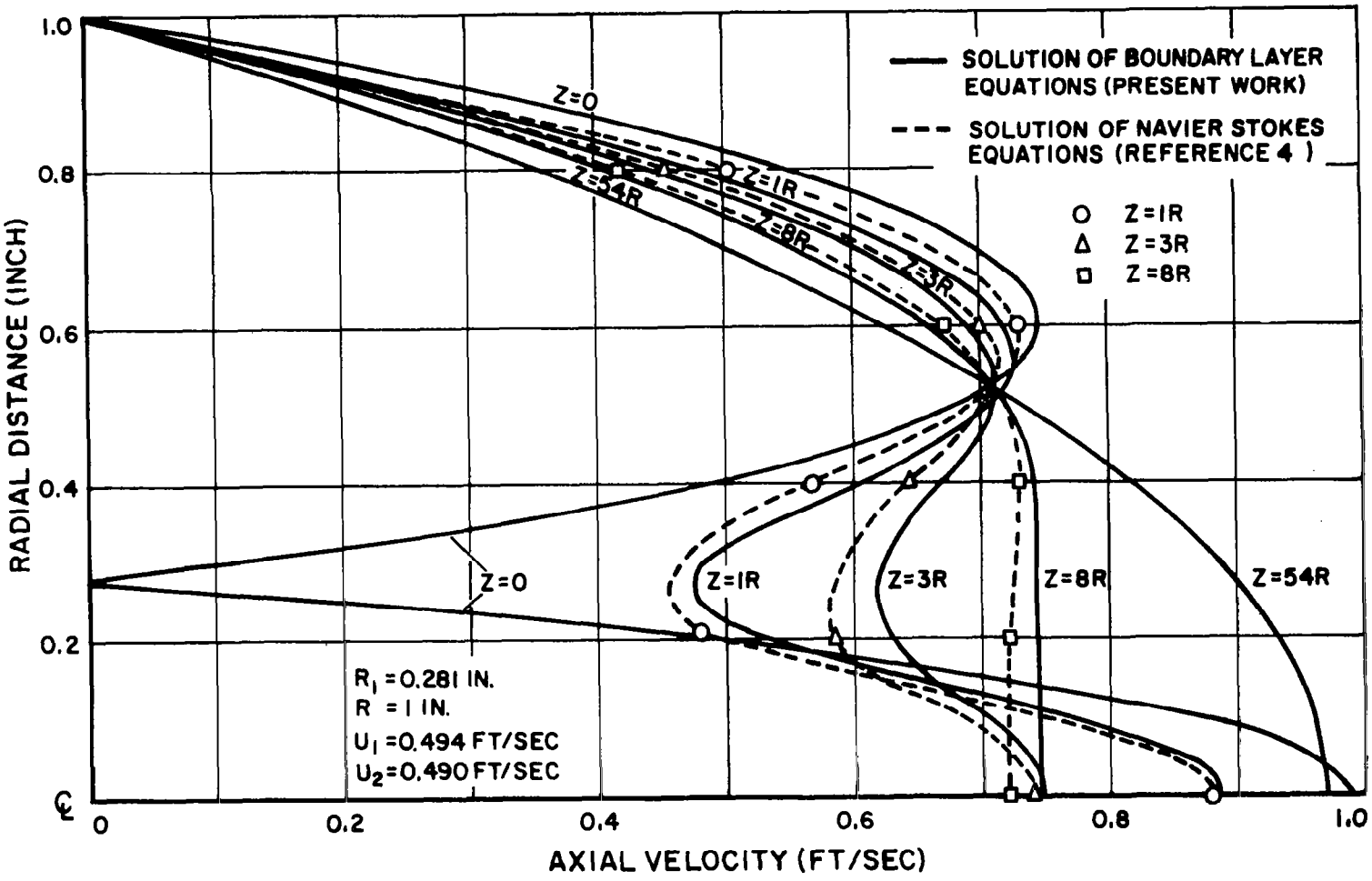

FIGURE 17. AXIAL VELOCITY PROFILES FOR STEADY CONFINED JET MIXING CONFIGURATION 3

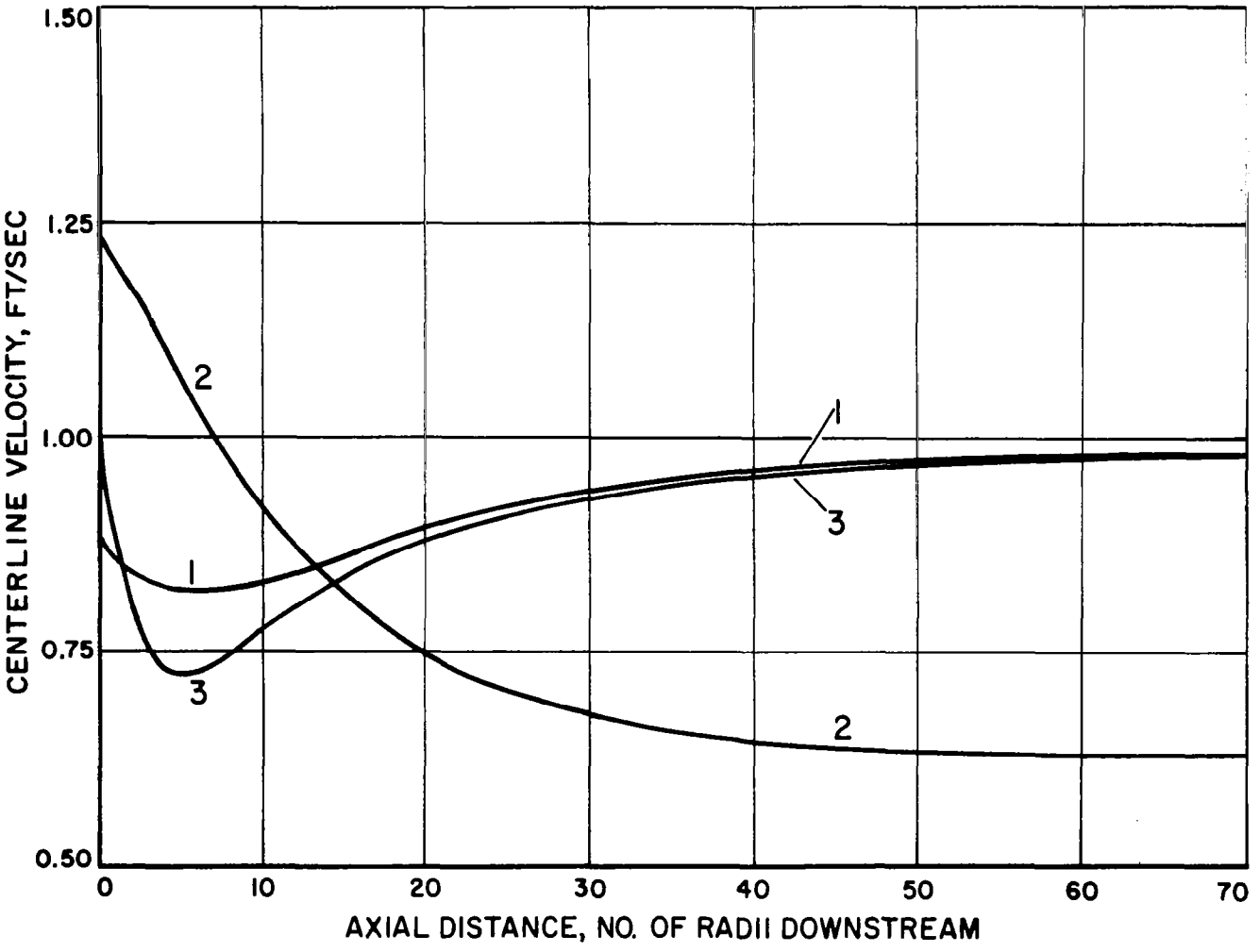

FIGURE 18. CENTERLINE VELOCITY VS AXIAL DISTANCE DOWNSTREAM FOR STEADY CONFINED JET MIXING CONFIGURATIONS 1, 2, 3

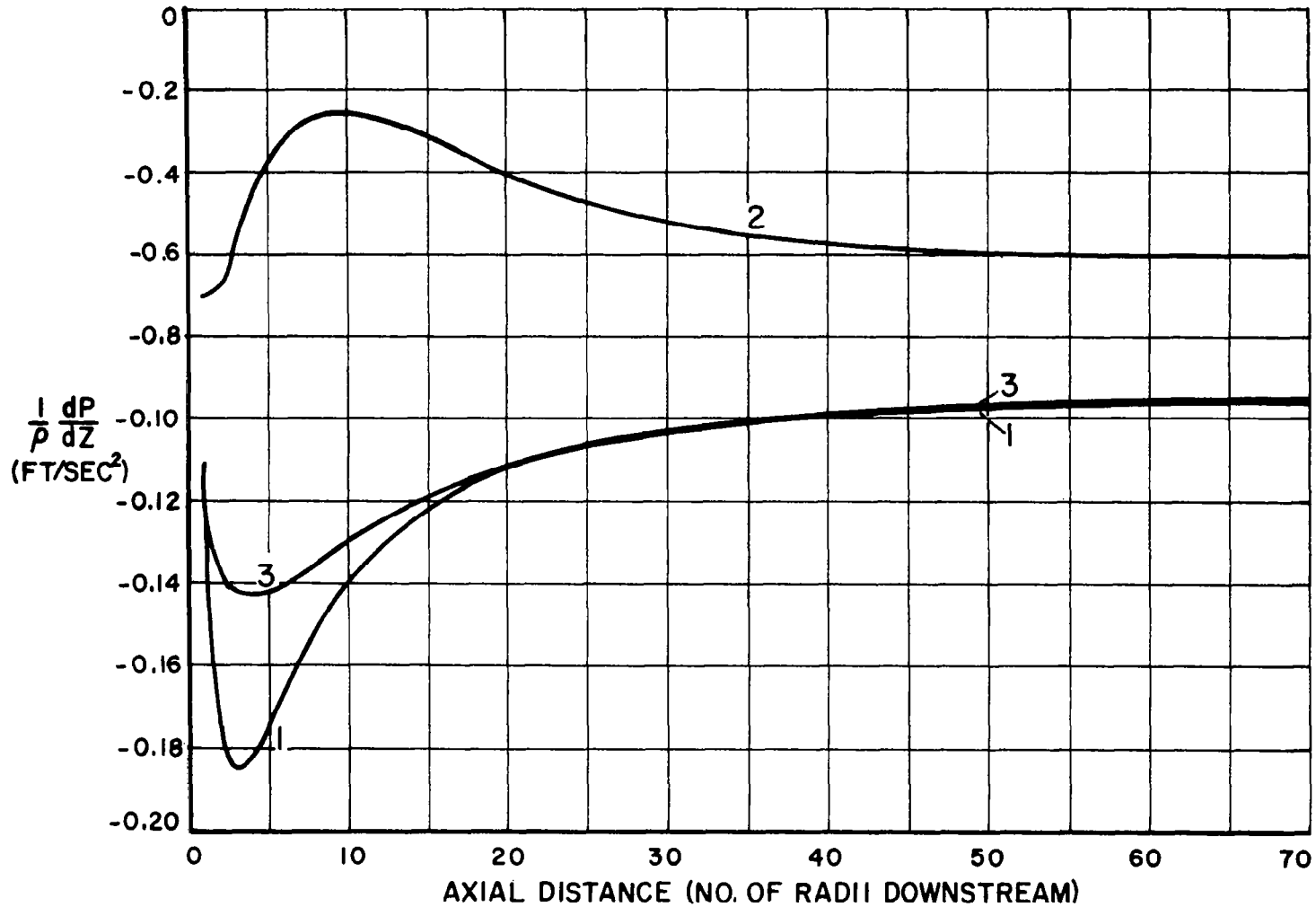

FIGURE 19. $\frac{1}{\rho}\frac{dP}{dZ}$ VS AXIAL DISTANCE DOWNSTREAM FOR STEADY CONFINED JET MIXING CONFIGURATIONS 1, 2, 3

maintained. The radial velocity is zero throughout. These conditions are maintained at the entrance section for all future times. Velocity profiles are then computed over the flow region as it develops with increasing time.

Figure 20 shows the developing axial velocity profiles at various axial positions. Comparison shows that the centerline velocities deviate by a maximum of twelve per cent, whereas the maximum deviation in the axial velocities near the wall, i.e., at $r = 0.8R$, is about 6.5 per cent. The results indicate that the time required to attain steady state increases with increasing downstream distance. The flow field investigated is limited to a downstream distance $z = 100R$. This region of the flow reaches its steady state in less than seven seconds. The steady state value of the centerline velocity at $z = 100R$ is about 1.77 times the initial uniform velocity. Thus, the development length for this impulsively started entrance flow is greater than 100R.

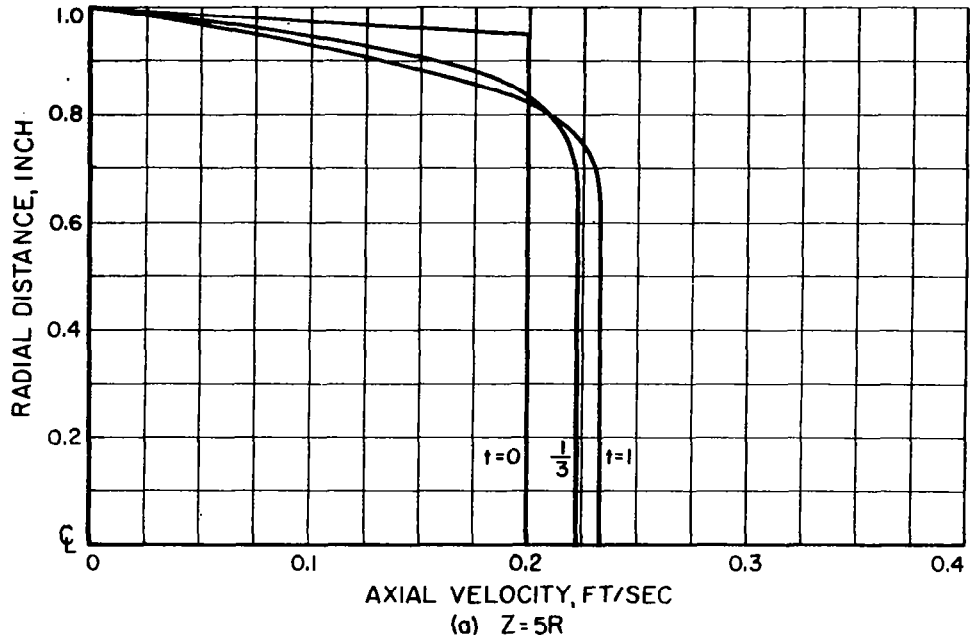

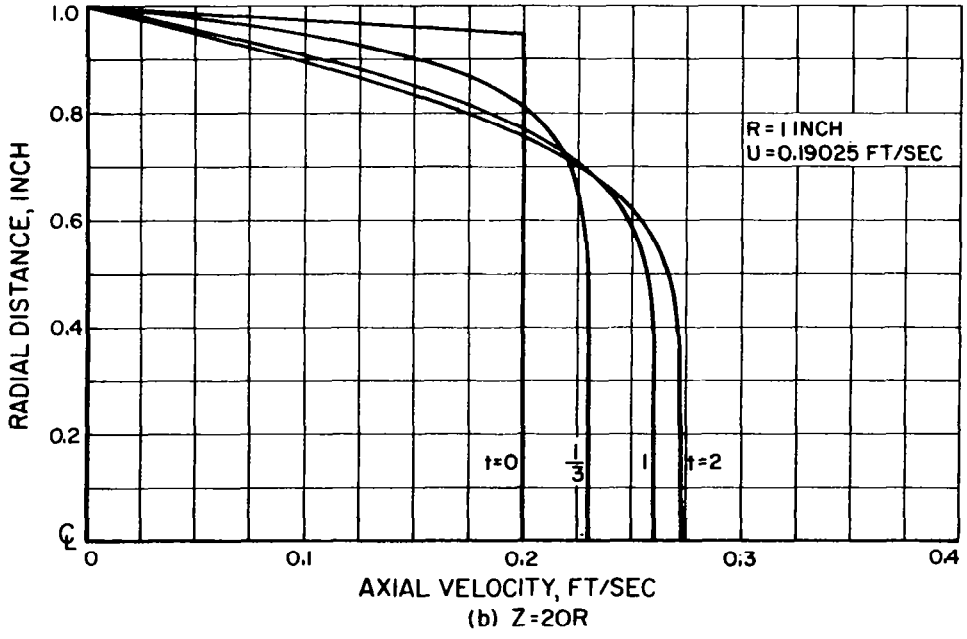

FIGURE 20. AXIAL VELOCITY PROFILES FOR IMPULSIVELY STARTED ENTRANCE FLOW

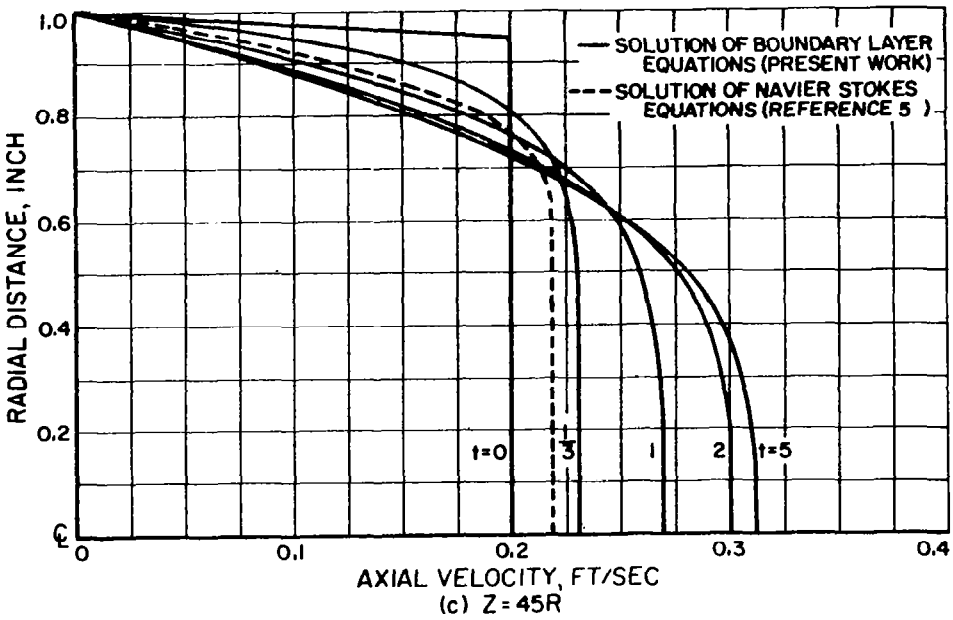

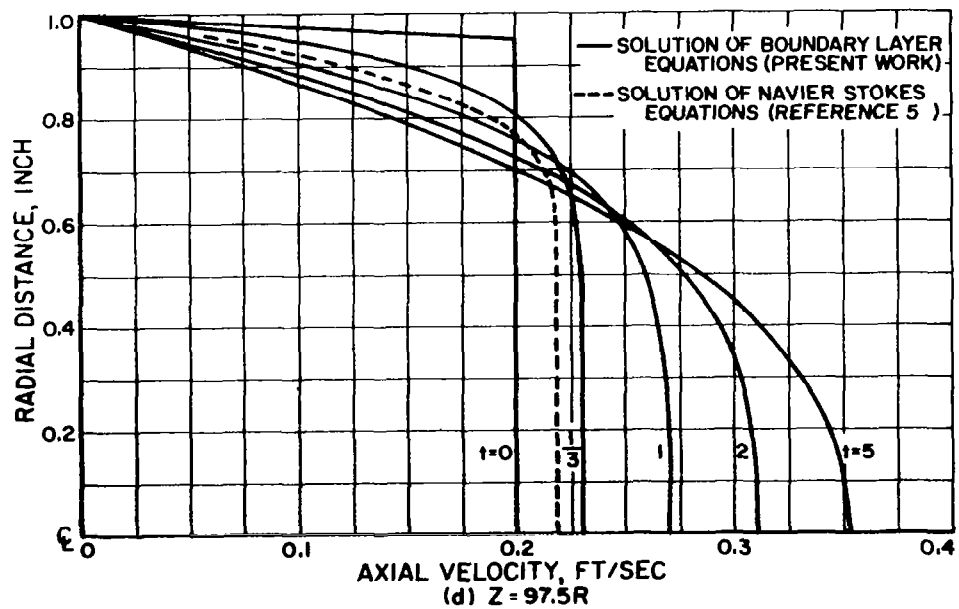

FIGURE 20. concluded. AXIAL VELOCITY PROFILES FOR IMPULSIVELY STARTED ENTRANCE FLOW

CHAPTER V
CONCLUSION

The method developed provides a means for numerical investigation of time-dependent laminar incompressible boundary layer flows with axial symmetry. The basic requirement for the applicability of the method is that the flow have an "open" downstream boundary. Hence, flows with obstacles in their path may not be effectively treated. The scheme of computation is explicit in all the independent variables of the initial-boundary value flow problem. Numerical stability is assured by satisfying Karplus' criterion at all points of the computation field.

The main features of the method are summarized in the following:

Any type of transverse boundary conditions, upstream boundary conditions and initial conditions can be handled without affecting the basic method of computation. No downstream boundary condition is needed.

Axial pressure gradient is computed at each axial location studied. Hence, flows confined within finite boundaries in the transverse direction can be directly studied.

Several of the assumptions of Chapter II are made only to reduce the number of computations. Some of these simplifying assumptions can be relaxed and the flow investigated, with no basic changes in the method of solution. Thus, specified variations of fluid properties like density and viscosity, inhomogeneity of the fluid media, heat transfer and chemical reaction can also be considered, though at the increased expense of computer time and memory.

The mesh size is limited by considerations of numerical stability

and required accuracy and problem resolution. Therefore, large computer memory and computer time are the major requirements for obtaining a solution. In fact, these requisites are always associated with all-numerical solution of problems involving more than two unbounded independent variables, regardless of whether the computation scheme is explicit or implicit. The explicit scheme involves simple and elementary computations at a large number of points for a given region. Unconditionally stable implicit schemes involve less straightforward computations (like iterations and matrix inversions) at a comparatively smaller number of points for the same region. Hence, obtaining the solution using either of the schemes may require comparable computer time. The investigation carried out for steady flows shows a much smaller computer time requirement for the explicit scheme while still maintaining close agreement with the results of the implicit scheme. Further, if high resolution is desired, small mesh size would have to be retained, and the increased computation time required would then render the use of implicit schemes less feasible [44]. Also, implicit schemes may not be recommended for solving a system of highly coupled equations in several variables because of the complicated computer program needed.

The method is used to obtain the transient response of steady, confined, jet mixing to superimposed velocity fluctuations. The investigation is mainly confined to the case with Reynolds' numbers of 1650 for the jet and 1400 for the surrounding annulus. A sinusoidal oscillation of amplitude equal to five per cent of the local axial velocity, is superimposed on the axial velocity at the jet exit section. The response of the mixing region is observed (numerically) for various

frequencies of the superimposed oscillation. Only a partial study was possible with the computer facilities available. No general conclusions may be drawn based on the results of these limited investigations although the following remarks can be made regarding the resulting flow:

The resulting flow field oscillates about its initial steady state at the same frequency as that of the superimposed fluctuations.

The transient time for the resulting flow field increases with increase in frequency of the superimposed oscillations.

The superimposed wave retains its sinusoidal form for low frequency oscillations, but undergoes distortion at higher frequencies, the extent of distortion increasing with increase in frequency.

For low frequencies, the envelope of the wave in the resulting flow, consists of nearly parallel straight lines, symmetric about the line of zero deviation from the steady state. At high frequencies, the envelope oscillates, though at a much reduced frequency. The axis of the envelope shifts in the direction of positive deviation from the initial steady state, the extent of this shift increases with increase in the superimposed frequency.

The high-frequency oscillations which undergo considerable distortion for the flow configuration with Reynolds' numbers of 1650 (jet), 1400 (surrounding annulus) and 2900 (overall flow) show no such behavior when the Reynolds' numbers are reduced to 250, 228, and 496 respectively. It may be mentioned here that the former flow undergoes transition to turbulence at a downstream distance of 1-1/2 pipe diameters while the latter remains laminar upto z = 40R downstream [4]. It may be, therefore, suspected that the difference in response of the two flow configurations

to the same superimposed oscillations may be due to hydrodynamic stability of the basic flows.

An impulsive change, or a step change, superimposed on the axial velocity along a circular ring near the jet exit shows no oscillations or any appreciable effects in the resulting flow.

The region of positive pressure gradient occurring close to the jet exit section is much smaller for the configuration with the reduced Reynolds' numbers than for the case with the higher Reynolds' numbers.

As previously mentioned, the limited downstream distance and physical time investigated and the limited parametric study carried out prevent conclusive statements to be made at this stage. Further investigations are indicated. Also, it may be worthwhile to carry out the same study using the time-dependent Navier Stokes equations in order to confirm the validity of the use of the boundary layer equations. If the general nature of the two solutions is similar, the possibility of the boundary layer equations being capable of predicting hydrodynamic stability of confined flows may be considered.

Several steady flow configurations are investigated and the results compared with the available corresponding solutions of either the boundary layer equations obtained by using implicit computation schemes or of the Navier Stokes equations obtained by using iterative methods. Comparison of results for time-independent problems with the corresponding solution of the Navier Stokes equations shows a maximum deviation of about twelve per cent. The general nature of both solutions is similar. The computer time required for solution is much smaller with the explicit scheme developed. Hence, flows for which the boundary layer approximations may be justified can be treated by

the method developed. This may however represent a compromise between the degree of correctness of the solution and the effort and time needed to obtain it.

APPENDIX A
DERIVATION OF EQUATION OF CONSTRAINT FROM THE DIFFERENTIAL FORM OF THE CONTINUITY EQUATION

The equation of constraint given by Equation (13) may be derived by integrating the continuity equation (4) over a complete cross-section.

Rewriting Equation (4) in the following form

$$\frac{\partial}{\partial r}(r\, v_r) + \frac{\partial}{\partial z}(r\, v_z) = 0 \tag{A.1}$$

and integrating with respect to r over the interval $0 \leq r \leq R$ leads to the equation

$$\int_0^R \frac{\partial}{\partial r}(r\, v_r)\, dr + \int_0^R \frac{\partial}{\partial z}(r\, v_z)\, dr = 0 \tag{A.2}$$

i.e.,

$$\left[r\, v_r\right]_{r=0}^{r=R} + \int_0^R r \frac{\partial v_z}{\partial z}\, dr = 0 \tag{A.3}$$

The first term in the above equation vanishes because of the center-line boundary condition (6) and the wall boundary condition (7). Therefore Equation (A.3) reduces to

$$\int_0^R r \frac{\partial v_z}{\partial z}\, dr = 0 \tag{A.4}$$

which is the same as Equation (13) in Chapter II.

APPENDIX B
DEFINITIONS OF CONSISTENCY, NUMERICAL STABILITY AND CONVERGENCE

A FDE is consistent with its corresponding PDE if the truncation error in the difference equation goes to zero as the spatial and the time steps approach zero.

A FDE is stable if its numerical solution remains uniformly bounded as the computations advance indefinitely under a set of time and space intervals, at least one of which is fixed (bounded). In general, stability is a function of only the difference equations and the boundary and initial conditions, and has no direct connection with the differential problem.

The exact solution of a FDE converges to the exact solution of its corresponding PDE if the truncation error of the solution goes to zero as the space and time steps approach zero.

Consistency and stability, considered individually, are only necessary, not sufficient for convergence. But consistency and stability together constitute the necessary as well as sufficient conditions of convergence for a properly posed initial value problem [40].

APPENDIX C
TRUNCATION ERRORS OF THE FINITE DIFFERENCE EQUATIONS

The finite difference approximations, given by expressions (20), (21), (22) are generated by expanding the function ϕ in a Taylor's series about the point (m,n,k). Thus

$$\phi(m+1,n,k) = \phi(m,n,k) + \Delta x \left.\frac{\partial \phi}{\partial x}\right|_{(m,n,k)} + \frac{(\Delta x)^2}{2!} \left.\frac{\partial^2 \phi}{\partial x^2}\right|_{(m,n,k)}$$

$$+ \frac{(\Delta x)^3}{3!} \left.\frac{\partial^3 \phi}{\partial x^3}\right|_{(m,n,k)} + \ldots \qquad (C.1)$$

Also,

$$\phi(m-1,n,k) = \phi(m,n,k) - \Delta x \left.\frac{\partial \phi}{\partial x}\right|_{(m,n,k)} + \frac{(\Delta x)^2}{2!} \left.\frac{\partial^2 \phi}{\partial x^2}\right|_{(m,n,k)}$$

$$- \frac{(\Delta x)^3}{3!} \left.\frac{\partial^3 \phi}{\partial x^3}\right|_{(m,n,k)} + \ldots \qquad (C.2)$$

The function $\phi(m,n,k)$ is assumed to possess continuous partial derivatives of the orders appearing in Equations (C.1) and (C.2) above.

The truncation errors of the finite difference approximations are then given as below:

$$E_{fda} = \left.\frac{\partial \phi}{\partial x}\right|_{m,n,k} - \frac{\phi(m+1,n,k) - \phi(m,n,k)}{\Delta x}$$

where E_{fda} is the truncation error in the forward difference approximation to the first derivative, as given by Equation (20), i.e.,

$$E_{fda} = -\frac{\Delta x}{2}\frac{\partial^2\phi}{\partial x^2}\bigg|_{m,n,k} - \frac{(\Delta x)^2}{6}\frac{\partial^3\phi}{\partial x^3}\bigg|_{m,n,k} - \quad . \quad . \tag{C.3}$$

$$E_{bda} = \frac{\partial\phi}{\partial x}\bigg|_{m,n,k} - \left[\frac{\phi(m,n,k) - \phi(m-1,n,k)}{\Delta x}\right]$$

$$= \frac{\Delta x}{2}\frac{\partial^2\phi}{\partial x^2}\bigg|_{m,n,k} - \frac{(\Delta x)^2}{6}\frac{\partial^3\phi}{\partial x^3}\bigg|_{m,n,k} + \ . \ . \ . \tag{C.4}$$

where E_{bda} is the truncation error in the backward difference approximation to the first derivative as given by Equation (21).

The central difference approximation (22) is obtained by subtracting (C.2) from (C.1) and the corresponding truncation error is

$$E_{cda} = \frac{\partial\phi}{\partial x}\bigg|_{m,n,k} - \left[\frac{\phi(m+1,n,k) - \phi(m-1,n,k)}{2\Delta x}\right]$$

$$= -\frac{(\Delta x)^2}{6}\frac{\partial^3\phi}{\partial x^3}\bigg|_{m,n,k} - \ . \ . \ . \tag{C.5}$$

where E_{cda} is the truncation error in the central difference approximation to the first derivative as given by Equation (22).

The approximation to the second derivative obtained by adding (C.1) and (C.2) involves a truncation error given by

$$E_{2c} = \frac{\partial^2\phi}{\partial x^2}\bigg|_{m,n,k} - \left[\frac{\phi(m+1,n,k) - 2\phi(m,n,k) + \phi(m-1,n,k)}{(\Delta x)^2}\right]$$

$$= -\frac{(\Delta x)^2}{12}\frac{\partial^4\phi}{\partial x^4}\bigg|_{m,n,k} - \ . \ . \ . \tag{C.6}$$

where E_{2c} is the truncation error in the finite difference approximation to the second derivative at the point (m,n,k).

The following expressions are also useful in determining the

truncation errors of the finite difference equations to be considered subsequently:

$$E_{c_{1/2}} = \left.\frac{\partial \phi}{\partial x}\right|_{(m-1/2,n,k)} - \left[\frac{\phi(m,n,k) - \phi(m-1,n,k)}{\Delta x}\right]$$

$$= -\frac{(\Delta x)^2}{24}\left.\frac{\partial^3 \phi}{\partial x^3}\right|_{(m-1/2,n,k)} - \ldots \qquad (C.7)$$

where $E_{c_{1/2}}$ is the truncation error in the central difference approximation to the first derivative, at the point (m-1/2,n,k).

$$E_{m_{1/2}} = \phi(m-1/2,n,k) - \left[\frac{\phi(m,n,k) + \phi(m-1,n,k)}{2}\right]$$

$$= -\frac{(\Delta x)^2}{8}\left.\frac{\partial^2 \phi}{\partial x^2}\right|_{m-1,n,k} - \frac{(\Delta x)^3}{16}\left.\frac{\partial^3 \phi}{\partial x^3}\right|_{m-1,n,k} - \ldots \qquad (C.8)$$

where $E_{m_{1/2}}$ is the error of approximating $\phi(m-1/2,n,k)$ by the arithmetic mean of the values of ϕ at the points (m,n,k) and (m-1,n,k).

The Time-Dependent Equations

Momentum Equation. Substituting the expressions obtained earlier for the truncation errors in the various approximations used, the truncation error E_{TM} in the finite difference approximation (given by Equation (55)) to Equation (3) at the point (m,n,k+1) is obtained as follows

$$E_{TM} = \frac{\partial v_z}{\partial t} + v_r \frac{\partial v_z}{\partial r} + v_z \frac{\partial v_z}{\partial z} + \frac{1}{\rho}\frac{\partial p}{\partial z} - \nu \frac{\partial^2 v_z}{\partial r^2} - \frac{\nu}{r}\left(\frac{\partial v_z}{\partial r}\right) -$$

$$\left[\frac{v_z(m,n,k+1) - v_z(m,n,k)}{\Delta t} + \frac{1}{\rho} \frac{\partial p}{\partial z}\Big|_{(n,k+1)} \right.$$

$$+ v_r(m,n,k+1)\left[\frac{v_z(m+1,n,k+1) - v_z(m-1,n,k+1)}{2\Delta r}\right]$$

$$+ v_z(m,n,k+1)\left[\frac{v_z(m,n+1,k+1) - v_z(m,n,k+1)}{\Delta z}\right]$$

$$- \nu\left[\frac{v_z(m+1,n,k+1) - 2v_z(m,n,k+1) + v_z(m-1,n,k+1)}{(\Delta r)^2}\right]$$

$$\left. - \frac{\nu}{r(m)}\left[\frac{v_z(m+1,n,k+1) - v_z(m-1,n,k+1)}{2\Delta r}\right] \right] \qquad (C.9)$$

$$= \frac{\Delta t}{2} \frac{\partial^2 v_z}{\partial t}\Big|_{(m,n,k+1)} - v_r(m,n,k+1) \frac{\Delta r^2}{6} \frac{\partial^3 v_z}{\partial r^3}\Big|_{(m,n,k+1)}$$

$$- v_z(m,n,k+1) \frac{\Delta z}{2} \frac{\partial^2 v_z}{\partial z^2}\Big|_{(m,n,k+1)}$$

$$+ \nu \frac{\Delta r^2}{12} \frac{\partial^4 v_z}{\partial r^4}\Big|_{(m,n,k+1)} + \frac{\nu}{r(m)} \frac{\Delta r^2}{6} \frac{\partial^3 v_z}{\partial r^3}\Big|_{(m,n,k+1)}$$

$$+ (\text{terms containing higher powers of } \Delta r, \Delta z, \Delta t) \qquad (C.10)$$

E_{TM} is the truncation error in the time-dependent momentum equation.

Since $\left[\frac{\partial p}{\partial z}\right]_{(n,k+1)}$ is evaluated by manipulation of the momentum and the continuity equations, no additional error is involved due to this term in Equation (C.9).

Since all quantities appearing in the expression (C.10) for E_{TM}

are evaluated at the point (m,n,k+1), the subscripts are omitted in the following expression and

$$E_{TM} = \Delta t\left[\frac{1}{2}\frac{\partial^2 v_z}{\partial t^2}\right] + \Delta z\left[-\frac{1}{2}v_z\frac{\partial^2 v_z}{\partial z^2}\right]$$

$$+ (\Delta r)^2\left[-\frac{1}{6}v_r\frac{\partial^3 v_z}{\partial r^3} + \frac{\nu}{12}\frac{\partial^4 v_z}{\partial r^4} + \frac{\nu}{6r(m)}\frac{\partial^3 v_z}{\partial r^3}\right]$$

$$+ (\text{terms containing higher powers of } \Delta r, \Delta z, \Delta t) \qquad (C.11)$$

Now, from physical considerations, it may be claimed that the quantities appearing as coefficients of Δt, Δz and $(\Delta r)^2$ in Equation (C.11) are bounded. Therefore, there exist three constants C_1, C_2 and C_3, such that these coefficients are less than or equal to the constants C_1, C_2 and C_3, respectively, i.e.,

$$E_{TM} \leq C_1\Delta t + C_2\Delta z + C_3\Delta r^2 \qquad (C.12)$$

Therefore, as Δt, Δz and Δr approach zero, the truncation error E_{TM} vanishes. This establishes that the FDE given by Equation (55) is a consistent representation of the PDE given by Equation (3).

Momentum Equation at the Centerline. The truncation error E_{TM_a} involved in approximating the centerline momentum Equation (3a) by the finite difference equation (62) is obtained as

$$E_{TM_a} = \frac{\partial v_z}{\partial t} + v_z\frac{\partial v_z}{\partial z} + \frac{1}{\rho}\frac{\partial p}{\partial z} - 2\nu\frac{\partial^2 v_z}{\partial r^2} -$$

$$\left[\frac{v_z(m,n,k+1) - v_z(m,n,k)}{\Delta t} + \frac{1}{\rho} \left.\frac{\partial p}{\partial z}\right|_{(n,k+1)} \right.$$

$$+ v_z(m,n,k+1) \left[\frac{v_z(m,n+1,k+1) - v_z(m,n+1,k+1)}{\Delta z} \right]$$

$$\left. - 2\nu \left[\frac{2v_z(m+1,n,k+1) - 2v_z(m,n,k+1)}{(\Delta r)^2} \right] \right] \qquad (C.13)$$

i.e.,

$$E_{TM_a} = \frac{\Delta t}{2} \left.\frac{\partial^2 v_z}{\partial t^2}\right|_{(m,n,k+1)} - v_z(m,n,k+1) \frac{\Delta z}{2} \left.\frac{\partial^2 v_z}{\partial z^2}\right|_{(m,n,k+1)}$$

$$+ 2\nu \frac{\Delta r^2}{12} \left.\frac{\partial^4 v_z}{\partial r^4}\right|_{(m,n,k+1)}$$

$$+ \text{(terms containing higher powers of } \Delta r, \Delta z, \Delta t) \qquad (C.14)$$

where E_{TM_a} is the truncation error in the time-dependent momentum equation at the centerline.

Dropping the subscripts (m,n,k+1),

$$E_{TM_a} = \Delta t \left[\frac{1}{2} \frac{\partial^2 v_z}{\partial t^2} \right] + \Delta z \left[-\frac{1}{2} v_z \frac{\partial^2 v_z}{\partial z^2} \right] + \left[\frac{\nu}{6} \frac{\partial^4 v_z}{\partial r^4} \right] (\Delta r)^2$$

$$+ \text{(terms containing higher powers of } \Delta r, \Delta z, \Delta t) \qquad (C.15)$$

This may be re-written as

$$E_{TM_a} \leq C_4 \Delta t + C_5 \Delta z + C_6 \Delta r^2 \qquad (C.16)$$

where C_4, C_5, C_6 are constants, used to replace the bounded coefficients

of $(\Delta r)^2$, Δz and Δt in Equation (C.15).

From (C.16), it follows that the truncation error E_{TM_a} vanishes as Δt, Δz, Δr approach zero, showing thereby that Equation (62) which approximates Equation (30) satisfies the consistency condition.

Continuity Equation. The truncation error E_{TC} in approximating the partial differential equation (4) by the finite difference equation (69) is given by

$$E_{TC} = \frac{v_r}{r} + \frac{\partial v_r}{\partial r} + \frac{\partial v_z}{\partial z}$$

$$\left[\frac{v_r(m,n+1,k+1) + v_r(m-1,n+1,k+1)}{r(m-1/2)} + \frac{v_r(m,n+1,k+1) - v_r(m-1,n+1,k+1)}{\Delta r} \right.$$

$$\left. - \frac{v_z(m,n+1,k+1) - v_z(m,n,k+1)}{2\Delta z} + \frac{v_z(m-1,n+1,k+1) - v_z(m-1,n,k+1)}{2\Delta z} \right] \qquad (C.17)$$

$$= - \frac{1}{r(m-1/2)} \cdot \frac{\Delta r^2}{8} \frac{\partial^2 v_r}{\partial r^2}\bigg|_{(m-1,n+1,k+1)} - \frac{\Delta r^2}{24} \frac{\partial^3 v_r}{\partial r^3}\bigg|_{(m-1/2,n+1,k+1)}$$

$$+ \frac{\Delta z}{2}\left[\frac{\partial^2 v_z}{\partial z^2}\bigg|_{(m,n+1,k+1)} + \frac{\partial^2 v_z}{\partial z^2}\bigg|_{(m-1,n+1,k+1)} \right]$$

$$- \frac{\Delta r^2}{8} \frac{\partial^2 v_z}{\partial r^2}\bigg|_{(m-1,n+1,k+1)}$$

$$+ \text{(terms containing higher powers of } \Delta r, \Delta z, \Delta t) \qquad (C.18)$$

$$= \Delta r^2 \begin{bmatrix} -\frac{1}{8}\frac{1}{r(m-1/2)} \cdot \left.\frac{\partial^2 v_r}{\partial r^2}\right|_{(m-1,n+1,k+1)} \\ -\frac{1}{24}\left.\frac{\partial^3 v_r}{\partial r^3}\right|_{(m-1/2,n+1,k+1)} \\ -\frac{1}{8}\left.\frac{\partial^2 v_z}{\partial r^2}\right|_{(m-1,n+1,k+1)} \end{bmatrix}$$

$$+ \Delta z \left[\frac{1}{2}\left.\frac{\partial^2 v_z}{\partial z^2}\right|_{(m,n+1,k+1)} + \frac{1}{2}\left.\frac{\partial^2 v_z}{\partial z^2}\right|_{(m-1,n+1,k+1)} \right] \qquad (C.19)$$

Again, the coefficients of $(\Delta r)^2$ and Δz, being bounded, expression (C.19) may be written as:

$$E_{TC} \leq C_7 \Delta r^2 + C_8 \Delta z \qquad (C.20)$$

where C_7 and C_8 are bounded constants.

Therefore, for sufficiently small Δz and Δr, the truncation error in the approximating equation goes to zero as Δz, Δr approach zero.

Hence the finite difference representation (69) of the continuity equation (4) satisfies the consistency condition.

The Time-Independent Equations

The essential differences in the differential equations describing the time-dependent problem and the time-independent problem are

i) the dependent variables in the time-dependent problem are functions of three independent variables - r, z, t. The dependent variables in the time-independent problem are function of r, z only, and

ii) the momentum equation for the time-dependent problem contains the additional term $\frac{\partial v_z}{\partial t}$ which vanishes in the time-independent problem.

The differencing scheme for the r and the z-derivatives is the same in both cases, i.e., r-derivatives are approximated by central differences, and z-derivatives by forward differences in the momentum equation and backward in the continuity equations.

The expressions for the truncation errors in the time-independent equations are therefore obtainable directly from the corresponding expressions for the time-dependent equations by setting $\Delta t = 0$.

Thus, the finite difference equations approximating the differential equations governing the time-independent problem may be shown to satisfy the consistency condition.

APPENDIX D
KARPLUS' CRITERION FOR NUMERICAL STABILITY OF FINITE DIFFERENCE EQUATIONS

Karplus [39] developed a criterion for stability of finite difference equations, based on the stability analysis of an electric network since the equilibrium equations for the network are similar to the FDE considered.

The FDE whose stability at the point (m,n,k) is to be considered is arranged in the following form

$$\sum_{i,j,\ell=0,1} A_{ij\ell} \left(\phi_{m\pm i,n\pm j,k\pm \ell} - \phi_{m,n,k}\right) = 0 \qquad (D.1)$$

where the subscript "m" refers to a bounded space co-ordinate. Then the FDE is stable if

i) the coefficients $A_{ij\ell}$ are all of the same sign (D.2)

or

ii) when all $A_{ij\ell}$ are not of the same sign then

a) for $A_{1,0,0} > 0$;

$$\sum_{i,j,\ell=0,1} A_{ij\ell} < 0 \qquad (D.3a)$$

and

b) for $A_{1,0,0} < 0$,

$$\sum_{i,j,\ell=0,1} A_{ij\ell} > 0 \qquad (D.3b)$$

In the above, i,j and ℓ are not equal simultaneously.

In general, it is always possible to arrange a FDE in the form of

Equation (D.1) if the FDE represents an approximation to a PDE.

The advantages of the above approach are that the criterion is simple to apply and does not require linearization of the equations. Without further complication, the criterion is also applicable to equations in several independent variables, and to equations in which the coefficients are functions of the independent variables. In several cases, the results are the same as those obtained by the more familiar methods of Hildebrand and von Neumann. The latter are comparatively complex to apply. Karplus' criterion is not over conservative if the specified boundary and initial conditions are taken into account.

APPENDIX E
STABILITY ANALYSIS OF THE FINITE DIFFERENCE EQUATIONS

The conditions for numerical stability of the FDE used in computing the problem variables are derived by using the method developed by Karplus [39].

The Time-Independent Equations

Momentum Equation. The FDE form of the momentum equation is given by Equation (23) which is used to compute the axial velocity $v_z(m,n+1)$ by the resulting explicit expression (24). To analyse the stability of Equation (23) it is re-written in the form corresponding to Equation (D.1), to yield the equation

$$\left[v_z(m+1,n) - v_z(m,n)\right]\left(\frac{v_r(m,n)}{2\Delta r} - \frac{\nu}{(\Delta r)^2} - \frac{\nu}{2r(m)\Delta r}\right)$$

$$+ \left[v_z(m-1,n) - v_z(m,n)\right]\left(-\frac{v_r(m,n)}{2\Delta r} - \frac{\nu}{(\Delta r)^2} + \frac{\nu}{2r(m)\Delta r}\right)$$

$$+ \left[v_z(m,n+1) - v_z(m,n)\right]\left(\frac{v_z(m,n)}{\Delta z}\right) - \frac{1}{\rho}\left(\frac{dp}{dz}\right)_n = 0 \qquad \text{(E.1)}$$

Next, it is necessary to determine the sign of the coefficients of the square bracketed terms in Equation (E.1)

i) Coefficient of $\left[v_z(m+1,n) - v_z(m,n)\right]$

a) If $v_r(m,n)$ is negative, the coefficient

$$\left(\frac{v_r(m,n)}{2\Delta r} - \frac{\nu}{(\Delta r)^2} - \frac{\nu}{2r(m)}\Delta r\right) < 0 \qquad \text{(E.2)}$$

with no restrictions on Δr.

b) If $v_r(m,n) > 0$, this coefficient is considered as

$$\frac{v_r(m,n)}{2\Delta r} - \frac{\nu}{(\Delta r)^2} - \frac{\nu}{2r(m)\Delta r}$$

$$= \frac{\nu}{(\Delta r)^2}\left(\frac{v_r(m,n)}{2\nu}\Delta r - 1 - \frac{\Delta r}{2r(m)}\right) \qquad (E.3)$$

Now,

$$r(m) = (m-1)\Delta r.$$

Therefore, Equation (E.3) may be re-written as

$$\frac{v_r(m,n)}{2\Delta r} - \frac{\nu}{(\Delta r)^2} - \frac{\nu}{2r(m)\Delta r}$$

$$= \frac{\nu}{(\Delta r)^2}\left(\frac{v_r(m,n)}{2\nu}\Delta r - 1 - \frac{1}{2m-2}\right)$$

$$= \frac{\nu}{(\Delta r)^2}\left(\frac{v_r(m,n)}{2\nu}\Delta r - \frac{2m-1}{2m-2}\right) \qquad (E.4)$$

Hence, for $v_r(m,n) > 0$, the coefficient under consideration is negative when

$$\frac{v_r(m,n)}{2\nu}\Delta r < \frac{2m-1}{2m-2} \qquad (E.5)$$

i.e.,

$$\Delta r < \frac{2\nu}{v_r(m,n)}\left(\frac{2m-1}{2m-2}\right) \qquad (E.6)$$

It may be noted that, if the inequality

$$\Delta r < \frac{2\nu}{v_r(m,n)} \qquad (E.7)$$

is satisfied, then inequality (E.6) will also be satisfied.

ii) Coefficient of $\left[v_z(m-1,n) - v_z(m,n)\right]$ may be written as

$$- \frac{v_r(m,n)}{2\Delta r} - \frac{\nu}{(\Delta r)^2} + \frac{\nu}{2r(m)\Delta r}$$

$$= \frac{\nu}{(\Delta r)^2}\left(- \frac{v_r(m,n)}{2\nu}\Delta r - 1 + \frac{\Delta r}{2r(m)}\right)$$

$$= \frac{\nu}{(\Delta r)^2}\left(- \frac{v_r(m,n)}{2\nu}\Delta r - 1 + \frac{1}{2m-2}\right)$$

i.e.,

$$- \frac{v_r(m,n)}{2\Delta r} - \frac{\nu}{(\Delta r)^2} + \frac{\nu}{2r(m)\Delta r}$$

$$= \frac{\nu}{(\Delta r)^2}\left(- \frac{v_r(m,n)}{2\nu}\Delta r - \frac{2m-3}{2m-2}\right) \qquad (E.8)$$

a) If $v_r(m,n) < 0$, Equation (E.8) yields that the coefficient under consideration is negative if

$$\Delta r < \frac{2}{|v_r(m,n)|}\left(\frac{2m-3}{2m-2}\right) \qquad (E.9)$$

b) If $v_r(m,n) > 0$, the coefficient is always negative.

iii) Coefficient of $\left[v_z(m,n+1) - v_z(m,n)\right]$ is positive for $v_z(m,n) > 0$. Since backflow is excluded from consideration, this coefficient will be only positive.

Thus, the coefficients are not all of the same sign. Hence, Equation (24) is not unconditionally stable.

The conditions for stability of Equation (24) are then obtained by employing the conditions (D.3a) and (D.3b) of Karplus' method.

a) If $v_r(m,n) < 0$, Equation (24) is stable if

$$- \frac{2\nu}{(\Delta r)^2} + \frac{v_z(m,n)}{\Delta z} > 0 \qquad \text{(E.10)}$$

i.e., if

$$\Delta z < \frac{v_z(m,n)}{2\nu} (\Delta r)^2 \qquad \text{(E.11)}$$

where Δr is not limited from stability considerations, and is selected by considering the physical problem.

b) If $v_r(m,n) > 0$, then the conditions of stability are given by the inequalities (E.7) and (E.11)

$$\Delta r < \frac{2\nu}{v_r(m,n)} \qquad \text{(E.7)}$$

and

$$\Delta z < \frac{v_z(m,n)}{2\nu} (\Delta r)^2 \qquad \text{(E.11)}$$

Momentum Equation at the Centerline. At the centerline the finite difference form of the momentum equation is given by Equation (29). Arranging it in the form corresponding to Equation (D.1) results in the equation

$$\left[v_z(m+1,n) - v_z(m,n)\right]\left(- \frac{4\nu}{(\Delta r)^2}\right)$$

$$+ \left[v_z(m,n+1) - v_z(m,n)\right]\left(\frac{v_z(m,n)}{\Delta z}\right) - \frac{1}{\rho}\left[\frac{dp}{dz}\right]_n = 0 \qquad \text{(E.12)}$$

It is necessary to examine the coefficients of the square bracketed

terms for their signs.

The coefficient of the first term is always negative.

The coefficient of the second term is positive for $v_z(m,n) > 0$, i.e., for flows without backflows like the ones under study.

Therefore, the conditions for stability of Equation (E.12) may be determined by using condition (D.3b) of Karplus' criterion.

Thus, Equation (E.12) is stable if

$$-\frac{4\nu}{(\Delta r)^2} + \frac{v_z(m,n)}{\Delta z} > 0 \qquad \text{(E.13)}$$

i.e., if

$$\Delta z < \frac{v_z(m,n)}{4\nu}(\Delta r)^2 \qquad \text{(E.14)}$$

where stability imposes no restriction on the size of Δr.

Continuity Equation. Equation (41) is the finite difference form of the continuity equation and is used to compute the radial velocity v_r by the resulting expression (43).

For investigating its numerical stability by Karplus' method, it must be arranged in the form corresponding to Equation (D.1). Since the continuity equation is written at the points (m-1/2,n+1), the various terms in v_r must be pivoted about the value $v_r(m-1/2,n+1)$. Since this value does not actually appear in Equation (41), such arrangement yields equal and opposite coefficients for the difference terms. Hence, no information regarding stability is obtainable in this manner.

Recalling that (m-1/2,n+1) are but fictitious points, Equation (41) is arranged to correspond to Equation (D.1) by pivoting the

terms in v_r about the value $v_r(m-1,n+1)$. Thus,

$$\left[v_r(m,n+1) - v_r(m-1,n+1)\right]\left(\frac{1}{2m-3} + 1\right)\frac{1}{\Delta r}$$

$$+ \left(\frac{2}{2m-3}\right)\frac{1}{\Delta r}\, v_r(m-1,n+1)$$

$$+ \frac{v_z(m,n+1) - v_z(m,n) + v_z(m-1,n+1) - v_z(m-1,n)}{2\Delta z}$$

$$= 0 \qquad \text{(E.15)}$$

Only one pertinent difference term appears so that the continuity equation is unconditionally stable. The terms in v_z may not enter the stability condition in any case, since they appear as known through earlier stable computations and cannot contribute to instability.

The Time-Dependent Equations

Momentum Equation. Equation (55) is the finite difference form of the time-dependent momentum equation. Re-arranging it to correspond to the form of Equation (D.1) gives

$$\left[v_z(m+1,n,k+1) - v_z(m,n,k+1)\right]\left(\frac{v_r(m,n,k+1)}{2\Delta r} - \frac{\nu}{(\Delta r)^2} - \frac{\nu}{2r(m)\Delta r}\right)$$

$$+ \left[v_z(m-1,n,k+1) - v_z(m,n,k+1)\right]\left(-\frac{v_r(m,n,k+1)}{2\Delta r} - \frac{\nu}{(\Delta r)^2} + \frac{\nu}{2r(m)\Delta r}\right)$$

$$+ \left[v_z(m,n+1,k+1) - v_z(m,n,k+1)\right]\left(\frac{v_z(m,n,k+1)}{\Delta z}\right)$$

$$+ \left[v_z(m,n,k) - v_z(m,n,k+1)\right]\left(-\frac{1}{\Delta t}\right) + \frac{1}{\rho}\left[\frac{\partial p}{\partial z}\right]_{(n,k+1)} = 0$$

(E.16)

The coefficients of the square bracketed quantities are next investigated for their sign.

i) Coefficient of $\left[v_z(m+1,n,k+1) - v_z(m,n,k+1)\right]$

a) If $v_r(m,n,k+1) < 0$, the coefficient is unconditionally negative.

b) If $v_r(m,n,k+1) > 0$, the coefficient is treated in a manner similar to that for the corresponding coefficient in Equation (23) of the time-independent problem.

Thus, for $v_r(m,n,k+1) > 0$, the coefficient is negative when

$$\Delta r < \frac{2\nu}{v_r(m,n,k+1)}\left[\frac{2m-1}{2m-2}\right] \tag{E.17}$$

The inequality (E.17) will be satisfied if

$$\Delta r < \frac{2\nu}{v_r(m,n,k+1)} \tag{E.18}$$

Condition (E.18) may be used rather than condition (E.17) to determine the value of Δr.

ii) Coefficient of $\left[v_z(m-1,n,k+1) - v_z(m,n,k+1)\right]$:

This coefficient is also considered by a similar approach as for the corresponding coefficient in Equation (23). Thus, the coefficient is re-written in the form

$$-\frac{v_r(m,n,k+1)}{\Delta r} - \frac{\nu}{(\Delta r)^2} + \frac{\nu}{2r(m)\Delta r}$$

$$= \frac{\nu}{(\Delta r)^2}\left(-\frac{v_r(m,n,k+1)}{2\nu} - \frac{2m-3}{2m-2}\right) \tag{E.19}$$

Therefore

a) If $v_r(m,n,k+1) < 0$, the coefficient under consideration is negative if

$$\Delta r < \frac{2\nu}{|v_r(m,n,k+1)|}\left(\frac{2m-3}{2m-2}\right) \qquad (E.20)$$

b) If $v_r(m,n,k+1) > 0$, the coefficient is always negative.

iii) Coefficient of $\left[v_z(m,n+1,k+1) - v_z(m,n,k+1)\right]$

For $v_z(m,n,k+1) > 0$, i.e., for flows without separation and backflow, this coefficient is positive. Since for the flows under consideration, $v_z(m,n,k+1)$ is non-negative, the coefficient $\frac{v_z(m,n,k+1)}{\Delta z}$ is unconditionally positive.

iv) Coefficient of $\left[v_z(m,n,k+1) - v_z(m,n,k)\right]$ is always negative.

Thus, the coefficients of the square bracketed terms in Equation (E.16) do not all have the same sign. Thus unconditional stability cannot be achieved under statement (D.2).

The sign of the first coefficient in Equation (E.16) is the factor for deciding which one of the conditions (D.3a) and (D.3b) provide the appropriate criterion for stability of Equation (55) and hence for the stability of Equation (56). Statement (D.3b) is found to be applicable. Therefore

a) For $v_r(m,n,k+1) < 0$, the scheme is stable if

$$-\frac{2\nu}{(\Delta r)^2} + \frac{v_z(m,n,k+1)}{\Delta z} - \frac{1}{\Delta t} > 0 \qquad (E.21)$$

From the inequality (E.21) it can be claimed that Equation (55), and hence Equation (56), is stable if

$$\Delta z < \frac{v_z(m,n,k+1)}{\frac{2\nu}{(\Delta r)^2} + \frac{1}{\Delta t}} \qquad (E.22)$$

where Δr and Δt are ascertained from physical considerations of the problem. Stability imposes no limitation on their magnitude.

b) For $v_r(m,n,k+1) > 0$, the conditions of stability are

$$\Delta r < \frac{2\nu}{v_r(m,n,k+1)} \qquad (E.23)$$

and

$$\Delta z < \frac{v_z(m,n,k+1)}{\frac{2\nu}{(\Delta r)^2} + \frac{1}{\Delta t}} \qquad (E.24)$$

where Δt is still free from stability restrictions.

Momentum Equation at the Centerline. The finite difference form of the centerline momentum equation is given by Equation (62). Re-arranging it in the form corresponding to Equation (D.1) results in the equation

$$\left[v_z(m+1,n,k+1) - v_z(m,n,k+1)\right]\left(-\frac{4\nu}{(\Delta r)^2}\right)$$

$$+\left[v_z(m,n+1,k+1) - v_z(m,n,k+1)\right]\left(\frac{v_z(m,n,k+1)}{\Delta z}\right)$$

$$+\left[v_z(m,n,k) - v_z(m,n,k+1)\right]\left(-\frac{1}{\Delta t}\right)$$

$$+\frac{1}{\rho}\left(\frac{\partial p}{\partial z}\right)_{(n,k+1)} = 0 \qquad (E.25)$$

An examination of the coefficients of the various square bracketed

terms reveals that

i) the first coefficient is always negative,

ii) the second coefficient is positive for the flows to be considered (i.e., for flows where $v_z \neq 0$)

iii) the third coefficient is always negative.

Therefore, statement (D.3b) of Karplus' criterion is applicable for determining the conditions for numerical stability of Equation (E.25) and hence of Equation (62). Consequently, Equation (62), and hence Equation (63) which resulted from Equation (62), is stable if

$$-\frac{4\nu}{(\Delta r)^2} + \frac{v_z(m,n,k+1)}{\Delta z} - \frac{1}{\Delta t} > 0 \qquad \text{(E.26)}$$

i.e., if

$$\Delta z < \frac{v_z(m,n,k+1)}{\frac{4\nu}{(\Delta r)^2} + \frac{1}{\Delta t}} \qquad \text{(E.27)}$$

where Δr and Δt are not limited by stability considerations.

APPENDIX F
DERIVATION OF EQUATION OF CONSTRAINT FROM FINITE DIFFERENCE FORM OF THE CONTINUITY EQUATION

The finite difference form of the continuity equation is given by Equation (43). This equation is re-written as follows

$$(m-1)\, v_r(m,n+1) - (m-2)\, v_r(m-1,n+1) + \frac{(2m-3)}{4} \frac{\Delta r}{\Delta z} \left[v_z(m,n+1) - v_z(m,n) + v_z(m-1,n+1) - v_z(m-1,n) \right] = 0 \qquad (F.1)$$

where $m=2,3,\ldots,M,M+1$.

For these values of m, Equation (F.1) yields

$$v_r(2,n+1) - v_r(1,n+1) + \frac{1}{4} \frac{\Delta r}{\Delta z} \left[v_z(2,n+1) - v_z(2,n) + v_z(1,n+1) - v_z(1,n) \right] = 0$$

$$2\, v_r(3,n+1) - v_r(2,n+1) + \frac{3}{4} \frac{\Delta r}{\Delta z} \left[v_z(3,n+1) - v_z(3,n) + v_z(2,n+1) - v_z(2,n) \right] = 0$$

$$\vdots \qquad (F.2)$$

$$(M-1)\, v_r(M,n+1) - (M-2)\, v_r(M-1,n+1) + \frac{2M-3}{4} \frac{\Delta r}{\Delta z} \left[v_z(M,n+1) - v_z(M,n) + v_z(M-1,n+1) - v_z(M-1,n) \right] = 0$$

$$M\, v_r(M+1,n+1) - (M-1)\, v_r(M,n+1) + \frac{2M-1}{4} \frac{\Delta r}{\Delta z} \left[v_z(M+1,n+1) - v_z(M+1,n) + v_z(M,n+1) - v_z(M,n) \right] = 0$$

Addition of the above equations results in the following equation

$$
\begin{aligned}
& M\, v_r(M+1,n+1) - v_r(1,n+1) \\
& \quad + \frac{1}{4}\,\frac{\Delta r}{\Delta z}\left[v_z(1,n+1) - v_z(1,n)\right] \\
& \quad + \frac{\Delta r}{\Delta z}\left[v_z(2,n+1) - v_z(2,n)\right] \\
& \quad + 2\,\frac{\Delta r}{\Delta z}\left[v_z(3,n+1) - v_z(3,n)\right] \\
& \quad + \ldots + (M-1)\,\frac{\Delta r}{\Delta z}\left[v_z(M,n+1) - v_z(M,n)\right] \\
& \quad = 0
\end{aligned}
\tag{F.3}
$$

From the centerline boundary condition (44)

$$v_r(1,n+1) = 0 \tag{F.4}$$

and from the wall boundary conditions (45)

$$
\begin{aligned}
v_r(M+1,n+1) &= 0 \\
v_z(M+1,n+1) &= 0 \\
v_z(M+1,n) &= 0
\end{aligned}
\tag{F.5}
$$

Using conditions (F.4) and (F.5), and dividing through by the non-zero constant common factor Δr, Equation (F.3) reduces to

$$
\begin{aligned}
& \frac{1}{4}\left[\frac{v_z(1,n+1) - v_z(1,n)}{\Delta z}\right] \\
& \quad + \sum_{m=2}^{M} (m-1)\left[\frac{v_z(m,n+1) - v_z(m,n)}{\Delta z}\right] = 0
\end{aligned}
\tag{F.6}
$$

which is the same as (52) of Chapter III.

BIBLIOGRAPHY

1. Hornbeck, R. W. The Entry Problem in Pipes with Porous Walls. Ph.D. Thesis, Carnegie Institute of Technology, 1961.

2. Uchida, S. "The Pulsating Viscous Flow Superimposed on the Steady Laminar Motion of Incompressible Fluid in a Circular Pipe." ZAMP, Vol. 7, 1956, p 403-422.

3. Lavan, Z. Investigation of Swirling Flows. Ph.D. Thesis, Illinois Institute of Technology, 1965.

4. Seider, W. D. Confined Jet Mixing in the Entrance Region of a Tubular Reactor. Ph.D. Thesis, University of Michigan, 1966.

5. Lavan, Z. Private Communications, Internal Memo, Illinois Institute of Technology.

6. Dixon, T. N. A Study on Stability and Incipient Turbulence in Poiseuille and Plane Poiseuille Flow by Numerical Finite Difference Simulation. Ph.D. Thesis, Rice University, April, 1966.

7. Trulio, J. G., Carr, W. E., Niles, W. J., and Rentfrom, R. L. "Calculation of Two-Dimensional Turbulent Flow Fields" NASA CR-430, 1965.

8. Schlichting. Boundary Layer Theory. McGraw Hill Book Company, 1962.

9. Lin, C. C. "Motion in the Boundary Layer with a Rapidly Oscillating External Flow." Proceedings 9th International Congress on Applied Mechanics, Brussels, 1957, Vol. 4, p 155.

10. Blasius, H. "Grenzschichten in Flüssigkeiten mit kleiner Reibung." Z. Math. u Phys. 56, 1, 1908.

11. Goldstein, S., and Rosenhead, L. "Boundary Layer Growth." Proceedings, Cambridge Philosophical Society 32, (1936), 392.

12. Watson, E. J. "Boundary Layer Growth." Proceedings, Royal Society A 231 (1955) 104.

13. Moore, F. K. "Unsteady Laminar Boundary Layer Flow." NACA TN 2471, 1951.

14. Ostrach, S. "Compressible Laminar Layer and Heat Transfer for Unsteady Motions of a Flat Plate." NACA TN 3569, 1955.

15. Cheng, S. I., and Elliot, D. "The Unsteady Laminar Boundary Layer on a Flat Plate." Transactions ASME, 79 (1957) 725.

16. Kestin, J., Maeder, P. F., and Wang, H. E. "On Boundary Layers Associated with Oscillating Streams." Applied Scientific Research, A10, 1961, 1.

17. Hori, E. "Unsteady Boundary Layers." Bulletin of JSME, 5, 1962, 461.

18. Schuh, H. Fifty Years of Boundary Layer Research. Braunschweig, 1955, 147-152.

19. Hayasi, N. "On the Quasi-Two-Dimensional Laminar Boundary Layer." Journal of Physical Society of Japan, 18 (1960), 208.

20. Hayasi, N. "On Semi-Similar Solutions of the Unsteady Quasi-Two-Dimensional Incompressible Laminar Boundary Layer Equations" Journal of Physical Society of Japan, 17 (1962) 194.

21. Cheng, S. I. "Some Aspects of Unsteady Laminar Boundary Layer on a Flat Plate." Quarterly of Spplied Mathematics, 14 (1957), 337.

22. Hassan, H. A. "On Unsteady Laminar Boundary Layers." Journal of Fluid Mechanics, 9 (1960), 300.

23. Yang, K. T. "On Certain Similar Solutions to Unsteady Laminar Boundary Layer Equations in Low Speed Flow." Journal Aerospace Sciences, 25 (1958), 471.

24. Stewartson, K. "The Theory of Unsteady Laminar Boundary Layers." Advances in Applied Mechanics, Vol. VI (1960), 1-37.

25. Karman, Th. von "Laminare und Turbulente Reibung." ZAMM 1 (1921), 235.

26. Pohlhausen, K. "Zur Näherungsweisen Integration der Differential Gleichung der Laminaren Grenzschicht." ZAMM 1 (1921), 252.

27. Lighthill, M. J. "The Response of Laminar Skin Friction and Heat Transfer to Fluctuations in the Stream Velocity." Proceedings Royal Society, A 224 (1954) 1.

28. Yang, K. T. "Unsteady Laminar Boundary Layers Over an Arbitrary Cylinder with Heat Transfer in an Incompressible Flow." Trans. ASME Series E, 81 (1959), 171.

29. Rozin, L. A. "An Approximation Method for the Integration of the Equations of a Non-Stationary Laminar Boundary Layer in an Incompressible Fluid." NASA TT F-22 (1960).

30. Yang, K. T. "On the Calculation of Unsteady Incompressible Laminar Boundary Layers Over Arbitrary Cylinders." TN 62-11, Notre Dame University, 1962.

31. Hayasi, N. "On the Approximate Solution of the Unsteady Quasi-Two-Dimensional Incompressible Laminar Boundary Layer Equations." Journal of Physical Socity of Japan, 17 (1962), 203.

32. Schlichting, H. and Ulrich, A. Report S 10 of the Lilienthalgesellschaft, 1940.

33. Friedrich, C. M. A Numerical Difference Equation Method for Determining Velocity Distribution in Co-Axial Jets. Ph.D. Thesis, Carnegie Institute of Technology, 1952.

34. Rouleau, W. T. and Osterle, J. F. "Finite Difference Methods for the Solution of Fluid Flow Problems Described by the Prandtl Equations." AFOSR Report prepared under Contract No. AF-18(600), 969, 1954.

35. Bodoia, J. R. The Finite Difference Analysis of Confined Viscous Flows. Ph.D. Thesis, Carnegie Institute of Technology, 1959.

36. Wu, J. C. "The Solution of Laminar Boundary Layer Equations by the Finite Difference Method." Douglas Report SM-37484, April, 1960.

37. Schuyler, F. L. and Torda, T. P. "An Aerothermochemical Analysis of Solid Propellant Combustion." To be published in a forthcoming issue of the AIAA Journal.

38. Farn, C., Arpaci, V. S., and Clark, J. A. "A Finite Difference Method for Computing Unsteady, Incompressible, Laminar Boundary Layer Flows." ARL Technical Report No. 3 prepared under Contract No. AF 33(657) - 8368.

39. Karplus, W. J. "An Electric Circuit Theory Approach to Finite Difference Stability." Transactions AIEE, Part I, May, 1958.

40. Lax, P. D. "Difference Approximation to Solution of Linear Differential Equations - An Operator Theoretical Approach." Lecture Series of the Symposium on Partial Differential Equations, University of Kansas Press, Lawrence, Kansas, 1957.

41. Wood, B. Diffusion in a Laminar Confined Jet. D. Sc. Thesis. Massachusetts Institute of Technology, (1964).

42. Hill, P. G. "Turbulent Jets in Ducted Streams." Journal of Fluid Mechanics, (1965), Vol. 22, part 1, pp 161-186.

43. Hildebrand, F. B. Methods of Applied Mathematics. Prentice Hall, Inc., 1942, p 328-355.

44. De Santo, D. F. and Keller, H. B. "Numerical Studies of Transition from Laminar to Turbulent Flow over a Flat Plate." Journal of the Society of Industrial and Applied Mathematics, Vol. 10, No. 4, December 1962, p 569-595.

"The aeronautical and space activities of the United States shall be conducted so as to contribute . . . to the expansion of human knowledge of phenomena in the atmosphere and space. The Administration shall provide for the widest practicable and appropriate dissemination of information concerning its activities and the results thereof."

—NATIONAL AERONAUTICS AND SPACE ACT OF 1958

NASA SCIENTIFIC AND TECHNICAL PUBLICATIONS

TECHNICAL REPORTS: Scientific and technical information considered important, complete, and a lasting contribution to existing knowledge.

TECHNICAL NOTES: Information less broad in scope but nevertheless of importance as a contribution to existing knowledge.

TECHNICAL MEMORANDUMS: Information receiving limited distribution because of preliminary data, security classification, or other reasons.

CONTRACTOR REPORTS: Scientific and technical information generated under a NASA contract or grant and considered an important contribution to existing knowledge.

TECHNICAL TRANSLATIONS: Information published in a foreign language considered to merit NASA distribution in English.

SPECIAL PUBLICATIONS: Information derived from or of value to NASA activities. Publications include conference proceedings, monographs, data compilations, handbooks, sourcebooks, and special bibliographies.

TECHNOLOGY UTILIZATION PUBLICATIONS: Information on technology used by NASA that may be of particular interest in commercial and other non-aerospace applications. Publications include Tech Briefs, Technology Utilization Reports and Notes, and Technology Surveys.

Details on the availability of these publications may be obtained from:

SCIENTIFIC AND TECHNICAL INFORMATION DIVISION

NATIONAL AERONAUTICS AND SPACE ADMINISTRATION

Washington, D.C. 20546